

New Insights into the Role of Citrullination for Antibody Levels and Reactivity in
Rheumatoid Arthritis and Influenza

By Aisha Maia Mergaert

A dissertation submitted in partial fulfillment of
the requirements for the degree of

Doctor of Philosophy
(Cellular and Molecular Pathology)

at the

UNIVERSITY OF WISCONSIN-MADISON

2021

Date of final oral examination: 4/29/2021

The dissertation is approved by the following members of the Final Oral Committee:

Miriam Shelef, MD PhD, Associate Professor, Medicine, Cellular and Molecular

Pathology Graduate Program

Marulasiddappa Suresh, MVSc DVM PhD, Professor, Pathobiological Sciences

Yun Liang, PhD, Assistant Professor, Microbiology & Immunology

John-Demian Sauer, PhD, Associate Professor, Medical Microbiology & Immunology

Judith Smith, MD PhD, Associate Professor, Pediatrics and Medical Microbiology and
Immunology

Abstract

Peptidylarginine deiminases (PADs) are responsible for the conversion of peptidylarginine to peptidylcitrulline. PAD2 is widely expressed in human tissue and, along with PAD4, is expressed in the rheumatoid joint and immune cells. PAD2 and PAD4 are both implicated in rheumatoid arthritis (RA) and citrullinated proteins are increased in RA patients. Autoantibodies to citrullinated proteins are a key diagnostic and pathologic feature of RA and these autoantibodies, called anti-citrullinated protein antibodies (ACPAs), appear preclinically and are associated with more severe disease. Here I investigate antibodies which target native and citrullinated histone and how these antibodies are related to a genetic variant within the PAD4 gene in North Americans. I find that the G allele at SNP rs2240335 is associated with reduced anti-histone antibodies to both native and citrullinated histone in rheumatoid arthritis subjects without known antibodies to citrullinated proteins. Additionally, I investigated epitope overlap between ACPAs and the other major autoantibody in RA, ie rheumatoid factor (RF, antibodies that bind the Fc portion of IgG). This investigation finds that RA subjects with both ACPAs and RF have significant IgG binding to IgG peptides that have been citrullinated as well as homocitrullinated, the post-translational modification of lysine to homocitrulline. Moreover, individual ACPAs can bind to intact, modified IgG Fc, demonstrating for the first time that IgG is a common antigen for ACPAs and RFs. Last, I investigate the role of PAD2 in inflammatory arthritis and normal immunity. Using mice which lack PAD2, I find that PAD2 is required for autoantibody levels in inflammatory arthritis. Further, in a new model of influenza A infection in DBA/1J mice, I found that PAD2 is required for robust levels of hemagglutination inhibiting antibodies and normal recovery after lethal influenza

rechallenge. Together these data demonstrate an important role for PAD2 in antibody responses in both normal immunity and autoimmunity. Taken together, these data contribute to our knowledge of citrullinating enzymes and antibodies in disease and should be further investigated to improve treatment strategies for both RA and influenza.

Acknowledgements

Reaching this remarkable milestone was not a solo effort. It required support, both personal and professional.

I would like to thank first and foremost my mother, Wendy, who has always believed in my ability to do great things and to accomplish my goals. I would not be writing this without her support and love. And thank you to my brother, Myell, for his encouragement over these seven years, he may have won the race to the “doctorate” finish line, but I get the medal for endurance.

A particular thank you goes to my husband, David, who supported me nearly the entire length of my PhD journey and helped me over unforeseen roadblocks. Such a feat would not have been possible without such a compassionate, kind person by my side.

Also, thank you to my fabulous female mentors. To Dr. Miriam Shelef, who bravely took me on in my fourth year and nurtured me into the scientist I am today. To Dr. Emer Clarke, who first showed me what a great immunologist looks like and encouraged me to pursue my PhD. And to Theresa Britschgi, who showed me how science can be a force for equity and justice and encouraged me in my studies since high school.

Table of Contents

Abstract.....	i
Acknowledgements	iii
Table of Contents.....	iv
Chapter 1: Introduction.....	1
1.1 Structure and function of antibodies.....	2
1.2 Antibodies in Autoimmune Disease.....	3
1.3 Citrullination	7
1.4 Peptidylarginine deiminases in disease	8
Chapter 2: Reduced anti-histone antibodies and increased risk of rheumatoid arthritis associated with a single nucleotide polymorphism in PADI4 in North Americans	12
2.1 Abstract.....	14
2.2 Introduction	15
2.3 Results.....	17
2.4 Discussion.....	20
2.5 Conclusions	23
2.6 Methods	23
2.7 Figures.....	29
Chapter 3: Divergent reactivities of rheumatoid factors and anti-modified protein antibodies converge on IgG epitopes.....	36
3.1 Abstract.....	38
3.2 Introduction	39

3.3 Results	40
3.4 Discussion.....	42
3.5 Methods	44
3.6 Figures.....	49
Chapter 4: PAD2 is Required for a Normal Antibody Response to Influenza Infection and Pathogenic Antibodies in Inflammatory Arthritis in Mice	69
5.1 Abstract.....	71
5.2 Introduction	71
5.3 Results.....	73
5.4 Discussion.....	76
5.5 Methods	79
5.6 Figures.....	87
Chapter 5: Conclusions and Future Directions.....	94
References.....	101
Appendix: Rheumatoid Arthritis: Two Murine Models.....	133
4.1 Abstract.....	135
4.2 Introduction	135
4.3 Collagen Induced Arthritis	138
4.4. TNF Induced Arthritis	142
4.5 Concluding remarks	143
4.6 Notes.....	143
4.7 Figures.....	145

Chapter 1: Introduction

1.1 Structure and function of antibodies

Immunoglobulins (Ig) are generated by plasmablasts and plasma cells in the bone marrow and secondary lymphoid tissues [1] and are composed of two light chains and two heavy chains. Each light chain is associated with a heavy chain via disulfide bonds and other non-covalent intermolecular interactions, forming a heterodimer, which is linked by a disulfide bond to an identical heterodimer [2]. The isotype of the heavy chain determines the Ig class of the molecule [3]. In mammals there are 5 classes of antibodies: IgG, IgM, IgA, IgE, IgD, each of which has a unique role in the immune system [4]. Antibody structure can also be described by its functional properties. The region of the antibody which interacts with antigen is called the fragment antigen binding domains (Fab), while the region of the antibody which interacts with the innate and adaptive immune system is termed the fragment crystallizable (Fc) region. Additionally, each heavy and light chain has a variable domain and constant domain within the Fab region. The heavy chain variable domain and light chain variable domain comprise the antigen binding site of the antibody, and diversity of antigen specificity is determined by genetic recombination and somatic hypermutation in these variable domains [3].

IgG, which is present exclusively in mammals, is one of the heavy lifters of humoral immunity, composing ~70% of Ig in human serum [4, 5]. While, IgM is a potent early responder to invading pathogens, IgG sustains the humoral immune response long term [6]. IgA responds to pathogens in the mucosal tissues, such as the lung, mouth and gastrointestinal tract, but can also be found at low levels in the serum [4, 5, 7, 8].

There are three central functions of antibodies. First, they directly bind antigen via their Fab region, second they activate immune cells via their Fc region, and third their Fc

region binds C1q to activate the classical pathway of the complement system [9]. In the context of viral infection, neutralizing antibodies mainly of the IgG isotype bind via their Fab region to viral particles and prevent entry to the target cell [10, 11]. Antibody-dependent cell-mediated cytotoxicity and antibody-dependent cellular phagocytosis are dependent not only on the Fab region but also on the ability of the Fc region to bind to effector cells [12-14]. These antibody dependent mechanisms are key components of the response to viral and bacterial infections [15-18] .

1.2 Antibodies in Autoimmune Disease

Although antibodies are largely beneficial, they are implicated in a wide variety of autoimmune diseases including RA, systemic lupus erythematosus (SLE), Sjögren's syndrome and multiple sclerosis (MS) [19-23], and are used extensively to diagnose autoimmune diseases [24-26]. Importantly, autoantibodies associated with a wide variety of autoimmune conditions can be detected before disease onset [27-30], and thus have a potential role in disease initiation. There is no clear mechanism by which autoantibodies develop in autoimmune disease. Thus, understanding the etiology of the loss in tolerance to self-protein could not only improve treatment once symptoms have developed, but also facilitate prevention strategies.

There are a variety of hallmark autoantibodies in rheumatic disease, one of which is anti-nuclear antibodies (ANA). ANA was first described in the bone marrow and peripheral blood of SLE patients in the 1940s and 1950s [21, 31, 32] as antibodies which bind to double stranded DNA and histones [33], though the current definition is broader and includes not only the nucleus but also some cytoplasmic proteins [34]. Although ANA

is found classically in SLE, ANA is also found in Sjögren's syndrome, systemic sclerosis and RA, and is classified by its pattern of binding within the cell [34, 35]. Importantly, ANA can be pathologic and drive disease, particularly in lupus nephritis [36-38]. Patients with RA commonly develop anti-histone antibodies, even before disease onset [39, 40].

Another early discovery among autoantibodies was rheumatoid factor (RF), an antibody which binds to the Fc region of IgG. RF was first described in 1939 by Waaler et al. who observed that RA serum had unique properties that included the ability to agglutinate sheep red blood cells sensitized by rabbit antibodies [19]. Since, RF has been identified in healthy subjects with an inflammatory process, such as infection, vaccination or smoking, and in a range of autoimmune diseases, including systemic SLE, Sjögren's syndrome [41]. In individuals without rheumatic disease *in vitro* studies show that RF functions to enhance neutralization of viruses [42] [43], function restoration of proteolytically cleaved IgG [44], and interacts with immune complexes to increase phagocytosis by macrophages and antigen presentation by RF positive B cells to T cells [45, 46].

RF can be pathologic through a variety of mechanisms. First, RF can bind to anti-citrullinated protein antibody (ACPA) immune complexes which can bind to macrophages via their Fc receptors and stimulate pro-inflammatory cytokines TNF- α , IL-1 β and IL-6 [47] [48]. RF can also enhance complement activation via ACPA immune complexes [49]. The deposition of proinflammatory RF-ACPA immune complexes in the rheumatoid joint indicates that RF may also contribute to synovitis through immune complex formation [50] [51]. Smoking, which is associated with the development of RA, is also a significant risk factor for RF-positive RA and smoking induces RF in mice [52, 53]. Low affinity,

polyreactive IgM-RF is typical of RF in healthy individuals, but those with RA have significantly more IgA and IgM RF compared to other rheumatic diseases [54, 55]. In RA, patients RF is typically IgM-RF, IgG-RF or IgA-RF, and these antibodies can occur simultaneously in as many as 52% of patients [41, 56]. Thus, break in tolerance to IgG within the T cell compartment is a well described characteristic of RA, but little is known about the mechanism by which this happens. Curiously, RF-positive disease has been reported to be decreasing, as outlined in retrospective study of 3 decades of RA incidence in Olmstead county, Minnesota [57]. The authors propose that decreased smoking and increased obesity rates may contribute to the shift of RF-positive disease, which could provide a basis for understanding the etiology of RF in RA patients.

In addition to RF, 75% of RA patients develop autoantibodies against proteins containing arginine that has been post-translationally modified to the non-standard amino acid citrulline, called ACPAs [58]. The discovery of ACPAs by Schellekens et al in 1998 has transformed RA research through the addition of an highly specific antibody to diagnose RA [58]. Like RF, smoking is a major risk factor for the development of ACPAs [52], but unlike RF, ACPA development is also highly associated with specific haplotypes of the MHC gene which confers an increased ability on the receptor to bind citrulline, called the shared epitope [52, 59-61]. Alternatively, the shared epitope could preferentially bind to PAD4 and result in the presentation of PAD4 citrullinated antigens in a hapten-carrier model [62]. ACPA positivity is controlled by both genetic factors and environmental factors. A GWAS study showed that ACPA-positive patients have different disease risk alleles from ACPA-negative RA patients [63] and another study showed ACPA-negative RA is associated with higher BMI, but not smoking [64]

Class switched ACPAs of the IgG isotype (IgG-ACPAs) are the first to be detected preclinically and can appear over a decade before RA is diagnosed [28], though likely IgM-ACPAs forms transiently before IgG-ACPAs. The presence of ACPAs may drive disease through the formation of pro-inflammatory immune complexes which increase joint destruction [50, 65]. Importantly, ACPA-negative patients differ in the early phase of disease, with less radiological progression and fewer swollen joints [66, 67] and have an altered cytokine signature and fewer leukocyte infiltrates in the synovium [68, 69].

Additional autoantibody reactivities in RA include autoantibodies to carbamylated (CarP) proteins which contain a lysine that is post-translationally modified to homocitrulline, acetylated-lysine (KAc) and malondialdehyde-acetaldehyde (MAA) adducted proteins [56]. Autoantibodies targeting post translational modifications, including citrulline, can be grouped together and are termed anti-modified protein antibodies (AMPAs). Using a competitive binding assay, Shi et al. showed that anti-CarP antibodies can be a distinct subset of antibody with a specific homocitrulline, rather than citrulline, containing epitope and that anti-CarP antibodies are present in both ACPA positive and ACPA negative RA patients [70]. Importantly, anti-CarP antibodies can be detected up to 10 years before RA onset [29], indicating a possible role on disease pathogenesis. Anti-KAc antibodies directed toward acetylated vimentin is described in ACPA-positive RA [71] and the mechanism by which this antibody arises is hypothesized to be linked to the microbiome [56, 72]. MAA is highly immunogenic [73] and anti-MAA antibodies are associated with ACPA levels [74], but anti-MAA antibodies appear after ACPA and RF indicating that it may not be the initiator of disease [75]. Of note, a subset of patients with RA are defined as seronegative due to negative serology for ACPAs and

RF, however there is growing evidence that RF and AMPAs are present in some of these patients [76, 77].

ACPAs, although traditionally thought to be specific to citrulline, can sometimes cross-react with other post-translational modifications [78, 79]. Sahlström et al. demonstrated that some human monoclonal ACPAs (mACPAs) isolated for their reactivities to citrullinated peptides also reacted with CarP peptides and KAc containing peptides [78]. Additionally, purified ACPA-IgG from the synovial fluid and serum bind not only to citrullinated vimentin peptide, but also CarP and KAc vimentin peptide [80]. Ultimately these studies demonstrate that many ACPAs are promiscuous binders to a range of post translational modifications beyond citrulline [78], which is important for understanding how a break in tolerance to self-protein occurs in RA.

1.3 Citrullination

Citrullination is a normal posttranslational modification present in healthy individuals, but appears to be dysregulated in RA patients and ACPAs are found almost exclusively in RA [58, 81-85] . Citrulline is the result of the enzymatic conversion of peptidylarginine to peptidylcitrulline by the peptidylarginine deiminase (PAD) family of enzymes [86]. This enzyme family consists of 5 isozymes, PAD1-4 and PAD6 [87-91], each of which has distinct patterns of substrate specificity and tissue and cellular localization [92-94]. The addition of a citrulline residue reduces the net charge of the protein by replacing positively charged arginine with a neutral citrulline. This effect can alter the protein's intermolecular interactions and cause a change in function and folding

[95-97]. An enzyme to reverse citrullination has not been described, indicating that citrullination is a permanent modification [98].

Evaluating the role of citrullination and citrullinating enzymes in RA has become a hot topic of research since Schellekens et al. discovered ACPAs in RA patients in 1998 [58]. The citrullination patterns, called the citrullinome, in humans has been described in several studies [81, 99-103]. Understanding disease pathology in RA necessarily means understanding the function of PADs in disease.

1.4 Peptidylarginine deiminases in disease

PAD2 and PAD4 are prominently expressed in a variety of immune cells [92, 104-107], and thus are of keen interest for researchers aiming to understand the generation of citrullinated autoantigens in RA. PAD2 is widely expressed in human tissue and, along with PAD4, is expressed in the rheumatoid joint [106, 108, 109], and both are both implicated in RA pathology more broadly [105, 110]. *PADI4*, the gene encoding PAD4, is a well known risk factor to RA development, with multiple GWAS studies showing a significant correlation between single nucleotide polymorphisms (SNPs) in *PADI4* and RA [111-116]. *PADI2*, the gene encoding PAD2, SNPs are also associated with RA but have not been identified in GWAS studies [117]. In general, far more research has explored PAD4 than PAD2 in the context of RA.

In the past 15 years, a refined mechanism of rheumatoid arthritis pathophysiology emerged which intersects PAD activity and neutrophil extracellular trap (NET) formation [118], as PAD4 is required for normal citrullinated NET formation [119, 120] and NETs are increased in RA patients [121]. Neutrophils are the first line of defense during an

infection or inflammatory insult [122]. They contain a variety of granules, specialized vesicles containing anti-microbial proteins, for which the traditional process of anti-microbial activity is the fusion of a granule with a phagosome containing a microbe [122]. NETosis is a unique form of cell death [123], distinct from apoptosis and necrosis, and serves a variety of purposes including the clearance of bacteria and fungi [124, 125]. When a neutrophil NETs, the chromatin decondenses and the nuclear envelope and granules disintegrate [122, 126]. The decondensed DNA and cytosolic contents are then extruded from the nucleus creating a complex structure of threads which ensnare and destroy fungi and bacteria [126, 127]. PAD4 enhances this process by citrullinating histones and allowing the chromatin to decondense [128]. Additionally, NETosis exposes PADs and citrullinated proteins to the extracellular space and is thus a proposed source of both intracellular and extracellular citrullinated antigen in RA, potentially driving disease [118, 121, 129]. Though PAD4 is widely described in NETosis, PAD2 could play a role in NET formation as it is present on NETs [129] and is the main source of citrullinated antigen in a mouse model of inflammatory arthritis [120]. While systematic analysis of NETs from mice found that PAD2 is not required for a wide variety of NETs in mice [130], loss of PAD2 has not been evaluated in human neutrophils.

PADs can also influence inflammation through direct modification of cytokines. PAD2 mediated citrullination of CXCL10 and CXCL11 is critical for some effector functions in T cells, resulting in decreased T cell chemotaxis and decreased calcium influx, both mediated through CXCR3 [131]. Also, citrullination of CXCL8 increases

neutrophil egress from the bone marrow and is thought to prolong neutrophils in the circulation [132].

Another mechanism by which PADs affect disease is through gene regulation and cell signaling. PAD4 is a well described regulator of gene activity, and a central mechanism by which it acts is through the modification of histones which are responsible for epigenetic regulation of gene expression [133-135]. PAD4 can act antagonistically to arginine methylation by converting monomethyl-Arg to citrulline, as shown in HL-60 granulocytes and kidney cell lines [136, 137]. Also, the P53 pathway, which is responsible for critical cell cycle activities, including responding to DNA damage, promoting apoptosis, and regulating senescence, is a well described target of PAD4 activity [138]. Specifically, it targets p53 histone binding and thus downregulates the downstream gene p21 [139]. Interestingly, PAD4 is the only PAD with a canonical nuclear localization signal (NLS), however there is evidence the PAD2 also translocates to the nucleus under homeostatic conditions [140, 141].

PAD2 also controls gene regulation and cell signaling, most notably through estrogen receptor signaling [141-144]. Decondensation at the loci surrounding the estrogen-response elements of target promoters is controlled by the citrullination of histone by PAD2, but not PAD4, and PAD2 directly associates with estrogen receptor α to mediate this effect [144]. Further studies into the role of PAD2 in estrogen receptor signaling and breast cancer is an area of ongoing research [145, 146].

Notably, PAD2 and PAD4 are expressed in T cells, macrophages, and neutrophils in human peripheral blood [104] [92] and possibly B cells [104]. Thus, these two PADs are of high interest to those investigating the role of citrullination in the immune system.

My research seeks to unravel the connection between citrullination in RA and disease pathology by investigating the activity and targets of PADs. GWAS studies have identified SNPs in *PADI4* associated with RA risk [111-116], and the G allele of SNP rs2240335 in *PADI4* is associated with reduced PAD4 levels in neutrophils [147]. Since PAD4 is required for citrullinated NETs and citrullinated NETs are a proposed source of citrullinated antigen in RA, it is possible the SNP rs2240335 is associated with NETs and autoantibodies in RA. Additionally, the two major types of autoantibodies in RA, RF and AMPAs, frequently co-exist but little is understood about why these two antibodies may arise simultaneously. One hypothesis is that post translationally modified IgG could act as antigen zero in RA by being a target for both RF and AMPAs. Lastly, mice lacking PAD2 have reduced serum IgG, plasma cells and arthritis in TNF-induced arthritis [120], but PAD2 has not been investigated in a mouse model with pathogenic autoantibodies or in normal immunity. My research investigates the above gaps in knowledge in relation PAD2 and PAD4 and autoantibody binding profiles in RA.

Chapter 2: Reduced anti-histone antibodies and increased risk of rheumatoid arthritis associated with a single nucleotide polymorphism in PADI4 in North Americans

This manuscript is published in the *International Journal of Molecular Sciences* (2019)

Funding for this study was provided by the University of Wisconsin School of Medicine and Public Health from the Wisconsin Partnership Program and the Doris Duke Charitable Foundation (2015099) to MAS. MAS was additionally supported by NIH/NIAMS K08AR065500 and CLH by NIH/NHLBI T32HL07899.

Reduced anti-histone antibodies and increased risk of rheumatoid arthritis associated with a single nucleotide polymorphism in PADI4 in North Americans

Aisha M. Mergaert ^{1,2}, Mandar Bawadekar ¹, Thai Q. Nguyen ¹, Laura Massarenti ³, Caitlyn L. Holmes ^{1,2}, Ryan Rebernick ¹, Steven J. Schrodi ⁴, and Miriam A. Shelef ^{1,5, *}

¹ Department of Medicine, University of Wisconsin-Madison, Madison, Wisconsin, USA; mergaert@wisc.edu, mandar.bawadekar@gmail.com, nguyen45@wisc.edu, cherndon@medicine.wisc.edu, reberya@gmail.com

² Department of Pathology and Laboratory Medicine, University of Wisconsin-Madison, Madison, Wisconsin, USA

³ Institute for Inflammation Research, Center for Rheumatology and Spine Diseases, Copenhagen University Hospital, Rigshospitalet, Copenhagen, Denmark; massarenti.laura@gmail.com

⁴ Center for Precision Medicine Research, Marshfield Clinic Research Institute, Marshfield, Wisconsin, USA; schrodi.steven@marshfieldresearch.org

⁵ William S. Middleton Memorial Veterans Hospital, Madison, Wisconsin, USA

* Correspondence: mshelef@medicine.wisc.edu

AM contributed to the manuscript by analyzing NET experiments in figure 1; performing and analyzing 90% of histone ELISA experiments; analyzing and assembling all data for the manuscript; making all of the figures, writing the original manuscript, reviewing and editing the final manuscript.

2.1 Abstract

Autoantibodies against citrullinated proteins are a hallmark of rheumatoid arthritis, a destructive inflammatory arthritis. Peptidylarginine deiminase 4 (PAD4) has been hypothesized to contribute to rheumatoid arthritis by citrullinating histones to induce neutrophil extracellular traps (NETs), which display citrullinated proteins that are targeted by autoantibodies to drive inflammation and arthritis. Consistent with this theory, PAD4-deficient mice have reduced NETs, autoantibodies, and arthritis. However, PAD4's role in human rheumatoid arthritis is less clear. Here, we determine if single nucleotide polymorphism rs2240335 in *PADI4*, whose G allele is associated with reduced PAD4 in neutrophils, correlates with NETs, anti-histone antibodies, and rheumatoid arthritis susceptibility in North Americans. Control and rheumatoid arthritis subjects, divided into anti-cyclic citrullinated peptide (CCP) antibody positive and negative groups, were genotyped at rs2240335. In homozygotes, *in vitro* NETosis was quantified in immunofluorescent images and circulating NET and anti-histone antibody levels by ELISA. Results were compared by t-test and correlation of rheumatoid arthritis diagnosis with rs2240335 by Armitage trend test. NET levels did not significantly correlate with genotype. G allele homozygotes in the CCP- rheumatoid arthritis group had reduced anti-native and anti-citrullinated histone antibodies. However, the G allele conferred increased risk for rheumatoid arthritis diagnosis, suggesting a complex role for PAD4 in human rheumatoid arthritis.

2.2 Introduction

Rheumatoid arthritis is an autoimmune destructive arthritis with a lifetime risk of 2.6% [148]. Most rheumatoid arthritis patients generate autoantibodies against citrullinated proteins. These anti-citrullinated protein antibodies (ACPAs) are diagnostic as measured by the anti-cyclic citrullinated peptide antibody (anti-CCP) test and pathologic [149, 150]. Although there may be multiple sources of citrullinated antigens in rheumatoid arthritis, neutrophil extracellular traps (NETs), extracellular structures composed of chromatin and antimicrobial proteins, have been hypothesized to be a significant source based on observations that NETs are increased in rheumatoid arthritis and contain some of the same citrullinated proteins targeted by ACPAs [121, 151, 152].

Citrullination, the post-translational modification of arginines to citrullines, is catalyzed by the peptidylarginine deiminases (PADs). In activated neutrophils, PAD4 citrullinates histones enhancing chromatin unraveling and NET formation [119, 128] and PAD4 is required for NETosis in response to a variety of stimuli [119, 120, 153-155]. Some of the earliest and most common ACPAs recognize citrullinated histones [39, 40, 156], sometimes more so if the histone is citrullinated by PAD4 as opposed to PAD2 [157]. In a murine model of rheumatoid arthritis, total IgG levels, autoantibodies, and arthritis are reduced in the absence of PAD4 [158]. These data suggest that PAD4 might contribute to the development of rheumatoid arthritis via enhanced NETosis and increased autoantibodies against histones driving disease. However, there is also data that would refute such a theory. Despite the importance of PAD4 for NETosis and the theory that NETs provide citrullinated antigen in rheumatoid arthritis, citrullination is not reduced in

the absence of PAD4 in serum, lungs, or joints in murine inflammatory arthritis [120, 158, 159]. Moreover, the importance of PAD4 in human rheumatoid arthritis is unclear.

Understanding the role of a protein in human disease is challenging. One method for approaching this problem is to seek genetic variants associated with disease. Genome-wide association studies have identified several single nucleotide polymorphisms (SNPs) in *PADI4*, the gene encoding PAD4, associated with rheumatoid arthritis [111, 113, 115]. SNP rs2240335 is particularly interesting since the G allele is associated with reduced PAD4 levels in neutrophils in Europeans [147]. Interestingly, the G allele of rs2240335 is associated with increased rheumatoid arthritis risk in East Asians [113, 115], the opposite of what would be expected based on lower PAD4 levels in Europeans and the requirement for PAD4 in murine arthritis [111, 158, 160]. To date, SNP rs2240335 has not been identified as associated with rheumatoid arthritis risk in Europeans in genome-wide association studies and no studies have evaluated rs2240335, PAD4-related biological phenomena, and rheumatoid arthritis risk together in a single human cohort.

The objective of this study is to determine if rs2240335 is associated with NETosis, anti-histone antibodies, and rheumatoid arthritis risk in a North American cohort to clarify the role of PAD4 in human rheumatoid arthritis. We found that the G allele of rs2240335 does not correlate with NETs, but does correlate with reduced anti-histone antibodies and increased risk of rheumatoid arthritis, suggesting that PAD4 has a complex role in human rheumatoid arthritis.

2.3 Results

Given the association of the G allele of rs2240335 with reduced PAD4 in human neutrophils [147] and the role for PAD4 in NETosis [119], we evaluated if the rs2240335 GG genotype would correlate with reduced NET formation in a North American cohort. Since rheumatoid arthritis [121, 151, 152] and potentially rheumatoid arthritis medications could affect NETosis, we evaluated NETs in control subjects homozygous for the G and T alleles of rs2240335. We assessed circulating NET levels by ELISA and percent NETosis in images of Sytox-stained neutrophils allowed to undergo NETosis *in vitro* using a semi-automated quantification tool [152]. We detected no reduction in either circulating NETs (Figure 1A) or *in vitro* NETosis (Figure 1B) in subjects homozygous for the G allele at rs2240335, suggesting that rs2240335 does not correlate with NET formation in our cohort.

We then sought to identify a correlation between rs2240335 and anti-histone antibody levels, since autoantibodies are reduced in arthritic mice in the absence of PAD4 [158]. Prior to this evaluation, we quantified anti-native and anti-citrullinated histone antibody levels by ELISA in control, CCP- rheumatoid arthritis, and CCP+ rheumatoid arthritis subjects in order to choose which group would be ideal for our experiments. We found that antibodies against histone H1 were not significantly different between control and rheumatoid arthritis subjects (Figure 2A). However, rheumatoid arthritis subjects had increased levels of antibodies against the other histones (Figure 2B-2E). More specifically, autoantibody levels were increased against both native and citrullinated histone H2A in CCP+ subjects, with no significant increase in CCP- rheumatoid arthritis (Figure 2B). As shown in Figure 2C and 2D, CCP+ subjects had higher levels of anti-

citrullinated histone H2B and H3 antibodies. Anti-citrullinated histone H4 antibodies in both CCP- and CCP+ subjects were significantly increased compared to controls (Figure 2E). Also, CCP- subjects had increased antibodies to native histone H4 compared to controls.

We also plotted each subject's titers against native versus citrullinated histones to identify a preference for citrullinated versus native histones in individual subjects. CCP+ subjects had a tendency towards reactivity against the citrullinated form of all five histones (Figure 3). However, a few CCP+ subjects targeted native histone H2A (Figure 3B). Also, a few CCP- subjects targeted native histone H2A and H3 (Figure 3B and 3D) and citrullinated histone H2B (Figure 3C).

Given the strong preference for citrullinated histones in CCP+ subjects, as expected, we compared serum IgG levels against citrullinated and native histones for CCP+ subjects homozygous for the G versus T allele of rs2240335. We found that there is no significant difference in anti-histone IgG between the GG versus TT genotypes in CCP+ subjects (Figure 4). Moreover, when plotting autoantibody levels against native versus citrullinated histones for each group, GG and TT subjects generally clustered similarly with a few GG subjects seeming to be outliers with increased autoantibodies to citrullinated and native histone H2A and citrullinated histone H4 (Figure 5).

Surprised by the results for the CCP+ subjects, we theorized that high levels of ACPAs, which are known to be cross-reactive [40, 161-163], may have obscured effects of rs2240335. Since some CCP- subjects were reactive to histones in our study, we hypothesized that these subjects might have detectable differences in anti-histone antibody levels between the homozygous alleles of rs2240335. Therefore, we compared

anti-histone antibody levels measured by ELISA between subjects homozygous for the G versus T alleles of rs2240335. We found that CCP- subjects homozygous for the G allele had reduced antibodies against native histones H2A, H2B, H3, and H4 and citrullinated histones H2B and H3 (Figure 6). Total IgG levels in homozygotes for the G allele of rs2240335 were not reduced (Supplementary Figure 2). When plotting native versus citrullinated titers for each genetic group, the TT or GG subjects clustered similarly with the majority of subjects showing no preference for citrullinated or native histone and a few TT subjects showing preference for native histone H2A (Figure 7). Together, these results suggest that the G allele of rs2240335, which is associated with reduced levels of PAD4 in neutrophils [147], is also associated with reduced levels of anti-histone antibodies in CCP- rheumatoid arthritis.

Finally, as noted above, the G allele of rs2240335 is associated with rheumatoid arthritis risk in East Asian populations [113, 115], yet reduced PAD4 levels were associated with the G allele in Europeans [147]. Therefore, we determined if rs2240335 is associated with rheumatoid arthritis in our North American cohort. For the 110 control and 452 White rheumatoid arthritis subjects in the University of Wisconsin Rheumatology Biorepository (94% of total subjects), we found that rs2240335 was associated with the rheumatoid arthritis/control endpoint using the Armitage trend test ($p=0.03$), where the G allele conferred increased risk for rheumatoid arthritis diagnosis compared to the T allele. Comparing the GG and TT homozygous genotypes, the odds ratio was calculated to be 2.14 with 95% CI (1.11, 4.12).

2.4 Discussion

Given the association between the G allele of rs2240335 in *PADI4* and increased rheumatoid arthritis risk in East Asians [113, 115], the reduction of PAD4 levels associated with the G allele of rs2240335 in Europeans [147], the role of PAD4 in NETosis, autoantibodies, and arthritis in mice [119, 158], and the link between NETs, ACPAs, and human rheumatoid arthritis [118, 121, 128], we determined if rs2240335 would be associated with NETs, anti-citrullinated histone antibodies, and rheumatoid arthritis in a North American cohort. Our data suggest that the relationships between rs2240335, biologic processes involving PAD4, and rheumatoid arthritis are quite complex.

For example, we detected no significant difference in NET levels between GG and TT homozygotes at rs2240335. There are several possible explanations for this finding. First, unlike the loss of NETs in the absence of PAD4 in *PAD4*^{-/-} mice [119], the reduction in PAD4 levels associated with rs2240335 may not be sufficient to reduce NETosis. Also, recent reports suggest that PAD4 is not required for the formation of NETs in response to some stimuli, particularly stimuli that do not induce citrullination [130, 164-166]. Thus, perhaps the NETosis that we measured simply does not require PAD4. Finally, our North American cohort may not be identical to the European cohort in which PAD4 was reduced in association with rs2240335 [147]. However, this last possibility is unlikely since 94% of our North American cohort is White and overwhelmingly reported Northwestern European ancestry similar to the European cohort [147]. Additionally, when analyses were repeated for NET and anti-histone antibody experiments using only White subjects, results were almost identical (data not shown).

In contrast to the lack of correlation between rs2240335 and NETs, we found that CCP- subjects homozygous for the G allele at rs2240335 had reduced autoantibodies against histones (Figure 6). There was no preference for binding to citrullinated versus native histones in the majority of subjects regardless of genotype (Figure 7), consistent with negative anti-CCP testing. The mechanism underlying these findings is unknown. Given the observed normal NET levels in the GG homozygotes (Figure 1), it is unlikely that reduced anti-histone antibody levels are due to a loss of NETs. Also, the reduction in anti-native histone antibodies suggests that the mechanism does not relate to an effect of rs2240335 in *PADI4* on citrullinated antigen. Consistent with this conclusion, no loss of gross protein citrullination was detected in arthritic PAD4-deficient mice [120, 158, 159]. Interestingly, the reduced anti-histone antibodies seen in the GG homozygotes at rs2240335 is similar to the reduced autoantibody levels against native and citrullinated antigens including histone H2B in PAD4-deficient mice [158], although GG homozygotes did not show a similar loss of total IgG (Supplementary Figure 2). Together these findings suggest a role for PAD4 in autoantibody development apart from providing citrullinated antigen.

We also found that the G allele at rs2240335 was associated with increased rheumatoid arthritis risk, although somewhat weakly, in North American Whites. Although this finding in North Americans agrees with findings in East Asians, increased rheumatoid arthritis risk associated with the G allele would not be predicted to co-associate with reduced PAD4 in neutrophils [147] or reduced anti-histone antibodies (Figure 6). Thus, there may be other effects of the G allele of rs2240335 on the development of rheumatoid arthritis. For example, the G allele of rs2240335 is associated with increased PAD4

expression in monocytes [147]. Although monocytes and macrophages are known to express PAD4 [104, 111, 140, 147], the function of PAD4 in this lineage is essentially unknown. Monocytes and macrophages can also make extracellular traps [167, 168] and thus could be a source of citrullinated antigen that is potentially PAD4-dependent. Additionally, rs2240335 could have effects in other cell types given the role of PAD4 in regulating gene expression [136, 169], modulating p53 effects [139], and regulating hematopoietic progenitor cells [170]. Further studies are needed to determine how rs2240335 might drive rheumatoid arthritis in PAD4-dependent or PAD4-independent pathways. Such studies will be important to understand disease pathophysiology and to inform the development of PAD4 inhibitors as potential treatments for rheumatoid arthritis.

The association between the GG homozygotes at rs2240335 with reduced anti-histone antibodies and increased rheumatoid arthritis risk also highlights a potential disconnect between autoantibodies and disease. While it is possible that the reduction of autoantibodies in GG homozygotes was too small to affect rheumatoid arthritis pathogenesis, another possibility is that not all autoantibodies are pathogenic. Studies have demonstrated a pathologic role for autoantibodies against a few citrullinated antigens [149, 150]. The autoantibodies that we evaluated did not specifically target citrulline, raising the possibility that pathogenicity lies primarily in ACPAs. Alternatively, autoantibodies may not be pathogenic in CCP- rheumatoid arthritis.

Finally, a peripheral contribution of our study is a comprehensive analysis of autoantibodies against all histones in CCP- and CCP+ rheumatoid arthritis. Multiple studies have identified citrullinated histones as autoantibody targets in rheumatoid arthritis [39, 40, 171]. Moreover, peroxynitrite-modified, 16 α -hydroxyestrone-adducted,

and acetylated histones have also been identified as autoantigens [172-174]. Although antibodies have been detected against native histones in rheumatoid arthritis [174, 175], our study provides a comprehensive evaluation of autoantibodies against all 5 histones including both citrullinated and native variants in both CCP- and CCP+ rheumatoid arthritis. The reactivity seen against native histone H2A (Figure 2 and 3) highlights the targeting of native antigens in rheumatoid arthritis, a commonly overlooked phenomenon. Further, the reactivity against histone H4 in CCP- subjects who also tested negative for rheumatoid factor (Figure 2 and data not shown) supports the theory that not all seronegative disease is truly seronegative. Together, these findings are useful for understanding the diversity of reactivity against histones and also reveal novel features of the autoantibody repertoire in rheumatoid arthritis.

2.5 Conclusions

We demonstrate that rs2240335 in *PADI4* correlates with reduced anti-histone antibodies and increased rheumatoid arthritis risk in North Americans. Taken together with the work of others, our data suggest that PAD4 may play a complex role in human rheumatoid arthritis. Additionally, we have provided a detailed evaluation of anti-histone antibodies in CCP- and CCP+ rheumatoid arthritis.

2.6 Methods

Human Subjects

All subjects gave their informed consent for inclusion before they participated in the study. The study was conducted in accordance with the Declaration of Helsinki, and the

protocol was approved by the Institutional Review Board of the University of Wisconsin-Madison (#2015-0156). All clinical data and biologic samples were obtained from the University of Wisconsin (UW) Rheumatology Biorepository first described in [152, 176]. Briefly, the biorepository contains data and samples from subjects at least 18 years old medically homeed at UW Health. Rheumatoid arthritis subjects were identified by having at least two outpatient visits with rheumatoid arthritis associated ICD codes within 24 months [177] or one visit and a positive anti-CCP test. Diagnosis was confirmed by manual review of rheumatology notes in the electronic medical record. Two categories of rheumatoid arthritis subjects were selected: those with a negative anti-CCP test (CCP-) and those with an anti-CCP test result twice the upper limit of normal (CCP+). Anti-CCP titers were determined using the Immunoscan CCPlus test kit (Eurodiagnostika, Malmö, Sweden) according to the manufacturer's instructions or generation II anti-CCP or anti-CCP3 ELISA (Inova, San Diego, USA) in the UW Health clinical lab. Controls were excluded if they had an autoimmune disease, inflammatory disease, or hematologic malignancy. Control subjects, CCP- rheumatoid arthritis subjects, and CCP+ rheumatoid arthritis subjects had similar demographic features for the GG versus TT genotype except for smoking in the CCP+ rheumatoid arthritis group (Supplementary Table 1).

DNA preparation

Peripheral blood was collected into EDTA vacutainers (BD, Franklin Lakes, USA). DNA was isolated using the Genra Puregene Blood Kit (Qiagen, Venlo, Netherlands) according to the manufacturer's instructions and stored at -80°C until use.

Plasma preparation

Peripheral blood was collected into EDTA vacutainers, centrifuged at 2000g for 10 minutes at room temperature without braking. Plasma was transferred to a new tube, centrifuged at 2000g for 5 minutes at room temperature with braking, transferred to a new tube, and stored at -80°C until use.

Genotyping

At the University of Wisconsin-Madison Biotechnology Center, DNA concentration was verified with Quant-iT PicoGreen dsDNA kit (Life Technologies, Grand Island USA). For the KASPar PCR reaction, DNA samples were standardized to 0.5 ng/μl using epMotion 5075 and 10 mM Ultrapure Tris-HCl pH 7.5 (Life Technologies). 2 μl of 0.5 ng/μl DNA and 2 μl of KASPar reaction mix [480 μl 2x KASP V4.0 2X Mastermix with standard ROX (KBioSciences, Hoddesdon, United Kingdom) and 13.2 μl assay mix (12 μM FWD Primer GAAGGTGACCAAGTTCATGCTCCCATGCAGGTACCATCACG, 12 μM REV Primer GAAGGTCGGAGTCAACGGATTACCCCATGCAGGTACCATCACT, 30 μM Common Primer AAGGAACAGAGGCCTGAAGGAGTTT, and 4.6 mM Tris HCl pH 7.5)] was dispensed into a 384 dark-well plate (Bio-Rad Microseal PCR plates, Bio-Rad, Hercules, USA). After brief centrifugation, 10 μl of Bio-Rad Chill-Out Liquid Wax was added and the following amplification protocol was used with an Eppendorf Mastercycler pro384: 94°C for 15:00 minutes; then a three-step protocol repeated 20 times: 94°C for 10 seconds, 59°C for 05 seconds, 72°C for 10 seconds; then another three-step protocol repeated 25 times: 94°C for 10 seconds, 59°C for 20 seconds, 72°C for 40 seconds; then 10°C until analysis. To determine the products of the PCR reaction, the plate is stored in

darkness at room temperature until the wax melts and become transparent. Then a Synergy 2 (BioTek, Winooski, USA) plate reader measures fluorescence using Gen5 software program.

NET enzyme linked immunosorbent assay (ELISA)

Similar to a previous NET ELISA assay [178], Costar 96-well high binding ELISA plates (Corning) were coated overnight at 4°C with 5 µg/ml anti-human myeloperoxidase (clone 4A4, Bio-Rad) diluted in 1X coating buffer from the Cell Death Detection ELISA kit (MilliporeSigma). Then, plates were washed four times with wash buffer (0.2% Tween-20 in PBS), blocked with 5% non-fat dry milk in PBS for 2 hours at room temperature, washed four times, and incubated overnight at 4°C with plasma samples diluted 1:50 in 1% BSA in PBS, washed four times, incubated for 2 hours at room temperature with anti-DNA-POD (Cell Death Detection ELISA kit, MilliporeSigma) diluted 1X in 1% BSA in PBS, washed four times, incubated with 1-Step Ultra TMB-ELISA Substrate Solution (Thermo Fisher Scientific) for 10 minutes, then stopped with 0.2N H₂SO₄. Absorbance was read at 450nm with 540nm plate correction using a Synergy 2 plate reader (BioTek) and normalized to a neutrophil NET standard. The neutrophil NET standard was generated by incubating a known number of purified neutrophils with phorbol 12-myristate 13-acetate and ionomycin overnight at 37°C with 5% CO₂. After 100% NETosis was visualized, NETs were scraped from the plate and stored at -80°C.

Quantification of *in vitro* NETosis

Neutrophils were purified and then incubated for 4 hours without any stimulant, followed by fixation, Sytox staining, imaging, and semi-automated quantification of NETosis using DNA Area and NETosis Analysis (DANA) as previously [152].

Citrullination of recombinant human histone

Recombinant human histones H1, H2A, H2B, H3 (New England Biolabs, Ipswich, USA) and H4 (MilliporeSigma, Burlington, USA) were citrullinated with recombinant human PAD4 (Cayman Chemical, Ann Arbor, USA) at a ratio of 2 μ g of PAD4 per mg of histone in a buffer of 100mM Tris-HCl pH7.5, 1mM DTT, and 5mM CaCl₂ at room temperature overnight with citrullination confirmed (Supplementary Figure 1).

Anti-histone ELISA

96 well plates (Corning, Corning, USA) were left uncoated or were coated with 10 μ g/ml of native or citrullinated histone, or the same concentration of PAD4 present in the citrullinated histone solution in phosphate buffered saline (PBS) overnight at 4°C. After washing 3 times (0.1% tween 20 in PBS), wells were incubated with block solution (5% nonfat dried milk in 0.2% Tween 20 in PBS) at room temperature for 2-4 hours, then serum (prepared as in [176]) diluted 1:200 in block solution for 2 hours at room temperature. Wells were then washed 5 times, incubated with anti-human IgG-HRP diluted 1:5000 in 5% nonfat dried milk in 0.2% Tween 20 in PBS for 2 hours at room temperature, washed again 5 times, and exposed to 1-Step Slow TMB-ELISA (Thermo Fisher Scientific, Waltham, USA) for 5-10 minutes, then stopped with 0.18M sulfuric acid.

Plates read at 450nm with 540nm plate correction using a Synergy 2 plate reader (BioTek). Samples were run in duplicate. Absorbance values from uncoated wells for each sample were subtracted from coated wells for each sample to reduce the effects of non-specific IgG binding to the plastic. Absorbance values from PAD4 coated wells were subtracted from citrullinated histone coated wells to normalize for anti-PAD4 IgG binding.

Statistical Analysis

T-tests and analysis of variance (*ANOVA*) were performed using Prism (GraphPad Software, San Diego, USA) with $p < 0.05$ considered statistically significant. The Armitage trend test with permutation routine was calculated using the XLISP-STAT programming language. 1M iterations of the permutation were performed to obtain a permuted p-value.

2.7 Figures

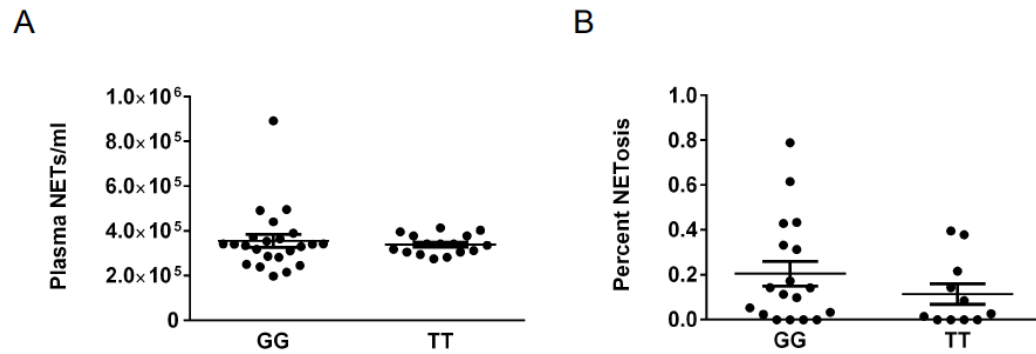


Figure 1. Genotype at rs2240335 Does Not Significantly Correlate with NET Levels.

A. Circulating NET levels measured in the plasma of control subjects by ELISA were compared for homozygotes for the G and T alleles at rs2240335 by t-test. B. Images of Sytox-stained peripheral blood neutrophils from control subjects allowed to NET for 4 hours were analyzed for percent NETosis and compared for homozygotes for the G and T alleles at rs2240335 by t-test. For all images, mean and SEM are graphed. No comparisons are significant. For ELISA, n= 23 GG and n=16 TT. For *in vitro* NETosis, n=18 GG and n=11 TT.

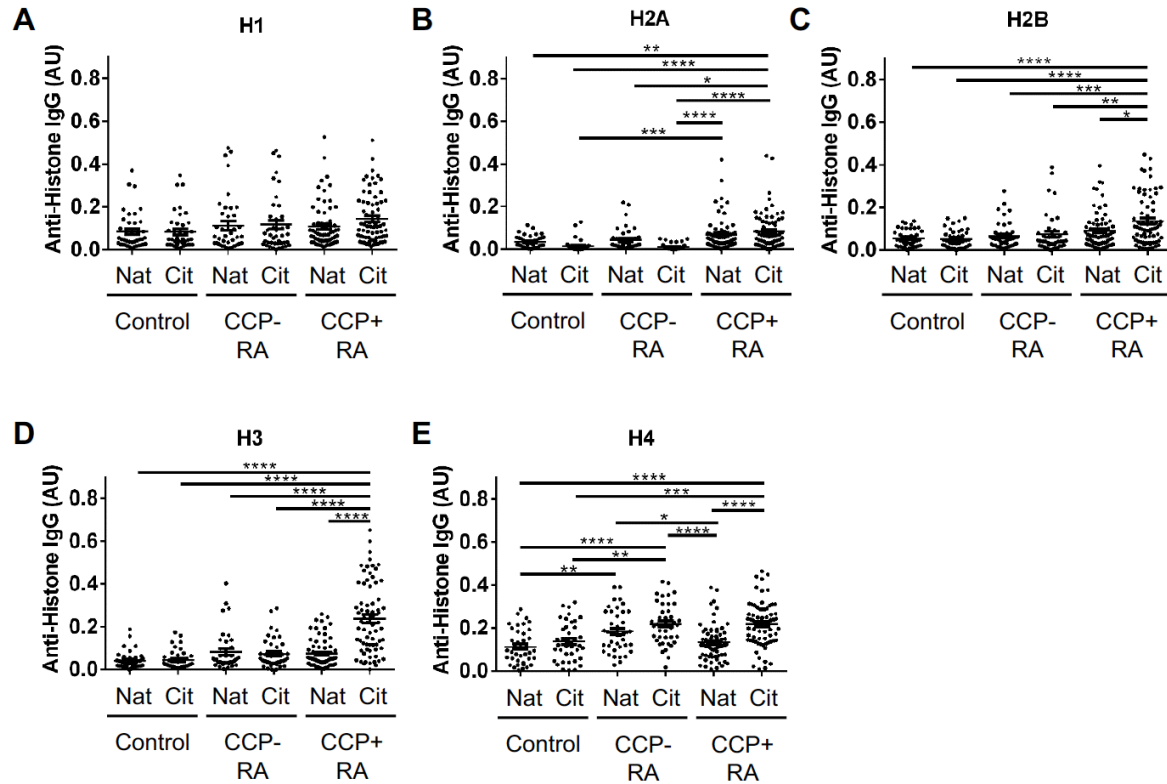


Figure 2. Anti-Histone IgG Levels in Controls and Rheumatoid Arthritis Subjects.

IgG levels against native (Nat) and citrullinated (Cit) histone H1 (A), histone H2A (B), histone H2B (C), histone H3 (D), and histone H4 (E) were measured by ELISA for controls, CCP- rheumatoid arthritis (RA) and CCP+ RA. Graphs depict average absorbance values in arbitrary units (AU) with SEM. Groups were compared by ANOVA. For all graphs, n=39 controls, 41 CCP- RA, 70 CCP+ RA; *p<0.05, **p<0.01, ***p<0.001, ****p<0.0001.

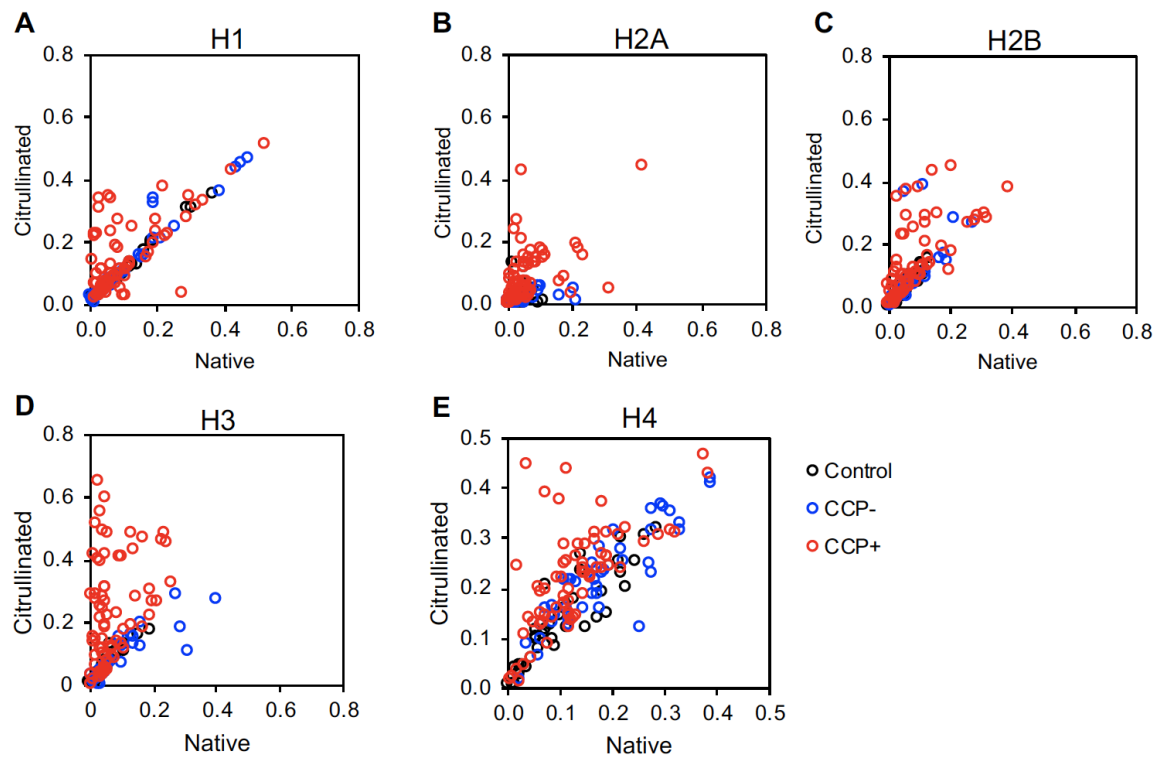


Figure 3. Native versus Citrullinated Histone Autoantibody Targeting in Controls and Rheumatoid Arthritis. IgG levels against native and citrullinated histone H1 (A), histone H2A (B), histone H2B (C), histone H3 (D) and histone H4 (E) measured by ELISA for controls, CCP- and CCP+ rheumatoid arthritis were compared by plotting anti-citrullinated histone antibody levels on the Y axis and anti-native histone antibody levels on the X axis. For all panels, n=39 controls, n=41 CCP- RA, n=70 CCP+ RA.

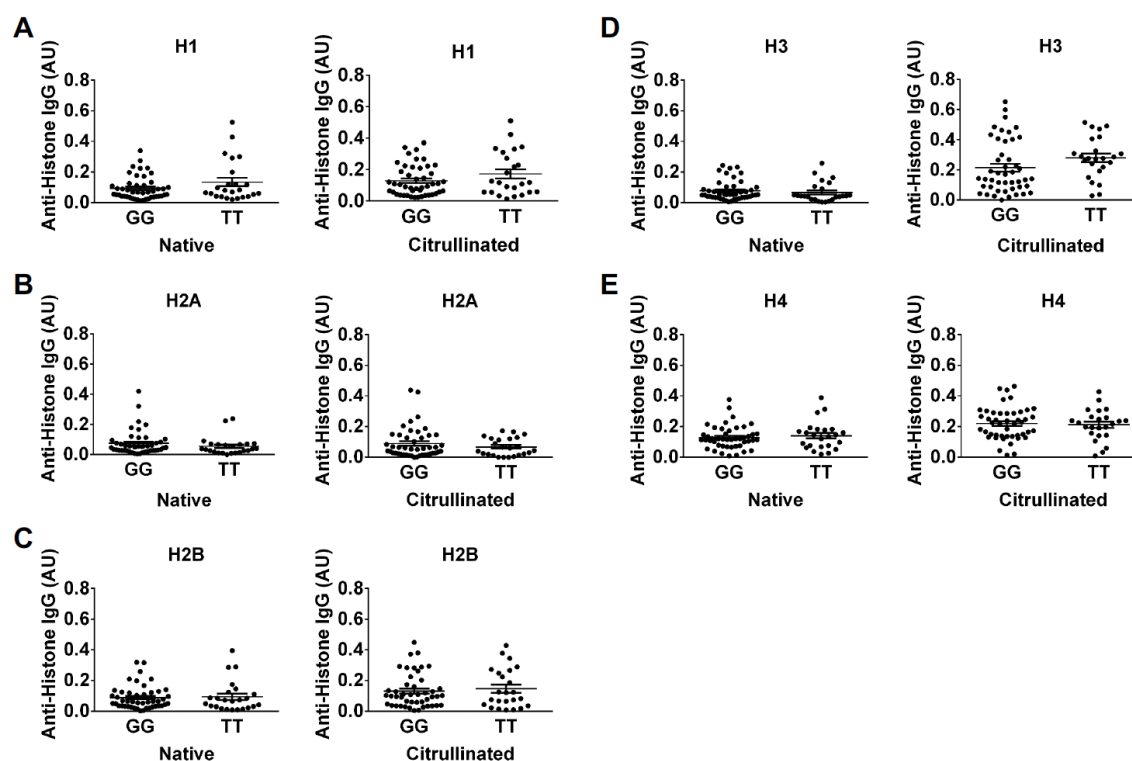


Figure 4. Anti-Histone IgG Levels in CCP+ Rheumatoid Arthritis Do Not Significantly Correlate with Genotypes at rs2240335. IgG levels against native and citrullinated histone H1 (A), histone H2A (B), histone H2B (C), histone H3 (D) and histone H4 (E) measured by ELISA in CCP+ rheumatoid arthritis subjects homozygous for the G or T allele at rs2240335 were compared by t-test. For all panels, graphs depict average absorbance values in arbitrary units (AU) \pm SEM, no comparisons were significant, and n=46 GG and 24 TT.

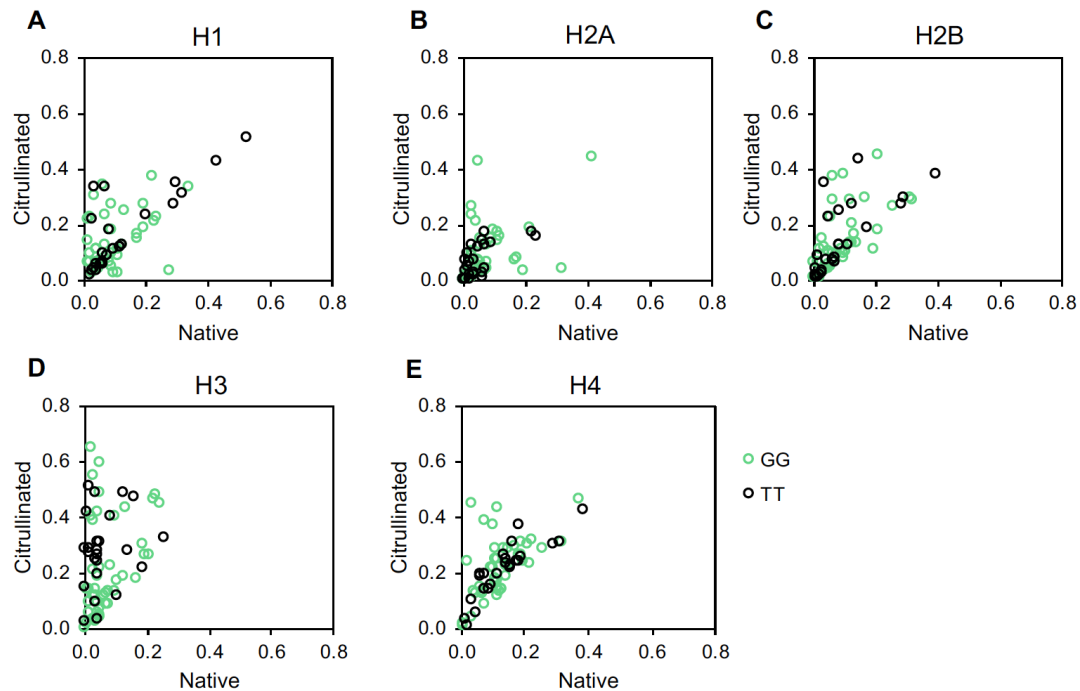


Figure 5. Native versus Citrullinated Histone Autoantibody Targeting in CCP+ Rheumatoid Arthritis. IgG levels against native and citrullinated histone H1 (A), histone H2A (B), histone H2B (C), histone H3 (D) and histone H4 (E) measured by ELISA for CCP+ rheumatoid arthritis subjects homozygous at rs2240335 were compared by plotting anti-citrullinated histone antibody levels on the Y axis and anti-native histone antibody levels on the X axis. For all panels, n=46 GG and 24 TT.

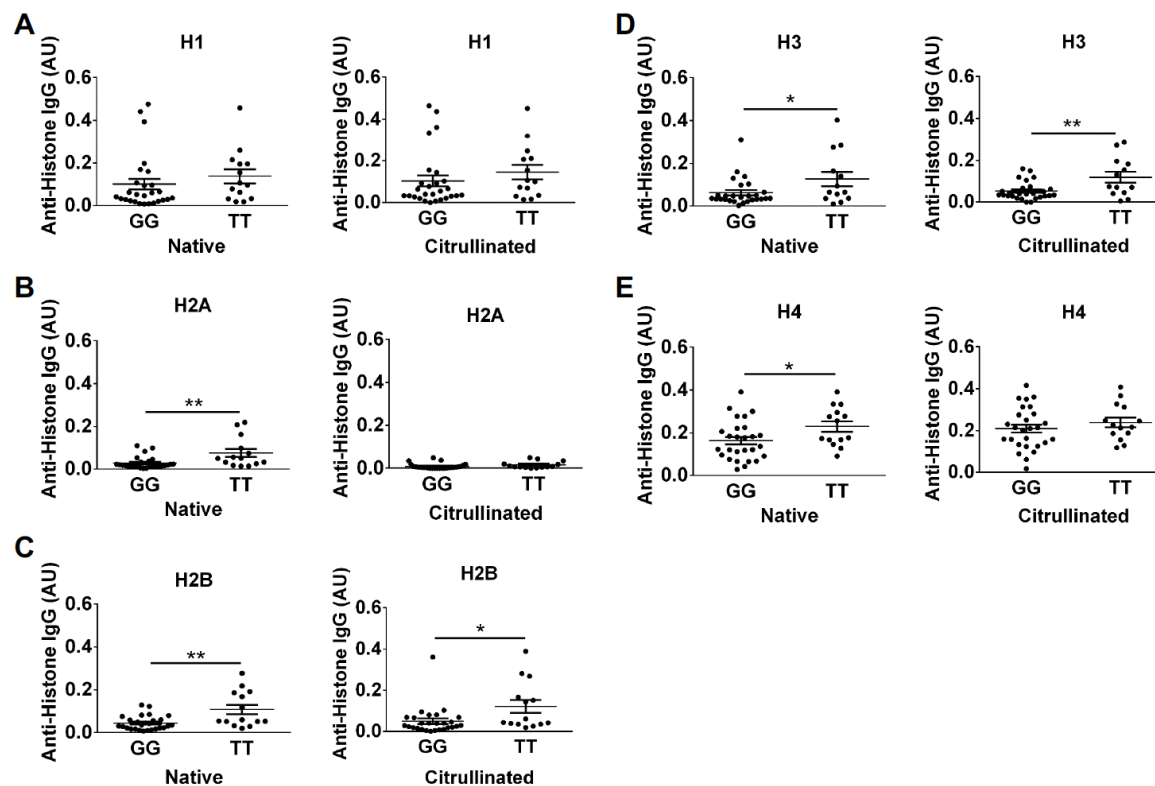


Figure 6. Reduced Anti-Histone IgG Levels in CCP- Rheumatoid Arthritis Subjects Homozygous for the G Allele at rs2240335. IgG levels against native and citrullinated histone H1 (A), histone H2A (B), histone H2B (C), histone H3 (D) and histone H4 (E) measured by ELISA in CCP- rheumatoid arthritis subjects homozygous for the G or T allele at rs2240335 were compared by t-test. For all panels, graphs depict average absorbance values in arbitrary units (AU) \pm SEM; * $p < 0.05$, ** $p < 0.01$; $n = 27$ GG and $n = 14$ TT.

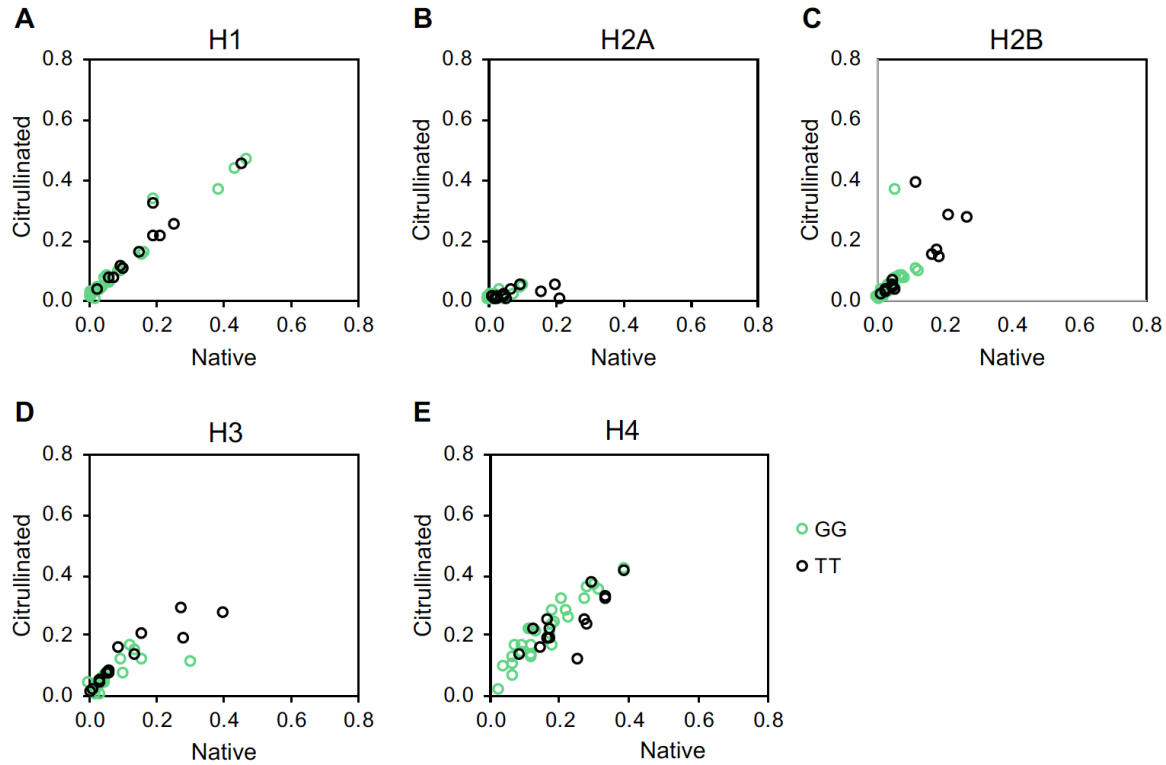


Figure 7. Autoantibodies against Native versus Citrullinated Histones in CCP-Subjects. IgG levels against native and citrullinated histone H1 (A), histone H2A (B), histone H2B (C), histone H3 (D) and histone H4 (E) measured by ELISA for CCP-rheumatoid arthritis subjects homozygous at rs2240335 were compared by plotting anti-citrullinated histone antibody levels on the Y axis and anti-native histone antibody levels on the X axis. For all panels, n=27 GG and n=14 TT.

Chapter 3: Divergent reactivities of rheumatoid factors and anti-modified protein antibodies converge on IgG epitopes.

This manuscript is under review at *Annals of Rheumatic Diseases* (2021)

Funding for this work was provided by the U.S. Army Medical Research Acquisition Activity through the Peer Reviewed Medical Research Program [W81XWH-18-1-0717] and the University of Wisconsin-Madison, Office of the Vice Chancellor for Research and Graduate Education with funding from the Wisconsin Alumni Research Foundation to M.A.S.. Additional support was provided by the National Institutes of Health's (NIH) National Heart, Lung, and Blood Institute [T32 HL007899] to A.M.M, the NIH's National Institute on Aging to M.F.A. [T32 AG000213], and the Clinical and Translational Science Award program through the NIH's National Center for Advancing Translational Sciences (UL1TR002373 and KL2TR002374) to S.S.M.. Monoclonal AMPA work was supported by the Swedish Research Council and the European Union/European Federation of Pharmaceutical Industries and Associations' Innovative Medicines Initiative 2 Joint Undertaking project RTCure (777357). We also thank Dr Daniel Mueller for his contributions to mACPA development.

Divergent reactivities of rheumatoid factors and anti-modified protein antibodies
converge on IgG epitopes.

Aisha M. Mergaert ^{1,3}, Zihao Zheng ^{2,3}, Michael F. Denny ³, Maya F. Amjadi ³, S. Janna
Bashar ³, Michael A. Newton ², Vivianne Malmström ⁴, Caroline Grönwall ⁴, Sara S.
McCoy ³, Miriam A. Shelef ^{3,5}

¹ Department of Pathology and Laboratory Medicine, University of Wisconsin-Madison,
Madison, USA

² Department of Statistics, University of Wisconsin-Madison, Madison, USA

³ Department of Medicine, University of Wisconsin-Madison, Madison, USA

⁴ Division of Rheumatology, Department of Medicine, Karolinska Institutet, Karolinska
University Hospital, Stockholm, Sweden

⁵ William S. Middleton Memorial Veterans Hospital, Madison, USA

AM contributed to the manuscript by selecting subjects in Figure 1; selecting peptides
with MAS and performing 80% of the ELISAs in figure 2; performing all ELISAs in figure
3; analyzing and assembling all data for the manuscript; making all of the figures, writing
the original manuscript, reviewing and editing the final manuscript.

3.1 Abstract

Objectives: Rheumatoid arthritis (RA) patients often develop rheumatoid factors (RFs), antibodies that bind IgG Fc, and anti-modified protein antibodies (AMPAs), multi-reactive autoantibodies that commonly bind citrullinated, homocitrullinated, and acetylated antigens. Recently, antibodies that bind citrulline-containing IgG epitopes were discovered in RA, suggesting that additional undiscovered IgG epitopes exist in rheumatic diseases and that IgG could be a shared antigen for RFs and AMPAs. The objective of this study was to reveal new IgG epitopes in rheumatic disease and to determine if cross-reactive AMPAs bind IgG.

Methods: Using RA, lupus, Sjögren's syndrome, and spondyloarthritis sera, IgG binding to native, citrulline-containing, and homocitrulline-containing linear epitopes of the IgG constant region were evaluated by peptide array with novel epitopes further evaluated by ELISA. Monoclonal AMPA binding to IgG-derived peptides and IgG Fc was evaluated by ELISA.

Results: Seropositive RA sera had high IgG binding to multiple citrulline- and homocitrulline-containing IgG-derived peptides, whereas only anti-SSA+ Sjögren's Syndrome had consistent binding to a single linear native epitope of IgG. AMPAs bound citrulline- and homocitrulline-containing IgG peptides and IgG Fc.

Conclusions: The repertoire of epitopes bound by AMPAs includes modified IgG epitopes, positioning IgG as a common antigen, connecting the divergent reactivities of RFs and AMPAs.

3.2 Introduction

Two main types of autoantibodies with high diagnostic value and possible pathogenic roles exist in rheumatoid arthritis (RA): rheumatoid factor (RF) and anti-citrullinated protein antibodies (ACPAs). RFs, antibodies of any isotype that bind the Fc portion of IgG, are common in RA, but are also found less frequently in systemic lupus erythematosus, anti-SSA+ Sjogren's syndrome, ankylosing spondylitis, some infections, hematologic malignancy, and smokers [53, 55, 179-182]. RFs commonly bind to two conformational epitopes after antigen binding, enzymatic degradation, or other change to the IgG molecule: one in the hinge region and one that includes parts of the CH2 and CH3 regions [181, 183-185]. In RA, additional epitopes are bound, affinity maturation occurs, and IgG-RF and IgA-RF are common [55, 181, 186], evidence of T cell help. However, why tolerance against IgG is lost in T cells in RA is unknown.

In addition to RF, ~75% of RA patients develop ACPAs, autoantibodies against proteins containing arginines that were post-translationally modified to citrullines [58]. Unlike RF, ACPAs are highly specific for RA and associated with shared epitope-containing HLA alleles [52], which may contribute to their development. Autoantibodies have also been identified in RA that bind to epitopes in which lysines have been converted to homocitrullines, i.e. homocitrullinated (carbamylated) antigens [70]. Moreover, individual ACPAs are often “anti-modified protein antibodies (AMPAs)” given their frequent reactivity to homocitrullinated and acetylated epitopes in addition to their multi-reactivity to many citrullinated targets [78, 79, 162]. Why AMPAs and RFs typically coexist in RA is a long-standing mystery. Perhaps each autoantibody type enhances the other's

production and/or a common antigen underlies the development of both autoantibodies [52, 187].

Recently, IgG in RA sera was shown to bind to citrulline-containing linear peptides present in the IgG heavy chain [188], raising the possibility that IgG could be a shared antigen for RFs and AMPAs. However, although RF is defined by binding to IgG, it is unknown if AMPAs could recognize modified IgG epitopes. Moreover, the use of modern technology to discover new IgG epitopes in a few RA patients raised the possibility of additional undiscovered IgG epitopes in RA and other rheumatic diseases with RF.

In this manuscript, we evaluate the full repertoire of IgG heavy chain derived linear peptides bound by IgG in rheumatic diseases and by monoclonal AMPAs (mAMPAs) to discover new IgG epitopes and to determine if IgG is a common antigen for AMPAs and RFs.

3.3 Results

To evaluate IgG epitopes bound in RA and other rheumatic diseases, we quantified IgG binding to every 12 amino acid linear peptide derived from human IgG1-4 using a high density peptide array [188] and sera from patients diagnosed with RA (anti-CCP+RF+ and anti-CCP-RF-), lupus, Sjögren's Syndrome (anti-SSA+ and anti-SSA-), or spondyloarthritis, and matched control subjects. Clinical and demographic features of subjects can be found in Supplementary Tables 1-4. As shown in Figure 1 and Supplementary Figure 1, anti-CCP+RF+ RA sera strongly bound to multiple citrulline- and homocitrulline-containing peptides in all IgG isotypes with minimal binding to corresponding arginine- and lysine-containing native peptides. Other diseases displayed

very limited binding to IgG-derived peptides with anti-SSA+ Sjögren's Syndrome and spondyloarthritis sera binding to native peptides in the hinge region. As expected [179], anti-CCP-RF- RA and anti-SSA- Sjögren's Syndrome had no areas of high binding to IgG-derived peptides.

We then selected highly bound regions of IgG1 (Supplementary Table 5), the most abundant IgG subclass [189], for further evaluation of IgG binding by ELISA. Anti-CCP+RF+ RA sera bound more greatly than control sera to 6/8 homocitrulline-containing, 2/3 citrulline-containing, 2/3 dually modified, and 1/9 native peptides (Figure 2A). Interestingly, for the peptide starting at position 289, binding was increased in RA as compared to control for the homocitrulline- and citrulline-containing peptide, but not the dually modified version. Anti-CCP-RF- RA sera showed no increased binding to any peptide (data not shown) and anti-SSA+ Sjögren's Syndrome sera had increased binding compared to controls to the hinge peptide (Figure 2B).

Given the different IgG epitopes bound in anti-CCP+RF+ RA versus other diseases and the frequent coexistence of AMPAs and RF in RA, we next determined if cross-reactive AMPAs could bind IgG epitopes. Five patient-derived mAMPAs with different multi-reactivity profiles and one negative control monoclonal antibody [161, 162] were evaluated for binding to IgG-derived peptides and IgG Fc by ELISA. As shown in Figure 3, three mAMPAs bound to many modified (especially homocitrulline-containing), but not native, IgG-derived peptides, with different patterns among clones. Further, two mAMPAs with high reactivity to modified IgG-derived peptides also bound to IgG Fc, particularly homocitrullinated Fc, bridging the divide between AMPAs and RFs.

3.4 Discussion

In this study, we evaluated IgG binding to all possible linear epitopes of the constant region of IgG heavy chain to reveal several key features of autoantibody reactivity in rheumatic disease. First, we identified novel homocitrulline-containing IgG epitopes not detected in a previous evaluation of 12 anti-CCP+RF+ RA subjects, perhaps due to patient heterogeneity [188]. Interestingly, reactivity to citrulline- or homocitrulline-containing epitopes did not guarantee reactivity with a dually modified version. Dual modification reduced reactivity to one peptide, suggesting that one modification may disrupt the epitope containing the other modification. Further, all citrulline- and homocitrulline-containing epitopes were not bound equally by RA sera or mAMPAs, supporting the idea that modification alone is insufficient for antibody binding. IgG binding did not closely correlate with the presence of previously identified dominating motifs for IgG binding in RA: citrulline-glycine, homocitrulline-glycine, or citrulline-serine [78, 188]. Thus, additional unknown features of epitopes drive modified antigen targeting that require further investigation.

In contrast to the extensive binding of linear IgG epitopes in anti-CCP+RF+ RA, we demonstrated consistent IgG binding to only one linear IgG epitope in one non-RA disease: a hinge region epitope bound in anti-SSA+ Sjögren's Syndrome. Conformational epitopes in the hinge and CH2/CH3 regions of IgG have been described in RA, hematologic malignancy, lupus, and healthy individuals [181, 183, 185]. Antibody binding to linear epitopes may be a relatively unique feature of RA, consistent with observed reactivity against structurally disordered citrulline-containing and native epitopes [188]. Of

note, this difference in reactivity against some IgG epitopes in RA versus other rheumatic diseases could be leveraged to refine diagnostic testing.

Finally, we demonstrated that some cross-reactive AMPAs bound to multiple IgG-derived peptides and homocitrullinated IgG Fc, albeit less than the synthetic peptides. AMPA binding to citrullinated Fc was less pronounced, due either to less binding or minimal citrullination (Supplementary Figure 2). Regardless, the binding of AMPAs to modified IgG epitopes allows for the possibility that IgG, potentially modified, conformationally altered, and/or degraded *in vivo*, could be a common antigen underlying the development of AMPAs and IgG-RFs in RA. If true, then tolerance might be lost against modified IgG through a shared epitope-related mechanism, leading to AMPAs and IgG-RFs via epitope spreading. This mechanism may not lead to all IgG-RF, including IgG-RF in lupus [55], a disease without citrulline reactivity. Moreover, this mechanism would not lead to IgM-RF, a major portion of RF in RA, which is likely a non-specific response to inflammation [187]. However, IgG as a common antigen provides at least a partial mechanism for the frequent occurrence of both AMPAs and IgG-RF in RA. Further studies are needed to evaluate anti-IgG antibodies in pre-clinical RA to determine the chronology of autoantibody development.

In summary, we discovered new IgG epitopes in rheumatic disease and demonstrated that IgG epitopes are bound by AMPAs, in addition to RF. These findings provide new insights into the loss of tolerance against IgG and the development of autoantibodies in RA and other rheumatic diseases.

3.5 Methods

Human Subjects

Human subjects research was approved by the University of Wisconsin Institutional Review Board and complied with the Helsinki Declaration. Sera were obtained from the University of Wisconsin (UW) Rheumatology Biorepository [130, 152], which has expanded to include systemic lupus erythematosus, Sjögren's Syndrome, and spondyloarthropathy. Subjects are ≥ 18 years old receiving care at UW Health. Rheumatoid arthritis subjects meet the 2010 American College of Rheumatology (ACR)/European League Against Rheumatism (EULAR) diagnostic criteria for RA [24, 190]. CCP+RF+ RA subjects have anti-cyclic citrullinated peptide (CCP) and RF levels greater than twice the upper limit of normal and CCP-RF- subjects tested negative for both markers in UW Health's clinical labs. Lupus subjects meet Systemic Lupus International Collaborating Clinics (SLICC) criteria [191]. Sjögren's Syndrome subjects all meet the 2016 ACR/EULAR classification criteria for primary Sjögren's Syndrome [26] except for two subjects: one with a positive SSA test and the other with a minor salivary gland biopsy with focus score >1 , but both with incomplete medical record documentation for objective sicca. Subjects with spondyloarthropathy were diagnosed with ankylosing spondylitis, psoriatic arthritis, or inflammatory bowel disease associated arthritis by a rheumatologist and all have radiographic evidence of sacroiliitis. Controls were matched by age and gender and carried none of the following diagnoses: RA, lupus, Sjögren's Syndrome, scleroderma, psoriasis, psoriatic arthritis, ankylosing spondylitis, reactive arthritis, ulcerative colitis, Crohn's disease, multiple sclerosis, type I diabetes, or

hematologic malignancy. Subject characteristics can be found in Supplementary Tables 1-4.

High Density Peptide Array

A high density peptide array (Roche Nimblegen, Madison, USA) was used to detect serum IgG that bound to overlapping 12 amino acid peptides derived from the constant region of the heavy chains of IgG1 (Uniprot P01857), IgG2 (P01859), IgG3 (P01860), and IgG4 (P01861) as previously [188]. Peptides were included in native form, with all arginines replaced by citrullines, and with all lysines replaced by homocitrullines.

Monoclonal AMPA (mAMPA)

Generation of the human monoclonal AMPAs from single B cells from RA patients have previously been described. Clones 1325:07E07 and 1325:04C03 were derived from synovial plasma cells [162] while clones 37CEPT1G09, 14CFCT3G09 and 37CEPF2C05 were derived from blood memory B cells [161]. The monoclonal antibodies were recombinantly expressed as hIgG1, purified and extensively quality controlled [192]. All AMPA clones bind CCP2 and multiple citrullinated peptides without native peptide reactivity [78]. Besides citrulline reactivity, 37CEPT1G09 has previously shown extensive multi-reactivity to homocitrulline and acetylated peptides [78, 174], and 1325:04C03 and 37CEPF2C05 have had reactivity to some homocitrullinated antigens. 1325:07E07 and 14CFCT3G09 were more citrulline restricted based on previous studies [78].

Enzyme Linked Immunosorbent Assay (ELISA)

For peptide ELISA, plates were coated with 5 µg/ml streptavidin (Thermo Fisher Scientific, Waltham, USA) for 1 hour at room temperature (RT), washed with PBS, then coated with 0.125 µM of peptide conjugated to biotin at the C terminus (Biomatik, Kitchener, Canada) for 1 hour at RT. Peptides are listed in Supplementary Table 5. For IgG Fc ELISA, plates were coated overnight at 4°C with 10 µg/ml IgG Fc (MilliporeSigma, Burlington, USA) in PBS, which had been previously depleted of residual contaminating IgM and light chain using streptavidin magnetic beads (Thermo Fisher Scientific) coated with biotin-conjugated goat IgG anti-human IgM, goat IgG anti-human kappa and goat anti-human lambda (Southern Biotech, Birmingham, USA), in 4 forms: treated with 2 µg of PAD2 and PAD4 per 1 mg of IgG Fc in 100 mM Tris-HCl pH7.5, 1 mM DTT, and 5 mM CaCl₂, treated with 0.1M KOCN in dH₂O, diluted in citrullination buffer, diluted in dH₂O. KOCN reaction was quenched by the addition of Tris pH 8.8 at 0.15 M. After washing with PBS, plates were blocked for 1 hour at RT with 5% non-fat dried milk in 0.2% Tween 20 in PBS (serum ELISA block) or 1% BSA in PBS (mAMPA ELISA block without 0.1% Tween 20). Sera diluted 1:200 or 1:2000 in serum ELISA block or 1µg/ml mAMPAs [161, 162] in mAMPA ELISA block were applied to plates overnight at 4°C. After three washes, plates were incubated with mouse monoclonal anti-human IgG conjugated to horse radish peroxidase (clone JDC-10, Southern Biotech) diluted 1:5000 in serum ELISA block or goat anti-human lambda and anti-human kappa IgG conjugated to horse radish peroxidase (Southern Biotech) diluted 1:5000 in mAMPA ELISA block. After one hour at RT, plates were washed four times, developed with 3,3',5,5'-tetramethylbenzidine (Thermo Fisher Scientific) for 10 minutes, then stopped with 0.18 M sulfuric acid. Plates were read on a FilterMAX F3 (Molecular Devices, San Jose, USA) at 450 and 562, with

562 values subtracted from 450 values for each sample. For each sample, absorbance values for uncoated wells were subtracted from peptide- or Fc-coated wells to exclude non-specific binding, and absorbance values for PAD-containing buffer were subtracted from wells coated with PAD-treated IgG Fc to exclude anti-PAD reactivity.

Each plate included a standard curve of purified human IgG ranging from 0.0169 to 1000 ng/ml. To generate the human IgG standard curve, wells were coated with streptavidin as above, followed by biotin-labeled goat IgG anti-human lambda and kappa (Southern Biotech) capture antibodies at a 1:5000 dilution. Following a blocking step, serially diluted purified human IgG (Bethyl Laboratories, Montgomery, USA) in blocking buffer was added to the wells. The serially diluted human IgG was detected using the same method as above. The background-corrected absorbance values for the patient serum samples were converted to ng/ml of human IgG by applying a four parameter nonlinear curve fit to the wells containing the human IgG standards (elisaanalysis.com).

Statistical analysis

To avoid making distributional assumptions about the array measurements, we used nonparametric statistical tests. ELISA data for disease groups versus controls were compared by a Mann-Whitney test. IgG binding to the native versus homocitrulline-containing version of each peptide was compared by Wilcoxon matched-pairs signed rank test and IgG binding to native, citrulline-containing, homocitrulline-containing, and dually modified versions of peptides were compared by a Friedman test. Analyses were performed using Prism (GraphPad Software, San Diego, CA, USA) and a p-value less than 0.05 was considered significant. For comparing disease versus control subjects in

Supplementary Tables 1-4, Pearson's chi-squared and Fisher's exact test was used for categorical variables and the Kruskal-Wallis rank test for age, a continuous variable, using STATA version 16 (College Station, USA).

3.6 Figures

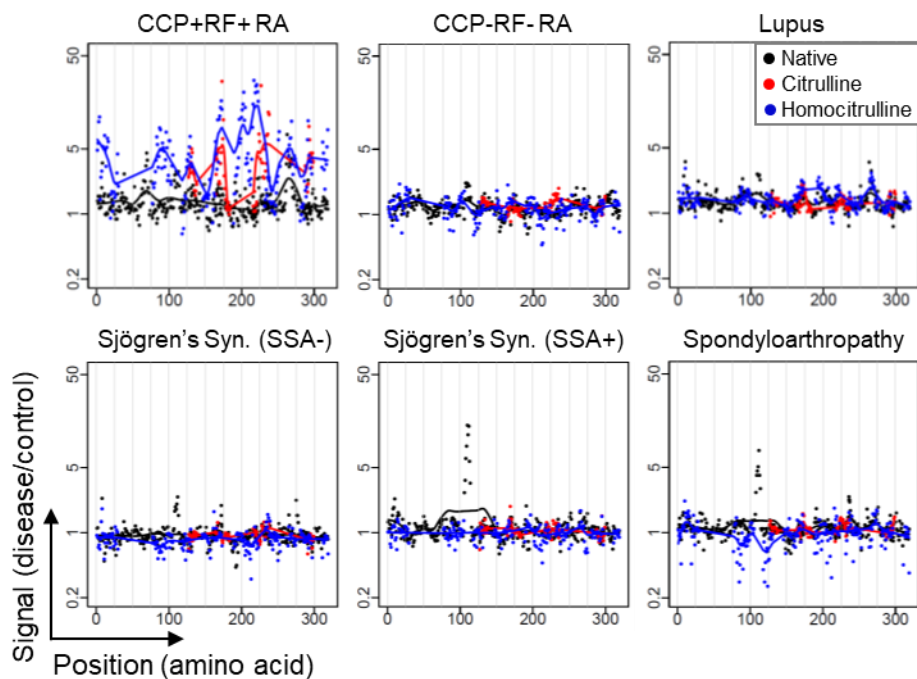


Figure 1. Serum IgG binding to IgG1-derived peptides in rheumatic diseases. IgG binding signal for each disease group divided by control binding signal is graphed for each peptide according to its position in the constant region of IgG1 (n=8, n=16 lupus).

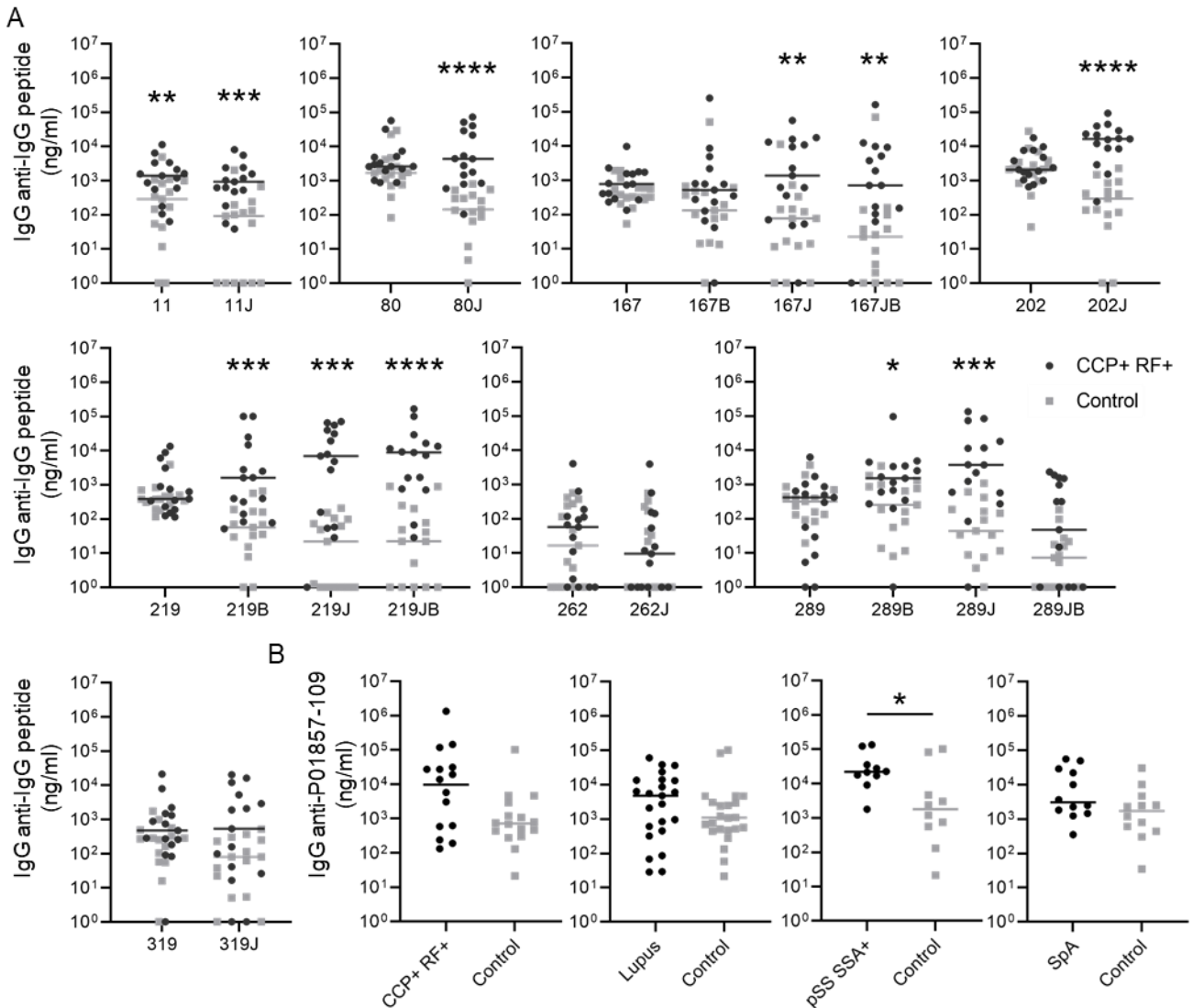


Figure 2. IgG from anti-CCP+RF+ RA patients binds multiple modified IgG-derived peptides with a native hinge peptide bound in Sjögren's Syndrome. A. Binding of IgG from anti-CCP+RF+ RA and control sera to native, citrulline (B)-containing, homocitrulline (J)-containing, and JB-containing peptides derived from the indicated amino acid position of IgG1 heavy chain was quantified by ELISA (n=15). **B.** Binding of IgG to a hinge peptide (position 109) was quantified by ELISA for anti-CCP+RF+ RA (n=16), lupus (n=23), anti-SSA+ primary Sjögren's Syndrome (pSS, n=10), spondyloarthritis (SpA, n=12), and controls. For all panels, disease groups were

compared to matched controls by Mann-Whitney test, bars indicate median, and * $p < 0.05$, ** $p < 0.01$, *** $p < 0.001$, **** $p < 0.0001$.

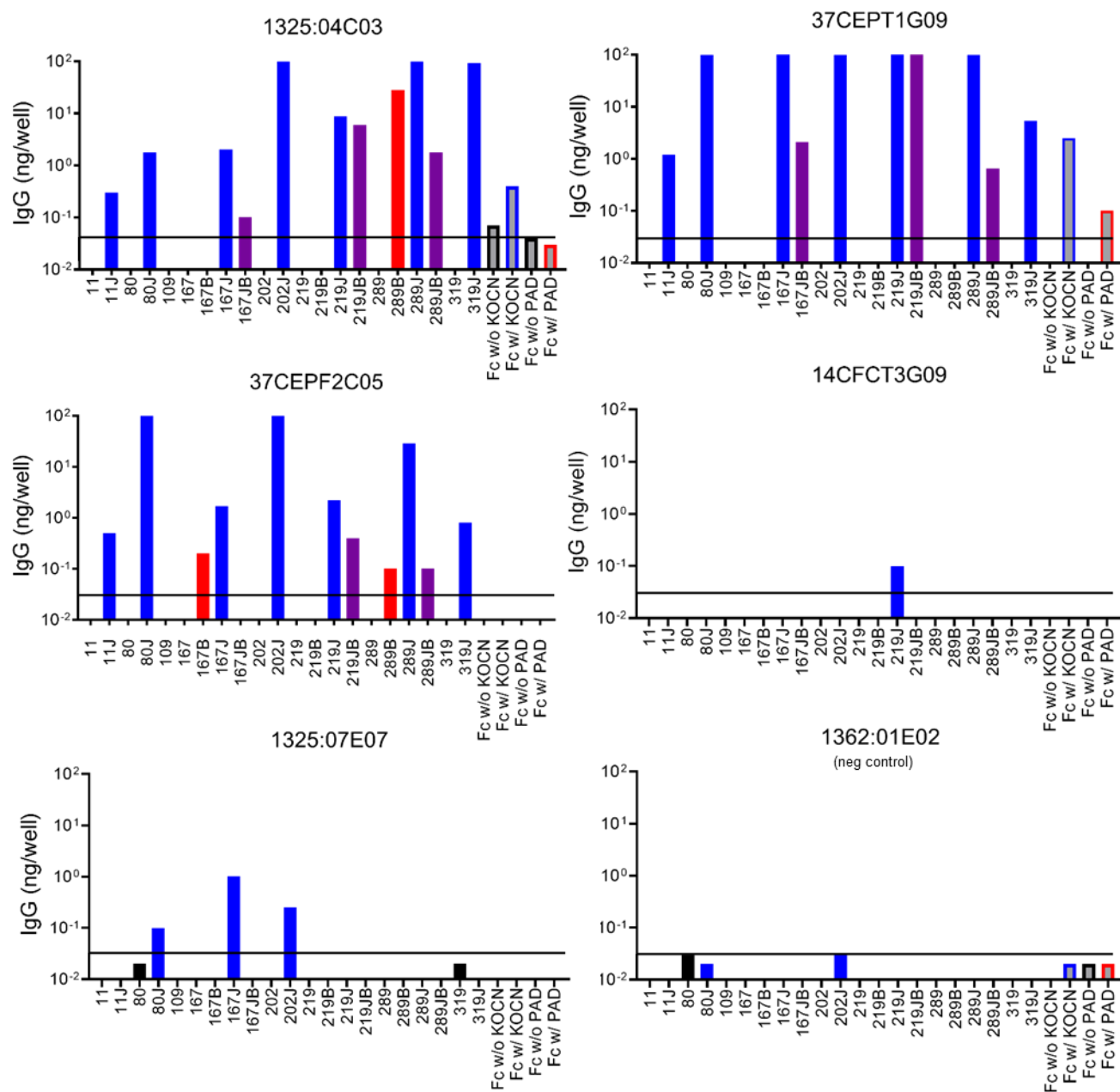


Figure 3. AMPAs bind citrulline- and homocitrulline-containing IgG-derived peptides and modified IgG Fc. Five patient-derived monoclonal AMPAs and one control monoclonal antibody were assessed by ELISA for binding to IgG1-derived peptides and human IgG Fc that was unmodified or treated with peptidylarginine deiminases (PADs) to

citrullinate or KOCN to homocitrullinate. Native peptides are in black, citrulline (B)-containing in red, homocitrulline (J)-containing in blue, and dually modified (JB) in purple. Line indicates highest level of binding detected for the negative control monoclonal antibody.

Supplementary Table 1. Characteristics of subjects with rheumatoid arthritis (RA) and controls.

Demographic	CCP+RF+ RA	CCP-RF- RA	Control	p value
N	16	16	16	
Sex, female, n (%)	14 (87.5)	14 (87.5)	14 (87.5)	1.000
Age, median (IQR)	54 (40, 62)	56 (40, 61)	55 (40, 61)	1.000
Race				0.319
White, n (%)	16 (100)	16 (100)	14 (87.5)	
Asian, n (%)	0 (0)	0 (0)	1 (6.25)	
Native American, n (%)	0 (0)	0 (0)	1 (6.25)	
Ethnicity, Hispanic, n (%)	3 (18.75)	0 (0)	0 (0)	0.097

Supplementary Table 2. Characteristics of subjects with lupus and controls.

Demographic	Lupus	Control	p value
N	23	23	
Sex, female, n (%)	22 (95.65)	22 (95.65)	1.000
Age, median (IQR)	48 (39, 57)	55 (40, 59)	0.386
Race			0.412
White, n (%)	20 (86.96)	18 (78.26)	
Black, n (%)	1 (4.35)	1 (4.35)	
Asian, n (%)	2 (8.70)	1 (4.35)	
Native American, n (%)	0 (0)	3 (13.04)	
Ethnicity, Hispanic, n (%)	2 (8.70)	0 (0)	0.489
Nephritis, n (%)	10 (43.48)	N/A	N/A

Supplementary Table 3. Characteristics of subjects with primary Sjögren's Syndrome (pSS) and controls.

Demographic	pSS SSA+	pSS SSA-	Control	p value
N	10	8	10	
Sex, female, n (%)	10 (100)	8 (100)	10 (100)	
Age, median (IQR)	63 (49, 64)	58 (48, 67)	58 (49, 69)	0.899
Race				1.000
White, n (%)	10 (100)	8 (100)	9 (90)	
Native American, n (%)	0 (0)	0 (0)	1 (10)	
Ethnicity, Hispanic, n (%)	0 (0)	0 (0)	0 (0)	

Supplementary Table 4. Characteristics of subjects with spondyloarthropathy (SpA) and controls.

Demographic	SpA	Control	p value
N	12	12	
Sex, female, n (%)	2 (16.67)	6 (50.00)	0.193
Age, median (IQR)	50 (36, 56)	45 (35, 57)	0.863

Race			1.000
White, n (%)	11 (91.67)	12 (100)	
Native American, n (%)	1 (8.33)	0 (0)	
Ethnicity, Hispanic, n (%)	0 (0)	0 (0)	

Supplementary Table 5. Peptides used in ELISA with array data for CCP+RF+ RA subjects and controls for each array peptide included in the ELISA peptides.

Name and amino acid position *	Sequence	CCP+R F+ RA Signal (Ave)	Contr ol Signal (Ave)	CCP+R F+ RA / Control	CCP+RF+ RA Subjects (number positive **)
P01857-11	LAPSSKSTSGGTAALGC				2
P01857-11J	LAPSSJSTSGGTAALGC				4
11	LAPSSKSTSGGT	269	164	1.6	2
11	LAPSSJSTSGGT	1157	167	6.9	3
12	APSSKSTSGGTA	89	91	1.0	0
12	APSSJSTSGGTA	418	87	4.8	2
13	PSSKSTSGGTAA	89	91	1.0	0
13	PSSJSTSGGTAA	660	203	3.3	2
14	SSKSTSGGTAAL	83	81	1.0	0
14	SSJSTSGGTAAL	350	67	5.2	2
15	SKSTSGGTAALG	70	71	1.0	0
15	SJSTSGGTAALG	417	65	6.5	3
16	KSTSGGTAALGC	97	63	1.6	0
16	JSTSGGTAALGC	380	64	6.0	3
	TYICNVNHKPSNTKVDKK				
P01857-80	VEPKSC				0

TYICNVNHJPSNTJVDJJV					
P01857-80J	EPJSC				5
80	TYICNVNHKPSN	69	64	1.1	0
80	TYICNVNHJPSN	147	69	2.1	1
81	YICNVNHKPSNT	82	74	1.1	0
81	YICNVNHJPSNT	208	73	2.8	2
82	ICNVNHKPSNTK	96	88	1.1	0
82	ICNVNHJPSNTJ	654	173	3.8	4
83	CNVNHKPSNTKV	105	134	0.8	0
83	CNVNHJPSNTJV	746	112	6.7	4
84	NVNHKPSNTKVD	108	122	0.9	0
84	NVNHJPSNTJVD	536	97	5.6	3
85	VNHKPSNTKVDK	86	69	1.2	0
85	VNHJPSNTJVDJ	700	221	3.2	4
86	NHKPSNTKVDDK	82	69	1.2	0
86	NHJPSNTJVDJJ	685	165	4.2	3
87	HKPSNTKVDDKV	99	73	1.4	0
87	HJPSNTJVDJJV	1120	133	8.4	4
88	KPSNTKVDDKVE	82	63	1.3	0
88	JPSNTJVDJJVE	988	124	8.0	4
89	PSNTKVDDKVEP	80	63	1.3	0
89	PSNTJVDJJVEP	514	105	4.9	3
90	SNTKVDDKVEPK	75	60	1.3	0

90	SNTJVDJJVEPJ	607	196	3.1	3
91	NTKVDKKVEPKS	69	65	1.1	0
91	NTJVDJJVEPJS	754	131	5.8	3
92	TKVDKKVEPKSC	69	58	1.2	0
92	TJVDJJVEPJSC	635	124	5.1	3
P01857-109	CPPCPAPELLGGPSV				4
109	CPPCPAPELLGG	390	201	1.9	2
110	PPCPAPELLGGP	490	172	2.9	3
111	PCPAPELLGGPS	408	192	2.1	2
112	CPAPELLGGPSV	515	193	2.7	3
	VHNAKTKPREEQYNSTY				
P01857-167	RVVSV				0
	VHNAKTKPBEEQYNSTY				
P01857-167B	BVVSV				7
	VHNAJTJPREEQYNSTYR				
P01857-167J	VVSV				5
P01857-167JB	VHNAJTJPBEEQYNSTYB				
	VVSV				8 ***
167	VHNAKTKPREEQ	201	126	1.6	0
167	VHNAKTKPBEEQ	592	130	4.5	2
167	VHNAJTJPREEQ	725	71	10.3	4
168	HNAKTKPREEQY	193	98	2.0	0
168	HNAKTKPBEEQY	461	93	5.0	2

168	HNAJTJPREEQY	235	65	3.6	1
169	NAKTKPREEQYN	127	149	0.9	0
169	NAKTKPBEEQYN	415	186	2.2	2
169	NAJTJPREEQYN	1011	98	10.3	4
170	AKTKPREEQYNS	103	73	1.4	0
170	AKTKPBEEQYNS	162	77	2.1	1
170	AJTJPREEQYNS	1189	106	11.3	5
171	KTKPREEQYNST	75	69	1.1	0
171	KTKPBEEQYNST	225	65	3.5	2
171	JTJPREEQYNST	1302	93	13.9	5
172	TKPREEQYNSTY	155	96	1.6	0
172	TKPBEEQYNSTY	371	82	4.5	1
172	TJPREEQYNSTY	1432	87	16.4	5
173	KPREEQYNSTYR	81	84	1.0	0
173	KPBEEQYNSTYB	2928	111	26.5	6
173	JPREEQYNSTYR	1162	87	13.3	5
174	PREEQYNSTYRV	181	112	1.6	0
174	PBEEQYNSTYBV	930	146	6.4	3
175	REEQYNSTYRVV	83	53	1.6	0
175	BEEQYNSTYBVV	674	66	10.2	3
176	EEQYNSTYRVVS	66	53	1.2	0
176	EEQYNSTYBVVS	148	58	2.6	0
177	EQYNSTYRVVSV	52	45	1.2	0

177	EQYNSTYBVVSV	115	61	1.9	0
P01857-202	YKCKVSNKALPAP				0
P01857-202J	YJCJVSNJALPAP				5
202	YKCKVSNKALPA	90	85	1.1	0
202	YJCJVSNJALPA	1654	109	15.1	5
203	KCKVSNKALPAP	69	73	1.0	0
203	JCJVSNJALPAP	2261	113	20.1	5
	ISKAKGQPREPQVYTLPP				
P01857-219	SRDEL				1
	ISKAKGQPBEPQVYTLPP				
P01857-219B	SBDEL				5
	ISJAJGQPREPQVYTLPP				
P01857-219J	SRDEL				6
P01857-219JB	SBDEL				8 ***
219	ISKAKGQPREPQ	194	198	1.0	0
219	ISKAKGQPBEPQ	205	193	1.1	0
219	ISJAJGQPREPQ	2245	112	20.0	5
220	SKAKGQPREPQV	191	188	1.0	0
220	SKAKGQPBEPQV	245	196	1.3	0
220	SJAJGQPREPQV	2195	93	23.5	5
221	KAKGQPREPQVY	167	183	0.9	0
221	KAKGQPBEPQVY	242	180	1.3	1

221	JAJGQPREPQVY	2667	109	24.5	5
222	AKGQPREPQVYT	168	92	1.8	0
222	AKGQPBEPQVYT	347	85	4.1	3
222	AJGQPREPQVYT	1923	94	20.5	5
223	KGQPREPQVYTL	76	71	1.1	0
223	KGQPBEPQVYTL	326	71	4.6	2
223	JGQPREPQVYTL	1128	70	16.2	4
224	GQPREPQVYTLPL	127	67	1.9	0
224	GQPBEPQVYTLPL	478	67	7.2	3
225	QPREPQVYTLPP	188	77	2.4	0
225	QPBEPQVYTLPP	458	77	5.9	3
226	PREPQVYTLPPS	150	106	1.4	0
226	PBEPQVYTLPPS	437	113	3.9	2
227	REPQVYTLPPSR	93	60	1.5	0
227	BEPQVYTLPPSB	1803	76	23.8	5
228	EPQVYTLPPSBD	274	77	3.5	2
228	EPQVYTLPPSRD	106	83	1.3	0
229	PQVYTLPPSRDE	183	114	1.6	1
229	PQVYTLPPSBDE	324	92	3.5	2
230	QVYTLPPSRDEL	267	248	1.1	1
230	QVYTLPPSBDEL	280	111	2.5	1
P01857-262	VEWESNGQPENNYKTT				5
P01857-262J	VEWESNGQPENNYJTT				4

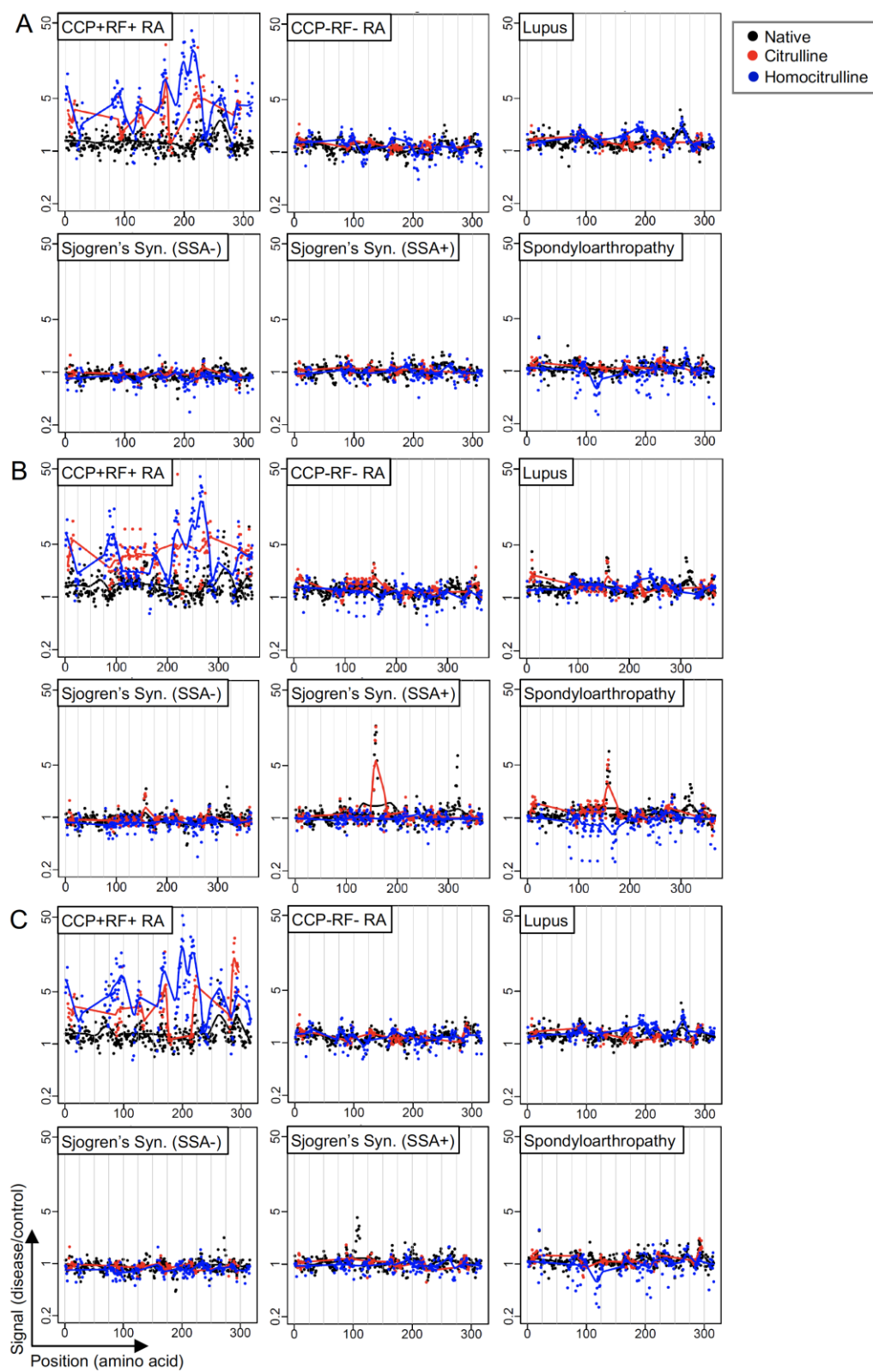
262	VEWESNGQPENN	372	109	3.4	1
263	EWESNGQPENNY	763	108	7.1	4
264	WESNGQPENNYK	816	174	4.7	4
264	WESNGQPENNYJ	986	209	4.7	4
265	ESNGQPENNYKT	513	122	4.2	3
265	ESNGQPENNYJT	419	101	4.2	3
266	SNGQPENNYKTT	683	213	3.2	3
266	SNGQPENNYJTT	642	118	5.5	3
	LYSKLTVDKSRWQQGNV				
P01857-289	FS				3
	LYSKLTVDKSBWQQGNV				
P01857-289B	FS				7
	LYSJLTVDJSRWQQGNV				
P01857-289J	FS				4
P01857-	LYSJLTVDJSBWQQGNV				
289BJ	FS				7 ***
289	LYSKLTVDKSRW	67	62	1.1	0
289	LYSKLTVDKSBW	223	72	3.1	1
289	LYSJLTVDJSRW	83	54	1.5	0
290	YSKLTVDKSRWQ	75	75	1.0	0
290	YSKLTVDKSBWQ	179	89	2.0	0
290	YSJLTVDJSRWQ	105	55	1.9	0
291	SKLTVDKSRWQQ	104	100	1.0	0

291	SKLTVDKSBWQQ	216	126	1.7	1
291	SJLTVDJSRWQQ	432	69	6.3	4
292	KLTVDKSRWQQG	164	107	1.5	0
292	KLTVDKSBWQQG	225	108	2.1	1
292	JLTVDJSRWQQG	826	83	9.9	4
293	LTVDKSRWQQGN	235	187	1.3	0
293	LTVDKSBWQQGN	1082	125	8.6	5
293	LTVDJSRWQQGN	433	102	4.2	3
294	TVDKSRWQQGNV	542	500	1.1	1
294	TVDKSBWQQGNV	1567	253	6.2	4
294	TVDJSRWQQGNV	1039	282	3.7	4
295	VDKSRWQQGNVF	618	603	1.0	1
295	VDKSBWQQGNVF	2079	496	4.2	5
295	VDJSRWQQGNVF	1635	530	3.1	4
296	DKSRWQQGNVFS	573	500	1.1	2
296	DKSBWQQGNVFS	1916	428	4.5	5
296	DJSRWQQGNVFS	1263	353	3.6	4
P01857-319	YTQKSLSLSPGK				0
P01857-319J	YTQJSLSLSPGJ				5
319	YTQKSLSLSPGK	142	126	1.1	0
319	YTQJSLSLSPGJ	1346	169	8.0	5

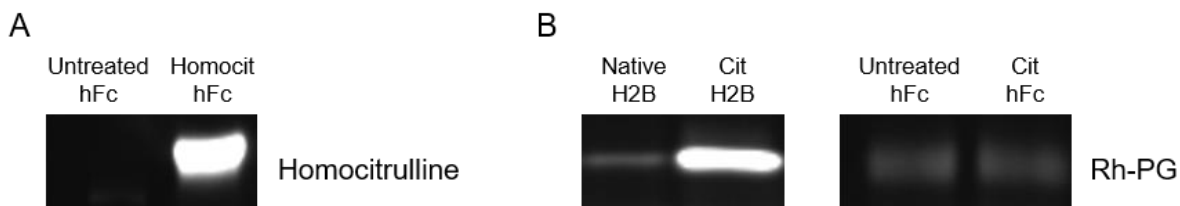
* Citrulline (B) and homocitrulline (J)

** A subject was considered positive if the signal value for the indicated peptide was greater than 3 standard deviations above the mean signal for the whole array. For ELISA peptides, the total positive subjects for any array peptide that was included in the ELISA peptide is listed.

*** Number of subjects with signal >3 standard deviations above the array mean for either citrulline or homocitrulline-containing peptides. The array does not contain peptides with both citrulline and homocitrulline.



Supplementary Figure 1. IgG binding to IgG-derived peptides in rheumatic diseases. IgG binding for each disease group (n=8 except n=16 for lupus) is graphed for each peptide according to its position in the constant region of IgG2 (A), IgG3 (B), and IgG4 (C).



Supplementary Figure 2. Detection of citrullination and homocitrullination of human IgG Fc. A. Human IgG Fc was treated with 0.1M KOCN in dH₂O or dH₂O alone. Then homocitrulline was detected using rabbit anti-homocitrulline IgG (Cayman Chemicals, Ann Arbor, USA) with goat anti-rabbit IgG conjugated to horse radish peroxidase (Invitrogen, Carlsbad, USA) as a detection antibody by western blot. B. Purified human IgG Fc or human recombinant histone H2B (New England Biolabs, Ipswich, UK) was treated at a ratio of 2 μ g of human PAD2 and PAD4 (Cayman Chemicals) per mg of protein in 100 mM Tris-HCl pH7.5, 1 mM DTT, and 5 mM CaCl₂ or exposed to buffer alone and then incubated with a citrulline-specific probe (rhodamine phenylglyoxal, Rh-PG, Cayman Chemicals) prior to SDS-PAGE with rhodamine detection at 365nm.

**Chapter 4: PAD2 is Required for a Normal Antibody Response to Influenza
Infection and Pathogenic Antibodies in Inflammatory Arthritis in Mice**

This manuscript was submitted to the *Journal of Immunology* (2021)

Funding for this work was provided by the U.S. Army Medical Research Acquisition Activity through the Peer Reviewed Medical Research Program [W81XWH-18-1-0717] to M.A.S.. Additional support was provided by the National Institutes of Health's National Heart, Lung, and Blood Institute [T32 HL007899] to A.M.M. and the National Institute of Allergy and Infectious Diseases [AI124299 and AI149793] to M.S..

PAD2 is Required for a Normal Antibody Response to Influenza Infection and
Pathogenic Antibodies in Inflammatory Arthritis in Mice

Aisha M Mergaert ^{1,2}, Michael F Denny ¹, Brock Kingstad-Bakke ³, Mandar Bawadekar ¹,
S. Janna Bashar ¹, Thomas F Warner ³, Marulasiddappa Suresh ³, and Miriam A Shelef^{1,4}

¹Department of Medicine, University of Wisconsin-Madison, Madison, WI, USA.

²Department of Pathology and Laboratory Medicine, University of Wisconsin-Madison,
Madison, WI, USA.

³Department of Pathobiological Sciences, University of Wisconsin-Madison, Madison, WI,
USA

⁴William S. Middleton Memorial Veterans Hospital, Madison, WI, USA.

AM contributed to the manuscript by performing all anti-collagen ELISAs in figure 1; preparation of tissue, performing and analyzing all flow cytometry analysis in figure 2; weekly scoring and paw thickness measurements, paw preparation for histology in figure 3; diluting virus for infection and daily measurement of survival in figure 4; performing all HI and anti-HA assays and daily monitoring of weight in figure 5 and 6; analyzing and assembling all data for the manuscript; making all of the figures, writing the original manuscript, reviewing and editing the final manuscript.

5.1 Abstract

The peptidylarginine deiminases (PADs) and the citrullinated proteins that they generate have key roles in innate immunity and rheumatoid arthritis, an inflammatory arthritis with antibodies that target citrullinated proteins. However, the importance of PADs, particularly PAD2, in adaptive immunity is newly emerging. In this study, we evaluated a requirement for PAD2 in collagen-induced arthritis (CIA), a T and B cell driven murine model of rheumatoid arthritis, and in the protective antibody response to murine influenza infection. Using PAD2^{-/-} and PAD2^{+/+} mice on the DBA/1J background, we found that PAD2 is required for maximal anti-collagen antibody levels, but not collagen-specific plasma cell numbers, T cell activation or polarization, or arthritis severity in CIA. However, using a new model of influenza infection for DBA/1J mice, we found that PAD2 is required not just for normal levels of persistent hemagglutination inhibiting antibodies, but also for full protection from lethal influenza rechallenge. Together these data provide evidence for a novel requirement for PAD2 in a normal anti-viral antibody response and in a pathogenic antibody response in inflammatory arthritis.

5.2 Introduction

The peptidylarginine deiminases (PADs) are essential components of normal and pathologic inflammation. They catalyze citrullination, the posttranslational modification of arginine to the nonstandard amino acid citrulline. PAD2 and PAD4 are expressed in hematopoietic cells [92, 104, 107], and many studies have evaluated their roles in innate immunity and inflammation. Most prominently, extensive evidence suggests that PAD4, more than PAD2, contributes to the normal formation of citrullinated neutrophil

extracellular traps [119, 120, 130], which have been implicated in a wide range of normal and pathologic immune responses [193]. More recent work demonstrates a requirement for the PADs in adaptive immune responses, and PAD2 appears to play a prominent role. It is required for production of IL-17A, but not IFN γ , by T cells from imiquimod-treated, but not untreated, mice [194] with a similar requirement for PAD2 in IL-17A production by *in vitro* differentiated Th17 cells [107]. PAD2 is also required to suppress IL-4 production by Th2-differentiated T cells, but has no effect on IFN γ production by Th1-differentiated cells [107].

PAD2 and PAD4 also appear to be important in rheumatoid arthritis, an autoimmune arthritis with autoantibodies that target citrullinated antigens [58]. PAD2 and PAD4 are present in the rheumatoid joint [106], have genetic variants associated with rheumatoid arthritis risk [111, 113, 117, 195], and are required for full arthritis severity in TNF-induced arthritis [120, 158], a murine model of innate inflammation in arthritis. Unlike in human rheumatoid arthritis, citrullinated antigens are not specifically targeted by antibodies in murine TNF-induced arthritis [158], suggesting that these two PADs provide distinct contributions to immune cell function in inflammatory arthritis. Although the exact mechanisms of these contributions are unclear, reductions in serum IgG levels and plasma cell numbers in PAD2-deficient mice with TNF-induced arthritis suggest involvement of lymphocytes [120].

Despite accumulating evidence for the importance of PAD2 for T and B cell function, a requirement for PAD2 has not been evaluated in an IL-17-driven [196] model of rheumatoid arthritis with pathogenic autoantibodies [197], such as collagen induced arthritis (CIA). Moreover, PAD2 has not been studied in a normal adaptive immune

response to a virus, such as the antibody-dependent response to influenza [198]. Such studies are important to fully define the implications of PAD inhibition, since PAD inhibitors have been proposed as therapeutic agents for the treatment of diseases in which citrullination is thought to be pathogenic, including rheumatoid arthritis, lupus, cardiovascular disease, thrombosis, multiple sclerosis, and cancer [199, 200].

In this manuscript, we evaluate the role of PAD2 in a pathogenic antibody response in a murine model of rheumatoid arthritis and in a protective antibody response using a murine model of influenza infection. We find that PAD2 is required for chronically elevated anti-collagen antibodies in CIA, but not for T cell activation or polarization, or arthritis severity. However, PAD2 is required for persistent levels of hemagglutination inhibiting antibodies and full protection from influenza in a novel DBA/1J-PR8-OVA model.

5.3 Results

To evaluate the role of PAD2 in a model of rheumatoid arthritis driven by T cells and pathogenic anti-collagen autoantibodies, we induced CIA in PAD2^{+/+} and PAD2^{-/-} mice on the DBA/1J background. Since IgG levels were reduced in the absence of PAD2 in TNF-induced arthritis [120], we first evaluated a requirement for PAD2 in anti-collagen IgG levels by ELISA. As shown in Figure 1A, anti-collagen IgG increased in all mice, but was reduced in PAD2^{-/-} as compared to PAD2^{+/+} mice, with a significantly lower level at 17 weeks post CIA induction. Next, we evaluated the number of anti-collagen IgG producing cells in the bone marrow at 17 weeks post CIA induction as measured by ELISpot and limiting dilution ELISA assay [201]. No difference in the number of anti-

collagen IgG producing cells could be detected between PAD2^{-/-} and PAD2^{+/+} mice (Figures 1B and C).

Given the role of PAD2 in IL-17 production, we next evaluated a requirement for PAD2 in the T cell compartment in CIA. PAD2^{-/-} and PAD2^{+/+} mice had similar numbers of CD3⁺ T cells in the spleen 17 weeks after the first CIA injection ($16.8 \times 10^6 \pm 11.7 \times 10^6$ and $16.9 \times 10^6 \pm 8 \times 10^6$, respectively). Moreover, there was no difference in the percent of CD3⁺ cells that were CD4⁺ or CD8⁺ (Figure 2A) or the frequencies of naïve, effector, or memory CD4⁺ or CD8⁺ T cells (Figure 2B-D). Finally, PAD2^{-/-} mice did not have altered frequencies of CD4⁺ cells that produced IL-17, IL-4, or IFN γ (Figure 2E and F).

Next, we evaluated arthritis severity in the absence of PAD2. Clinical scores and paw thickness were determined weekly for 12 weeks starting on the date of the final CIA injection. As shown in Figures 3A and 3B, PAD2^{-/-} mice did not have reduced arthritis compared to PAD2^{+/+} mice by either measurement. Additionally, paws were analyzed for histological differences and showed that synovitis, cartilage destruction, and ankylosis at 17 weeks post-initial injection were unaltered in the absence of PAD2 (Figure 3C, D). Taken together, these data suggest that PAD2 is required for persistently high levels of anti-collagen IgG in CIA, but not for the number of anti-collagen IgG secreting cells, T cell activation or polarization, or arthritis severity.

Given the reduction of anti-collagen IgG levels in PAD2-deficient mice with CIA as well as the importance of protective antibodies for immunity against influenza [198], we wanted to assess the role of PAD2 in antibody-based immunity to PR8, a mouse-adapted H1N1 influenza virus. However, we could find no reports of the use of PR8 in DBA/1J mice. Thus, we first established appropriate viral dosing in the DBA/1J strain. We infected

DBA/1J mice with a range of PFUs of PR8. As shown in Figure 4, even extremely low PR8 doses were highly lethal to DBA/1J mice. We then infected mice with 10 or 50 PFU of PR8-OVA, a modified PR8 virus that contains the SIINFEKL peptide of chicken ovalbumin in its neuraminidase stalk [202], based on our informal observations of reduced virulence. Only the very low dose of 10 PFU of PR8-OVA allowed for survival. Therefore, this dose was chosen for further experiments.

We next evaluated the requirement for PAD2 in a primary response to influenza infection. PAD2^{+/+} and PAD2^{-/-} mice were infected with 10 PFU of PR8-OVA and serum was collected prior to infection as well as 3 and 12 weeks after infection to quantify hemagglutination inhibiting antibodies by HI assay and anti-HA antibodies by ELISA. No hemagglutination inhibiting antibodies were detected in any mouse before exposure to PR8-OVA. As shown in Figure 5A, PAD2^{-/-} mice had equivalent HI titers at 3 weeks post-infection, but reduced titers compared to PAD2^{+/+} mice at 12 weeks post-infection. There was no corresponding reduction of anti-HA IgG, IgA, or IgM levels in PAD2^{-/-} mice at 12 weeks post-infection (Figure 5B). We also evaluated weight loss, a measure of influenza disease severity, in the PAD2^{+/+} and PAD2^{-/-} mice after infection and saw essentially no difference in weight loss between PAD2^{+/+} and PAD2^{-/-} mice (Figure 5C).

Given the reduced HI titers at 12 weeks post-infection with PR8-OVA and the importance of hemagglutination inhibiting antibodies for protective immunity against influenza [198], we next evaluated the role of PAD2 in a rechallenge influenza infection using a viral dose of PR8 lethal to naïve DBA/1J mice. Twelve weeks after initial infection with PR8-OVA, we rechallenged PAD2^{+/+} and PAD2^{-/-} mice with 3,000 PFU of PR8 and performed the same assays as above. We found that PAD2^{-/-} mice had reduced HI titers

compared to PAD2^{+/+} mice two weeks after challenge, with a corresponding reduction in anti-HA IgM levels (Figure 6A and 6B). Moreover, PAD2^{-/-} mice had twice as much weight loss and required three times longer to return to their starting weight than PAD2^{+/+} mice after the lethal rechallenge (Figure 6C). Taken together, these data suggest that PAD2 is required for normal antibody titers and full protection from influenza reinfection in DBA/1J mice.

5.4 Discussion

In this manuscript, we demonstrate a novel role for PAD2 in persistent anti-collagen antibody levels in a murine model of rheumatoid arthritis, as well as a requirement for PAD2 for normal levels of hemagglutination inhibiting antibodies and full protection from influenza using a newly established model of influenza infection in DBA/1J mice.

In response to growing evidence of the importance of PAD2 for B and T lineage cells, this study is the first to evaluate the role of PAD2 in CIA. A pan-PAD inhibitor was shown to reduce CIA severity [203], but this may have been due to inhibition of multiple PADs or potentially just PAD4, which is required for full arthritis severity in this model [160]. In this manuscript, we show that PAD2 is not required for arthritis severity in CIA (Figure 3). In contrast, we previously identified a requirement for PAD2 in TNF-induced arthritis severity [120]. Thus, PAD2 may be important in the innate immune cells thought to be the predominant drivers of TNF-induced arthritis, with a less critical role in the adaptive immune processes in CIA. Although not required for neutrophil extracellular trap formation [120, 130], PAD2 is required for optimal inflammasome assembly and IL-1 β

release by macrophages [204]. Since TNF can drive IL-1 β secretion via the NLRP3 inflammasome [205], the role of PAD2 in TNF-induced arthritis may be macrophage-dependent. We did observe a reduction of anti-collagen antibodies (Figure 1A), which are known to be able to drive arthritis [197], but the ~35% reduction of anti-collagen antibodies late in disease in PAD2^{-/-} mice may have been insufficient to reduce arthritis severity in a detectable manner in CIA, a model with notoriously high variability.

Additionally, PAD2 was seemingly dispensable in the T cell compartment at 17 weeks post-induction of CIA (Figure 2). The absence of a requirement for PAD2 in Th17 cells in CIA may have contributed to the lack of a detectable reduction in arthritis in PAD2-deficient mice. In contrast, previous studies demonstrated a requirement for PAD2 in Th17 cells [107, 194], a T cell subset important in CIA [196, 206, 207]. The reason for the discrepant findings is unknown. Perhaps PAD2 is only required in some contexts for Th17 polarization and IL-17 production, such as in the imiquimod-mediated model of lupus [194] or in *in vitro* differentiated Th17 cells [107], but not in Th17 cells in CIA. In CIA, the multiple injections of collagen plus adjuvant might overcome mild defects in Th17 cells due to loss of PAD2. Timing may also be a factor. We examined T cell responses about four months after CIA induction, while other studies evaluated Th17 cells earlier in disease [206, 208, 209]. However, even if Th17 responses were altered in PAD2^{-/-} mice earlier in CIA, there was no effect on arthritis severity.

In contrast to the lack of a detectable role for PAD2 in Th17 cells in CIA, PAD2 was required for persistent anti-collagen antibody levels (Figure 1A). This finding is consistent with reduced antibodies in PAD2-deficient mice with TNF-induced arthritis [120]. Curiously, numbers of anti-collagen IgG secreting cells were unaltered in PAD2^{-/-}

mice, suggesting either low sensitivity of the assays that quantify these cells, or that the reduced anti-collagen IgG resulted from other mechanisms such as lower IgG production in each cell or an alteration of IgG half-life in PAD2^{-/-} mice.

We also found that PAD2 was required for robust levels of hemagglutination inhibiting antibodies in response to influenza infection (Figure 5, 6). The reduction in HI titers did not always correspond with a reduction in total levels of anti-HA Ig (Figure 5). While both tests measure anti-viral antibodies, the HI assay quantifies functional antibodies, which typically correlate with protective immunity, while the anti-HA ELISA measures total antibody levels, irrespective of functional capacity. Thus, the differences seen between the two assays could reflect inherent caveats in assay sensitivities or a decrease in the relative amount of functional antibodies within the total anti-HA antibody repertoire [210, 211]. However, two weeks after the lethal challenge infection, anti-HA IgM levels were reduced in PAD2-deficient mice. Although IgG is typically considered the Ig isotype of long-lived plasma cells conferring protection from re-infection, influenza-specific neutralizing IgM antibodies can persist for 18 months and protect mice from influenza-mediated death [212, 213].

Consistent with reduced HI titers in PAD2^{-/-} mice, protection from influenza virus induced weight loss was reduced in the absence of PAD2, a novel role for PAD2 or any PAD. PAD4-deficient mice had no increase in weight loss compared to wild type mice after primary infection with influenza A/WSN/33/H1N1, but rechallenge infection was not evaluated [214]. Further studies to determine the mechanism by which PAD2 regulates protection from influenza are needed in a genetic background for which there are more immunological tools, such as C57BL/6 mice. Nonetheless, our study provides the first

evidence that PAD2 could be a therapeutic avenue to pursue to improve antibody responses to viral infection. Our work also highlights a potential area of concern for PAD inhibition as a treatment for disease.

Of note, in order to demonstrate a role for PAD2 in influenza, we developed a model for influenza A infection in DBA/1J mice (Figure 4). We showed that PR8, even at exceedingly low doses, is lethal to DBA/1J mice (Figure 4A), but PR8-OVA, which appears to have attenuated virulence, is sublethal at a very low dose (Figure 4B). Consistent with these findings, mice of a related strain, DBA/2J, are highly susceptible to influenza [215-218], and DBA/1J mice are more susceptible than BALB/c mice to a H3N2 influenza virus strain [219]. Notably, non-lethal PR8 infection is often studied in C57BL/6 and BALB/c mice [220]. The cause of increased susceptibility of DBA mice to influenza infection is not known, but is likely related to a multiple genetic factors known to be important in an anti-influenza immune response, including MHC haplotypes [221, 222]. Our DBA/1J-PR8-OVA model may help future studies to solve this mystery.

In conclusion, we demonstrate a novel requirement for PAD2 in the abnormal anti-collagen antibody response in CIA and in the normal antibody response to influenza. Future investigation is needed to define the mechanisms behind this requirement and to utilize these findings to improve human health.

5.5 Methods

Mice

PAD2^{-/-} mice [223] backcrossed to the DBA/1J background [130] and age- and sex-matched DBA/1J PAD2^{+/+} controls were used for all experiments. Mice of both

genotypes were co-housed whenever possible and when not, bedding was mixed for CIA experiments. Absence of PAD2 was confirmed in several PAD2^{-/-} mice by western blot of bone marrow lysates. Mice were maintained in specific-pathogen-free conditions and experiments were approved by the University of Wisconsin Animal Care and Use Committee.

Collagen Induced Arthritis Induction

Arthritis was induced in 7-8 week old mice by intradermal tail injection of 50-100 μ l of an emulsion of equal parts 1mg/ml chick type II collagen (Chondrex, Redmond, USA) and complete Freund's adjuvant (CFA, BD, Franklin Lakes, USA) followed by intraperitoneal injection of 100 μ l of an emulsion of equal parts 1mg/ml chick type II collagen with incomplete Freund's adjuvant (IFA, BD) 21 and 42 days after the initial injection. After initial injection, mice were fed a high fat diet (2019 diet, Teklad, Madison, USA).

Influenza Infection

To determine optimum infection conditions, mice were infected intranasally with 100, 33, 10 or 3 plaque forming units (PFU) of A/PR/8/34 H1N1 [224] or 50 or 10 PFU of A/PR/8/34 H1N1-OT-I (PR8-OVA) [202, 224] in PBS. Influenza virus was prepared in the laboratory of Professor Yoshihiro Kawaoka (University of Wisconsin-Madison). For PAD2^{-/-} experiments, 8-9 week old mice were infected with 10 PFU of PR8-OVA in 50 μ l of PBS. After 3 months, mice were infected with 3,000 PFU of PR8 in 50 μ l of PBS. Mice were

weighed daily and monitored for health for 14 days after each infection. Mice with severe disease defined by 20%-30% weight loss were euthanized.

Enzyme Linked Immunosorbent Assay (ELISA)

Flat bottom high bind 96-well plates (Corning, Tewksbury, USA) were incubated with 40 ng/ml PR8 hemagglutinin (HA, BEI Resources, Manassas, USA) in PBS or with bovine collagen (Chondrex) at 10µg/ml in 50mM carbonate-bicarbonate buffer overnight at 4°C. Wells were washed with wash buffer (0.1% Tween 20 in PBS) followed by blocking with 5% nonfat dried milk with 2% fetal bovine serum (FBS, Atlanta Biologicals, Flowery Branch, USA) in wash buffer (HA block) or with 1% BSA in wash buffer (collagen block) for 2 hours at room temperature (RT). For collagen ELISA, serum was applied to the plate at a 1:10,000 dilution in collagen block and incubated at 4°C overnight, followed by washing, then application of a 1:5000 dilution of goat anti-mouse IgG Fc conjugated to horseradish peroxidase (HRP, Southern Biotech, Birmingham, USA). For HA ELISA, serum was applied to the plate at 1:1000 (Anti-IgG ELISA) or 1:200 (anti-IgM and IgA) dilutions in HA block and incubated at RT for 1 hour. Then, plates were washed, followed by incubation for 1 hour at RT with dilutions of 1:10,000 goat anti-mouse IgG Fc-HRP (Southern Biotech), 1:5000 goat anti-mouse IgM-HRP (Southern Biotech), or 1:1000 goat anti-mouse IgA Fc-HRP (LSBio, Seattle, USA) in PBS. All plates were then washed, developed with Slow-TMB ELISA solution (ThermoFisher, Waltham, USA), stopped with 0.2M H₂SO₄, and read using a Synergy 2 plate reader (BioTek, Winooski, USA) plate reader equipped with Gen5.0 software or a FilterMAX F3 equipped with SoftMax Pro

software (Molecular Devices, San Jose, USA). The 540 nm signal was subtracted from the 450 nm signal and values for blank wells were subtracted.

To standardize anti-collagen ELISAs, a standard curve was performed on each plate using serially diluted (from 1:1000 to 1:1024000) CIA reference serum (Hooke Labs, Lawrence, USA). The standard curve was used to convert experimental sample absorbance values into a relative value compared to the CIA reference.

For HA ELISA, absorbance values were converted to ng/ml of Ig using a standard curve. Each plate included a standard curve, which was generated by coating wells with streptavidin, followed by 5 ug/ml biotin conjugated goat anti-mouse IgG (Mabtech, Nacka Strand, Sweden), rabbit anti-mouse IgM (Mabtech) or rat anti-mouse IgA (Biolegend, San Diego, USA). Serial dilutions of purified mouse IgG (Jackson ImmunoResearch, West Grove, USA) or IgM (Millipore, Burlington, USA) ranging from 0.0169 to 1000 ng/ml or IgA (Invitrogen, Carlsbad, USA) ranging from 0.0085 to 500ng/ml were applied to appropriate wells followed by the same steps as above. After correcting for background, absorbance values for mouse sera were converted to ng/ml of Ig using a four parameter nonlinear curve fit for the standard curve wells. (elisaanalysis.com).

Enzyme-Linked Immune Absorbent Spot (ELISpot)

Bone marrow cells were flushed from mouse femurs under aseptic conditions with sterile PBS, dispersed by several passages through a 21 gauge needle, and strained through a 100 micron nylon mesh filter, followed by immersion in 0.8% NH₄Cl red blood cell lysis solution (Stemcell Technologies, Vancouver, Canada). Cells were resuspended in B cell media (RPMI 1260 with 10% FBS, 50 µM beta-mercaptoethanol, L-glutamine,

streptomycin, and penicillin). PVDF filter plates were prepared per manufacturer's instructions (Millipore). Wells were incubated overnight at 4°C with 10ug/ml bovine type II collagen, washed with PBS, and blocked with RPMI 1640 (Thermo Fisher Scientific) with 2% FBS, penicillin, streptomycin, and 50uM beta-mercaptoethanol at 37°C for 2 hours. Bone marrow cells in B cell media were applied in triplicate to wells and incubated overnight in a humidified incubator at 37°C with 5% CO₂. Plate membranes were then washed with PBS, then with wash buffer, then incubated with 0.5 ug/ml biotinylated goat anti-mouse IgG (Mabtech) in PBS with 1% BSA and 0.2% Tween 20 (ELISpot wash) for 2 hours at RT or overnight at 4°C, washed with wash buffer, incubated with avidin-HRP at 1:10,000 in wash buffer for 1 hour at RT, washed twice and developed with fresh 2 mg/ml aminoethylcarbazole in acetate solution for up to 20 minutes, neutralized with tap water, and left to dry. Spots were counted by eye in a blinded manner.

Limiting-Dilution Assay (LDA)

Bone marrow cell suspensions of 2.5 ml each at densities of 2.0×10^6 , 1.33×10^6 , 0.5×10^6 , and 0.2×10^6 cells/ml in B cell media were prepared from the femurs of each mouse. A round bottom 96-well tissue culture plate was filled by aseptically transferring 0.1 ml of each suspension density into a total of 24 wells. The plates containing the bone marrow cells in culture were incubated for 20 hours at 37°C in a humidified 10% CO₂ tissue culture incubator, with each plate corresponding to one mouse sample. To detect wells containing collagen-specific antibody secreting cells, a corresponding 96-well collagen ELISA plate was prepared. RIA/EIA binding plates (Corning) were coated overnight at 4°C with 10 µg/ml chick collagen type II in 50mM carbonate-bicarbonate

buffer (pH>8.0). ELISA wells were washed and blocked for 2 hours at RT with collagen block. The blocking buffer was removed, and 85µl of the conditioned B cell media from the overnight incubation of bone marrow cells was directly transferred into the corresponding well of the collagen ELISA plate. The collagen ELISA plates were incubated and developed as described above for the anti-collagen ELISA, except the collagen standard curve for relative titer determination was omitted. In non-immunized DBA1/J mice, a background subtracted OD450 of 0.03 is approximately 9 standard deviations above mean background absorbance for negative wells. The frequency of anti-collagen type II antibody secreting cells at each cell density was calculated based upon the Poisson distribution of limiting dilution analysis. The number of antibody secreting cells was calculated for each cell density using the equation $m = -\ln(F_0)$, where m is the number of antibody secreting cells and F_0 is the fraction of wells that are negative for anti-collagen reactivity. A linear regression was applied to the graph of anti-collagen IgG producing bone marrow cell number versus plated bone marrow cell density, and the frequency of antibody secreting cells calculated by solving for the cell density at the point where $\ln(F_0)=-0.368$,

Flow Cytometry

Splenocytes were resuspended in a buffer of 1% BSA, 2% FBS, 0.03% sodium azide and 2 mM EDTA in PBS for staining with CD8b-Alexa Fluor 488 (H35-17.2, Invitrogen), CD4-PE-CF594 (RM4-5, BD), CD62L-PE-Cy7 (MEL-14, Tonbo Biosciences, San Diego, USA), CD44-Brilliant Violet 421 (IM7, Biolegend), CD3e-APC (145-2C11, Biolegend), and/or ghost dye (Red 780, Tonbo Biosciences) and were fixed in 2% PFA in

PBS after staining. Helper T cell characterization was performed using a mouse Th1/Th2/Th17 Phenotyping Kit (BD Biosciences, San Jose, USA) per manufacturer's instructions. Samples were acquired using a LSRII machine and data was analyzed using FlowJo software (BD Biosciences).

Arthritis Scoring

Paws were scored weekly by A.M.M. in a blinded manner for range of motion (normal 0, reduced in digits 1, reduced in wrist/ankle or more 2), usage (normal 0, abnormal weight bearing or loss of grip strength 1, non-use 2), swelling (none 0, any digit 1, paw 2, wrist/ankle 3, entire limb 4), erythema (none 0, slight 1, extreme 2). Each limb was scored according to each parameter and scores for all limbs averaged for each mouse to create a final score. Paw thickness was measured with a digital caliper (SPI, Melville, USA) weekly with measurements of all paws averaged for a final measurement.

Histology

Front paws were fixed and decalcified in Decalcifier I (Leica, Buffalo Grove, USA), embedded in paraffin, sectioned, and stained with hematoxylin and eosin. Carpal, carpometacarpal, metacarpophalangeal, and interphalangeal joints were scored on a scale of 0 to 8 by T.F.W. in a blinded manner for each of the following characteristics: pannus with synovitis, cartilage destruction, and ankylosis. Scores were averaged for each mouse.

Hemagglutinin Inhibition (HI) Assay

Sera were treated with receptor destroying enzyme II (Denka Seiken, Tokyo, Japan) per manufacturer's instructions, then mixed with 4 HA units of PR8 virus in a round bottom 96 well plate (Corning). After a 30 minute incubation at 37°C, 0.5% chicken red blood cells (Lampire Biological Laboratories, Pipersville, USA) in PBS were added and mixed. Assay was incubated for a minimum of 30 minutes at RT. The lowest titer at which hemagglutination of red blood cells occurred was recorded.

Statistics

A paired t-test was used for all analyses with $p < 0.05$ considered significant.

5.6 Figures

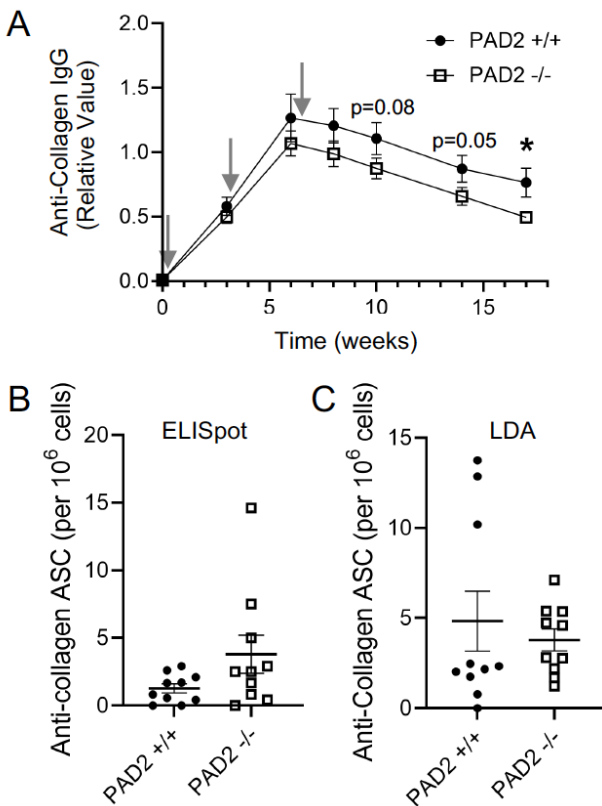


Figure 1. In collagen-induced arthritis (CIA), PAD2 is required for normal anti-collagen IgG levels, but not numbers of anti-collagen antibody secreting cells. CIA was induced in PAD2^{+/+} and PAD2^{-/-} mice on the DBA/1J background with the first injection at week zero. A. Sera were collected at indicated time points post-CIA induction and anti-collagen IgG levels quantified by ELISA and expressed as a value relative to a CIA serum standard (mean \pm SEM, n=23 mice, 6 experiments). Gray arrows indicate CIA-inducing injections. Bone marrow derived anti-collagen IgG antibody secreting cells (ASCs) were quantified by (B) *ELISpot* and (C) anti-collagen ELISA limiting dilution assay (LDA) 17 weeks post-CIA induction (symbols indicate ASC numbers in individual mice, horizontal bar indicates mean \pm SEM, n=10 mice, 3 experiments). For all panels, PAD2^{+/+} versus PAD2^{-/-} data were compared by paired t test and *p<0.05.

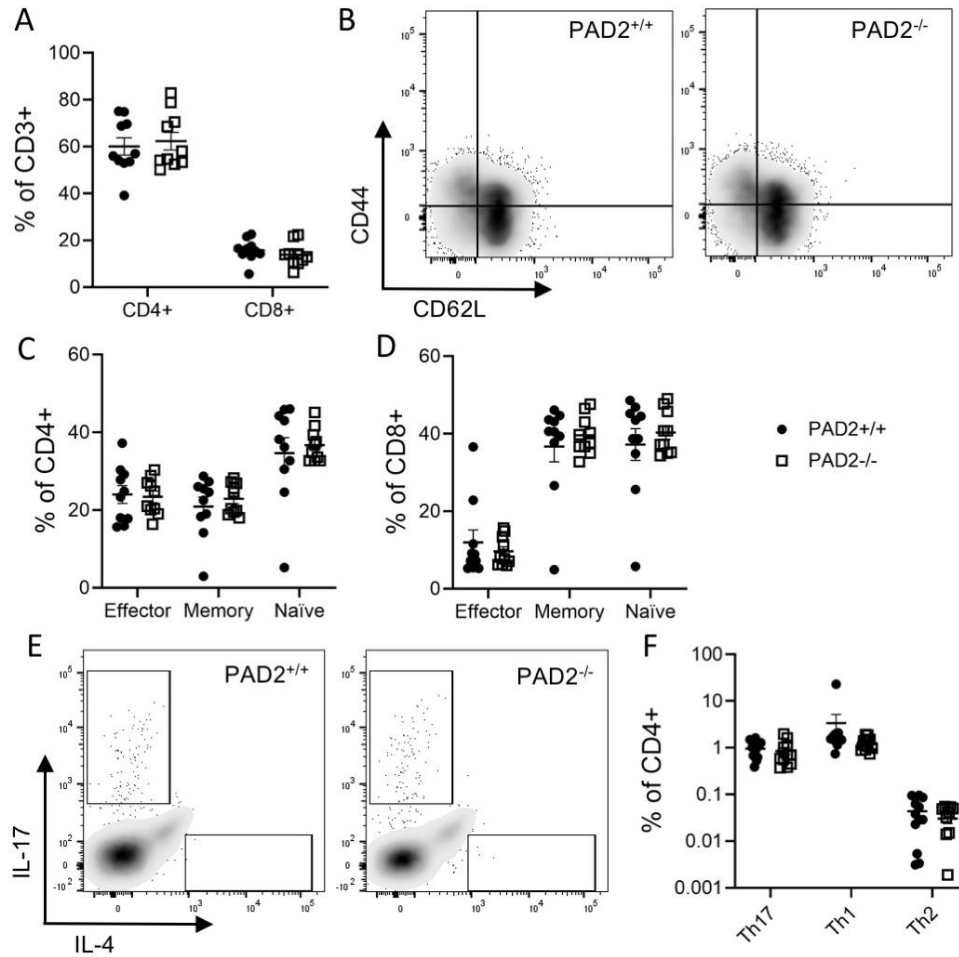


Figure 2. T cells in CIA are unaffected by loss of PAD2. Seventeen weeks after the first injection to induce CIA, splenocytes were harvested and stained for flow cytometry. Debris, clustered cells, and dead cells were excluded using forward scatter, side scatter, and a viability dye. A. Percent of CD3⁺ splenocytes that are CD4⁺ and CD8⁺ (n=10 mice, 3 experiments). Activation status of these CD3⁺ cells was evaluated with (B) representative plots as well as mean percent \pm SEM of (C) CD4⁺ and (D) CD8⁺ populations that are effector (CD62L⁻CD44⁺), memory (CD62L⁺CD44⁺), and naïve (CD62L⁺CD44⁻) shown. The percent of CD4⁺ cells that produce IL-17A, IL-4, and IFN γ were also quantified with (E) representative plots and (F) mean percent \pm SEM graphed

(n=12 mice, 3 experiments). For all panels, PAD2^{+/+} versus PAD2^{-/-} data were compared by paired t test and no comparisons were significant.

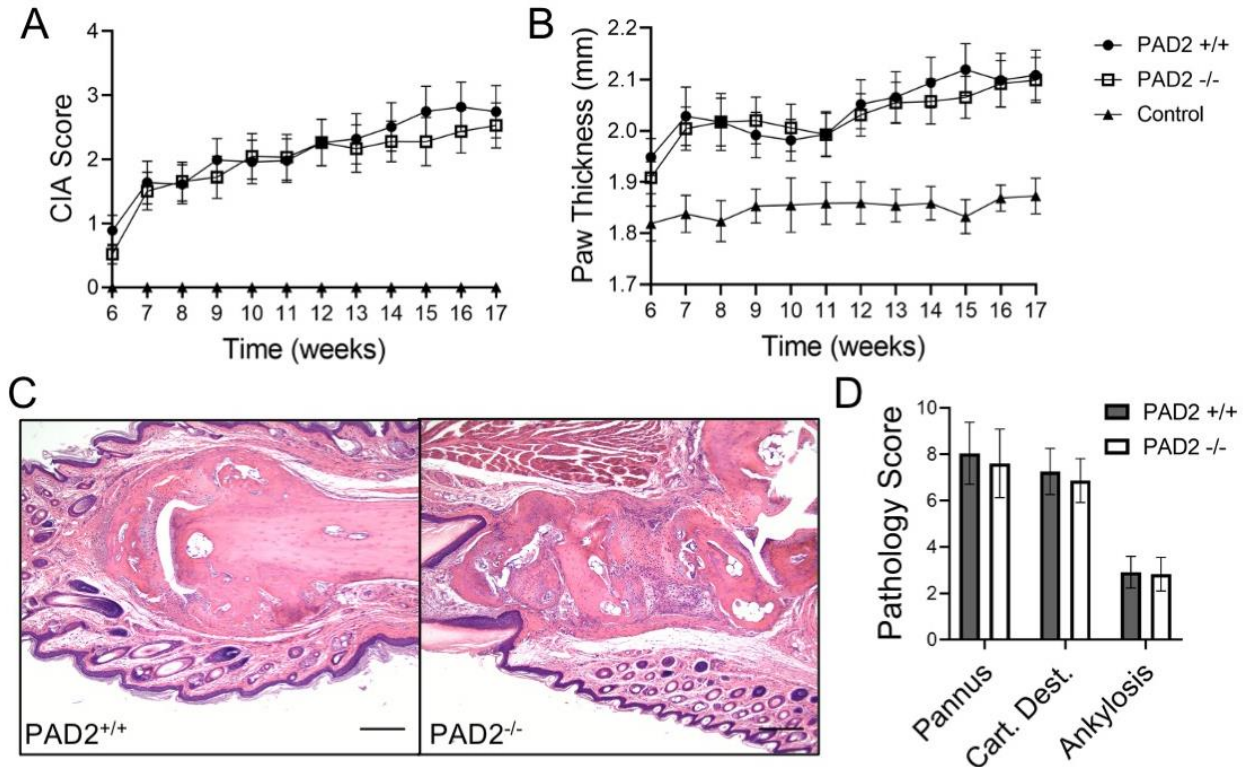


Figure 3. Arthritis severity in collagen-induced arthritis (CIA) is unaltered in the absence of PAD2. Six weeks after the first injection to induce CIA, (A) clinical scores and (B) paw thickness were assessed weekly (n=23 mice, 6 experiments). Controls (n=9), which received no injections and were co-housed with experimental mice, were also evaluated. At 17 weeks after the first injection, the front paws were fixed, embedded, sectioned, and stained with hematoxylin and eosin. C. Representative images at 100x. Bar indicates 200 microns. D. The extent of pannus development, cartilage destruction, and ankylosis were scored in a blinded manner (n=23 mice, 6 experiments). All graphs depict mean \pm SEM. PAD2^{+/+} versus PAD2^{-/-} data were compared by paired t test and no comparisons were significant.

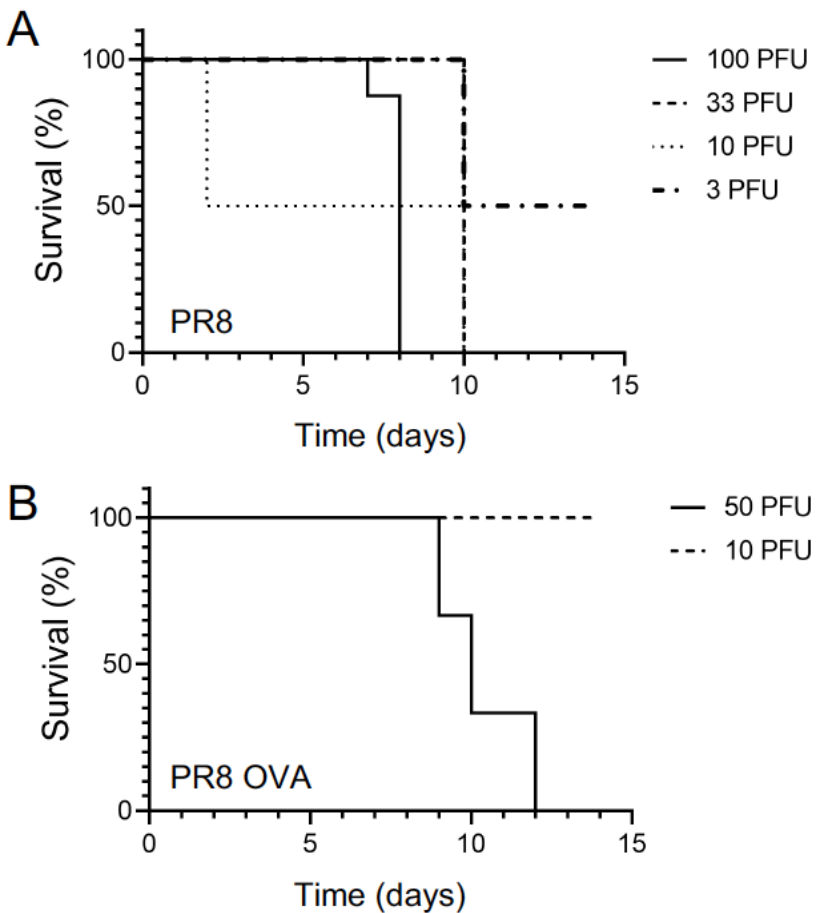


Figure 4. DBA/1J mice are highly susceptible to influenza infection. Mice were infected with different doses of PR8 or PR8-OVA followed by daily health monitoring. Kaplan–Meier curves depict survival of DBA/1J mice after (A) PR8 infection (100 PFU n = 8, 33.3 PFU n=2, 10 PFU n=2, 3 PFU n=2) or (B) PR8-OVA infection (50 PFU n=3, 10 PFU n=2).

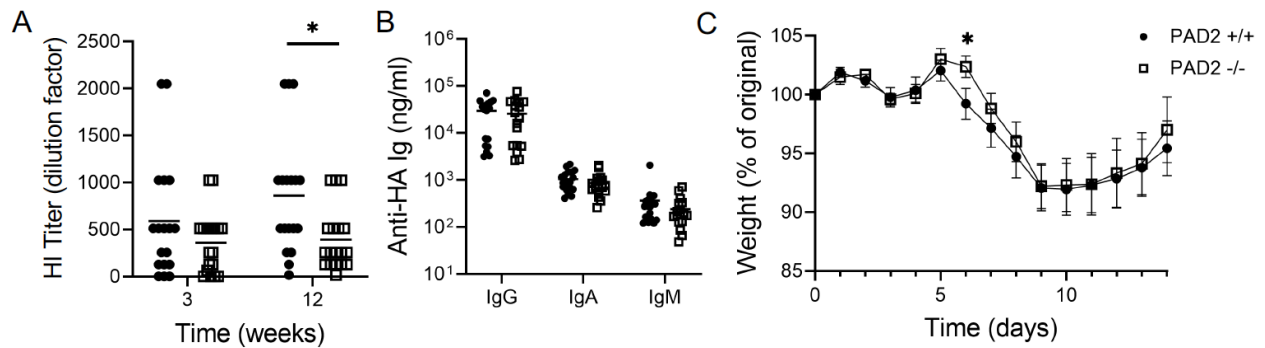


Figure 5. PAD2 is required for hemagglutination inhibiting antibody titers in DBA/1J mice after influenza infection. PAD2^{+/+} and PAD2^{-/-} mice on the DBA/1J background were infected with PR8-OVA. A. Sera were collected at the indicated time points and used in a hemagglutination inhibition (HI) assay (n=18, 5 experiments). B. Sera at 12 weeks post-infection were used to detect anti-hemagglutinin (HA) IgG, IgM and IgA by ELISA (n=17-18). C. Body weights were obtained daily for 14 days post-infection and reported as percent of weight on the day of infection (n=18, 5 experiments). For all panels, PAD2^{+/+} versus PAD2^{-/-} data were compared by paired t test, graphs depict mean ± SEM, and *p<0.05.

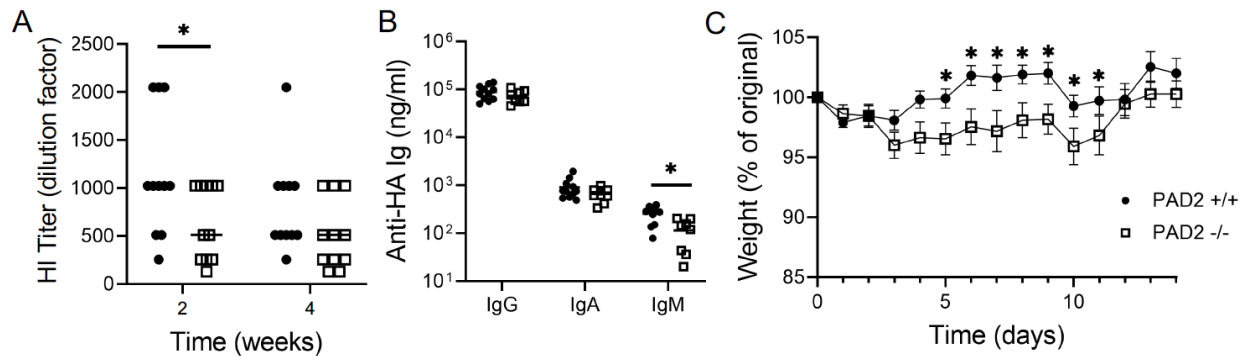


Figure 6. PAD2 is required for normal protection from influenza infection. $PAD2^{+/+}$ and $PAD2^{-/-}$ mice on the DBA/1J background were infected with PR8-OVA, followed by lethal challenge 12 weeks later with PR8. A. Sera were collected at the indicated time points and used in a hemagglutination inhibition (HI) assay ($n=11$, 3 experiments). B. Sera from two weeks post-challenge were used to detect anti-hemagglutinin (HA) IgG, IgM and IgA by ELISA ($n=9-11$). C. Body weights were obtained daily for 14 days post-challenge infection and reported as percent of weight on the day of challenge infection ($n=11$, 3 experiments). For all panels, $PAD2^{+/+}$ versus $PAD2^{-/-}$ data were compared by paired t test, graphs depict mean \pm SEM, and * $p<0.05$.

Chapter 5: Conclusions and Future Directions

In conclusion, the above work demonstrates the role of citrullination and the PAD enzymes for antibodies in both normal immunity and autoimmune disease (Figure 1). My work shows that citrullinating enzymes influence the production of antibodies in RA patients and in two mouse models. Additionally, I show that antibodies in anti-CCP+ RF+ RA patients bind post-translationally modified epitopes of IgG and thus are a possible linchpin in RA development, potentially joining some AMPAs and RFs in a unified mechanism for loss of tolerance to self-proteins (reviewed in [187]).

First, I described how a SNP in *PADI4* (rs2240335) influences RA risk, NET levels and autoantibodies in RA. Early ACPAs often target histones [39]. NETs, which contain histones, are a proposed source of autoantigens in RA [118, 129] and PAD4 is required for citrullinated NETs [130]. Therefore, I investigated the possible connection between NET formation and autoantibody production to histones associated with rs2240335. I find that allele G at SNP rs2240335 is associated with RA risk in our North American cohort but is not associated with different levels of NETs in controls, as measured by two methods. Interestingly, I find that the G allele is not associated with anti-histone antibodies in CCP+ subjects but is correlated with reduced anti-histone antibodies to both native and citrullinated histones in CCP- subjects. The mechanisms of this finding are unknown, but further study of the role of rs2240335 in our population could provide a mechanism.

To investigate the mechanism responsible for reduced autoantibodies associated with rs2240335 in our cohort, a series of experiments could be conducted. First, the citrullination status of NETs produced by homozygotes in our cohort should be evaluated

using F95 and DAPI immunofluorescent staining, as previously described [130]. This would identify if rs2240335 affects the ability of PAD4 to produce citrullinated NETs. Also, previous literature demonstrated a correlation between the G allele and decreased PAD4 levels in neutrophils and increased PAD4 levels in monocytes, both of which make extracellular traps [124, 147, 225]. It is possible that our findings are mediated through increased PAD4 expression in monocytes rather than neutrophils, so the frequency of monocyte extracellular traps could also be investigated. Also, the levels of PAD4 mRNA in neutrophils and monocytes isolated from our subjects who are homozygous for the G or T alleles should be assessed using qPCR. Last, synonymous SNPs can affect mRNA stability and thus protein production and enzymic activity [226]. Therefore, mRNA stability in neutrophils of homozygotes could be assessed. To do this, cells would be cultured with a transcription inhibitor, such as Actinomycin D, and PAD4 mRNA levels would be assessed over time between homozygotes [111, 227].

Second, I showed that reactivities of rheumatoid factors and anti-modified protein antibodies converge on IgG epitopes. Using a high-density peptide array and ELISA, I showed that CCP+ RF+ RA subjects have increased binding to citrulline and homocitrulline containing epitopes of IgG and that monoclonal ACPAs bind these epitopes and modified IgG Fc. This study demonstrates for the first time that ACPAs can act as RF by binding to the Fc region of IgG. RA patients frequently have antibodies to modified protein and IgG Fc. Tolerance against modified, in particular citrullinated, proteins is likely due to shared epitope containing HLA alleles, but nothing is known about how a break in tolerance might occur against IgG to generate IgG-RF. One mechanism that has been proposed that would unify how tolerance is lost leading to these two types

of autoantibodies is IgG as a common antigen [187, 228]. The mechanism proposed is that modified peptides derived from IgG are presented by RF+ B cells to T cells via the shared epitope, which preferentially binds citrulline. The activated T cell is then able to provide help to a citrullinated IgG-binding B cell. This in turn could potentially give rise to an IgG antibody that is both a RF and an ACPA simultaneously (reviewed in [187]). Through epitope spreading, the initial loss of tolerance to modified IgG could possibly build the broader ACPA and RF repertoires.

The next step to evaluate the common antigen model of RA is to further investigate RF in human subjects. Purification of RF using Fc conjugated magnetic beads should be performed, and the resulting RF should be evaluated in ELISA for binding to native, citrullinated or homocitrullinated IgG peptides to determine if RF binds modified epitopes like monoclonal ACPAs bind IgG epitopes. Additionally, mapping of the precise locations of endogenous citrulline and homocitrulline in IgG is necessary to determine existent epitopes that could drive disease. Mass spectrometry of IgG isolated from humans is currently under investigation in the lab; however, the small mass shift of citrulline compared to arginine, and other technological issues, has proved a challenge for accurate detection of all citrulline residues so far [229]. Lastly, antibodies to both citrullinated and homocitrullinated IgG epitopes in pre-clinical RA should also be measured. Before arthritis onset, patients develop autoantibodies in a period of pre-clinical RA [28, 230], but not all people with autoantibodies develop RA [28]. Epitope spreading is well described in RA, and it has been demonstrated that initial loss of tolerance is narrowly focused and spreads with time [39]. If IgG is an initiating antigen and not a late target of ACPAs, we would detect autoantibodies to modified IgG before

other ACPAs. These anti-modified IgG antibodies could be developed into an early diagnostic tool to be used in conjunction with CCP to diagnose pre-clinical RA. Also, this study would reveal which epitopes are targeted in pre-clinical RA and would be the next step in understanding how a break in tolerance occurs and thus also possibly how to intervene in at risk individuals.

Last, I showed that PAD2 is required for antibodies in inflammatory arthritis and for a normal antibody response to influenza infection in mice. PAD2 is necessary for antibody levels, plasma cell numbers and arthritis severity in a TNF α driven form of inflammatory arthritis [120]. I investigated if this phenotype translates to an arthritis model with pathogenic autoantibodies and found that although PAD2 is not required for arthritis severity, ASCs or T cells, it is required for autoantibody levels. Next, I evaluated the role of PAD2 in a normal immune response to influenza and found that PAD2 is also required for hemagglutinin inhibition (HI) antibody titers, anti-HA IgM levels and normal weight recovery post lethal challenge. PAD2 has not previously been described in immunity to influenza, and these results indicate a novel role for PAD2 in protection from influenza, which could have implications for anti-viral therapeutics or vaccination strategies.

To further investigate our above CIA findings, additional experiments could be performed. First, although there was no observed effect from the loss of PAD2 on ASC number, the total amount of antibody secreted from those cells could vary from cell to cell. So direct measurement of antibody secretion per ASC is necessary. To do this, bone marrow and spleen plasma cells would be isolated using CD138 positivity and cultured on a stromal cell layer in media supplemented with APRIL [231] and total IgG measured in the supernatant via ELISA. Alternatively, the effect of PAD2 on anti-collagen antibodies

specifically could be determined by simultaneously performing ASC culture followed by anti-collagen ELISA and anti-collagen ELISpot. This would allow for the quantification of both the number of anti-collagen ASCs and the amount of antibody they produce. Next, as Th17 cells are critical for CIA and PAD2 is known to affect T cell polarization [107, 194], Th17 polarization should be assessed by flow cytometry near to arthritis onset as the role of Th17 in CIA is often investigated at the time of arthritis onset [206, 208, 209]. Our finding that PAD2 does not affect helper T cell polarization in CIA is possibly due to assessing this population after arthritis has fully manifested and Th17 cells are no longer critical. This work is important because PAD inhibitors are in development as an RA treatment and understanding the role of PAD2 within a translatable mouse model can give researchers guidance on human therapy [199].

Additionally, the finding that PAD2 is required for antibodies and protection in an influenza model warrants further investigation. First, it should be determined if the inability for PAD2^{-/-} mice to recover quickly post lethal challenge is the result of deficient antibody function. To do this, a serum transfer should be performed by transferring serum from PAD2^{+/+} and PAD2^{-/-} mice after non-lethal PR8-OVA infection to naïve mice and challenging them with a lethal dose of PR8 [198, 232]. A significant difference between mice that received PAD2^{+/+} and those that received PAD2^{-/-} serum would indicate that the antibodies are mediating the PAD2 dependent effect on protection. Furthermore, examination of the effect of PAD2 on the PR8 neutralizing antibody repertoire could be assessed using a plaque reduction neutralization test [233]. Determination of isotypes affected by the loss of PAD2 in these assays could also be assessed by selectively depleting isotypes from the serum, i.e., assess IgG neutralization in a plaque assay by

depleting IgA and IgM. Understanding neutralizing antibody titers for each isotype via the plaque reduction neutralization test would clarify the anti-HA data which did not always show significantly different anti-HA binding. Also, as a reduction of anti-HA IgM levels was observed post lethal challenge, long-lived IgM secreting cells could be measured in the bone marrow using ELISpot using an HA coated plate before and after lethal challenge [213]. Finally, loss of PAD2 should be assessed on the C57BL/6 background where there are more immunological tools to assess antigen specific immune responses, such as tetramers.

In conclusion, these investigations show that the PADs and citrullination are important for antibody responses in normal immunity and autoimmune disease. Further investigation is necessary to expand on these findings to improve human health and fight disease.

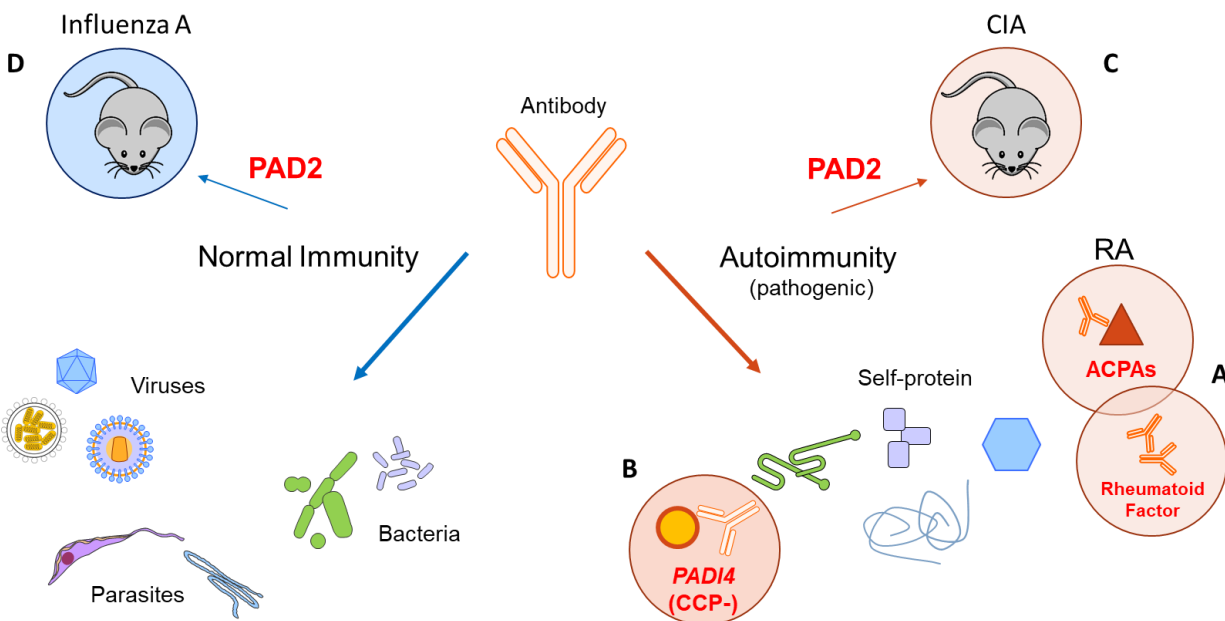


Figure 1. Antibodies and the Role of Citrullination and Citrullinating Enzymes in Immunity. In normal immunity, antibodies respond to foreign antigens, such as those derived from viruses, parasites, and bacteria. However, antibodies are also present in autoimmunity, where they target self proteins and are associated with pathology. In RA, there are two categories of antibodies that are used diagnostically, ACPAs and RFs. I show that these two antibody types, previously viewed as distinct, in fact have overlapping reactivity (A). Additionally, my work demonstrates that a *PADI4* genetic variant is associated with reduced anti-native and anti-citrullinated histone antibodies in CCP- RA, but not in CCP+ RA (B). Last, I used two mouse models to investigate the role of PAD2 using PAD2 deficient mice: in autoimmunity through CIA (C) and then in normal immunity through the development of a novel influenza infection model in DBA/1J mice (D), finding that PAD2 is required for antibody levels in both CIA and influenza.

References

1. Tellier, J. and S.L. Nutt, *Plasma cells: The programming of an antibody-secreting machine*. Eur J Immunol, 2019. **49**(1): p. 30-37.
2. Huber, R., et al., *Crystallographic structure studies of an IgG molecule and an Fc fragment*. Nature, 1976. **264**(5585): p. 415-20.
3. Chiu, M.L., et al., *Antibody Structure and Function: The Basis for Engineering Therapeutics*. Antibodies (Basel), 2019. **8**(4).
4. Bradley, J., *Immunoglobulins*. J Med Genet, 1974. **11**(1): p. 80-90.
5. Fahey, J.L., *Antibodies and immunoglobulins. I. Structure and function*. JAMA, 1965. **194**(1): p. 71-4.
6. Pike, R.M., *Antibody heterogeneity and serological reactions*. Bacteriol Rev, 1967. **31**(2): p. 157-74.
7. Crabbe, P.A., A.O. Carbonara, and J.F. Heremans, *The Normal Human Intestinal Mucosa as a Major Source of Plasma Cells Containing Gamma-a-Immunoglobulin*. Lab Invest, 1965. **14**: p. 235-48.
8. Tomasi, T.B., Jr., et al., *Characteristics of an Immune System Common to Certain External Secretions*. J Exp Med, 1965. **121**: p. 101-24.
9. Hoffman, W., F.G. Lakkis, and G. Chalasani, *B Cells, Antibodies, and More*. Clin J Am Soc Nephrol, 2016. **11**(1): p. 137-54.
10. Edwards, M.J. and N.J. Dimmock, *Hemagglutinin 1-specific immunoglobulin G and Fab molecules mediate postattachment neutralization of influenza A virus by inhibition of an early fusion event*. J Virol, 2001. **75**(21): p. 10208-18.

11. Murin, C.D., I.A. Wilson, and A.B. Ward, *Antibody responses to viral infections: a structural perspective across three different enveloped viruses*. Nat Microbiol, 2019. **4**(5): p. 734-747.
12. Wang, Y.Y., et al., *IgG in cervicovaginal mucus traps HSV and prevents vaginal herpes infections*. Mucosal Immunol, 2014. **7**(5): p. 1036-44.
13. Sissons, J.G. and M.B. Oldstone, *Antibody-mediated destruction of virus-infected cells*. Adv Immunol, 1980. **29**: p. 209-60.
14. Shibuya, A., et al., *Fc alpha/mu receptor mediates endocytosis of IgM-coated microbes*. Nat Immunol, 2000. **1**(5): p. 441-6.
15. Hellwig, S.M., et al., *Targeting to Fc gamma receptors, but not CR3 (CD11b/CD18), increases clearance of Bordetella pertussis*. J Infect Dis, 2001. **183**(6): p. 871-9.
16. Kohl, S. and L.S. Loo, *Protection of neonatal mice against herpes simplex virus infection: probable in vivo antibody-dependent cellular cytotoxicity*. J Immunol, 1982. **129**(1): p. 370-6.
17. Yang, K.D., et al., *Mechanisms of bacterial opsonization by immune globulin intravenous: correlation of complement consumption with opsonic activity and protective efficacy*. J Infect Dis, 1989. **159**(4): p. 701-7.
18. Tay, M.Z., K. Wiehe, and J. Pollara, *Antibody-Dependent Cellular Phagocytosis in Antiviral Immune Responses*. Front Immunol, 2019. **10**: p. 332.
19. Waaler, E., *On the occurrence of a factor in human serum activating the specific agglutination of sheep blood corpuscles*. 1939. APMIS, 2007. **115**(5): p. 422-38; discussion 439.

20. Lee, S.L., S.R. Michael, and I.L. Vural, *The L.E. (lupus erythematosus) cell; clinical and chemical studies*. Am J Med, 1951. **10**(4): p. 446-51.
21. Holborow, E.J., D.M. Weir, and G.D. Johnson, *A serum factor in lupus erythematosus with affinity for tissue nuclei*. Br Med J, 1957. **2**(5047): p. 732-4.
22. Deutscher, S.L., J.B. Harley, and J.D. Keene, *Molecular analysis of the 60-kDa human Ro ribonucleoprotein*. Proc Natl Acad Sci U S A, 1988. **85**(24): p. 9479-83.
23. Archelos, J.J., et al., *Isolation and characterization of an oligodendrocyte precursor-derived B-cell epitope in multiple sclerosis*. Ann Neurol, 1998. **43**(1): p. 15-24.
24. Aletaha, D., et al., *2010 Rheumatoid arthritis classification criteria: an American College of Rheumatology/European League Against Rheumatism collaborative initiative*. Arthritis Rheum, 2010. **62**(9): p. 2569-81.
25. Aringer, M., et al., *2019 European League Against Rheumatism/American College of Rheumatology Classification Criteria for Systemic Lupus Erythematosus*. Arthritis Rheumatol, 2019. **71**(9): p. 1400-1412.
26. Shiboski, C.H., et al., *2016 American College of Rheumatology/European League Against Rheumatism Classification Criteria for Primary Sjogren's Syndrome: A Consensus and Data-Driven Methodology Involving Three International Patient Cohorts*. Arthritis Rheumatol, 2017. **69**(1): p. 35-45.
27. Theander, E., et al., *Prediction of Sjogren's Syndrome Years Before Diagnosis and Identification of Patients With Early Onset and Severe Disease Course by Autoantibody Profiling*. Arthritis Rheumatol, 2015. **67**(9): p. 2427-36.

28. Kelmenson, L.B., et al., *Timing of Elevations of Autoantibody Isotypes Prior to Diagnosis of Rheumatoid Arthritis*. *Arthritis Rheumatol*, 2020. **72**(2): p. 251-261.
29. Shi, J., et al., *Anti-carbamylated protein (anti-CarP) antibodies precede the onset of rheumatoid arthritis*. *Ann Rheum Dis*, 2014. **73**(4): p. 780-3.
30. Eriksson, C., et al., *Autoantibodies predate the onset of systemic lupus erythematosus in northern Sweden*. *Arthritis Res Ther*, 2011. **13**(1): p. R30.
31. Hargraves, M.M., H. Richmond, and R. Morton, *Presentation of two bone marrow elements; the tart cell and the L.E. cell*. *Proc Staff Meet Mayo Clin*, 1948. **23**(2): p. 25-8.
32. Haserick, J.R., L.A. Lewis, and D.W. Bortz, *Blood factor in acute disseminated lupus erythematosus; determination of gamma globulin as specific plasma fraction*. *Am J Med Sci*, 1950. **219**(6): p. 660-3.
33. Godman, G.C. and A.D. Deitch, *A cytochemical study of the L. E. bodies of systemic lupus erythematosus. I. Nucleic acids*. *J Exp Med*, 1957. **106**(4): p. 575-92.
34. Wiik, A.S., *Anti-nuclear autoantibodies: clinical utility for diagnosis, prognosis, monitoring, and planning of treatment strategy in systemic immunoinflammatory diseases*. *Scand J Rheumatol*, 2005. **34**(4): p. 260-8.
35. Op De Beeck, K., et al., *Detection of antinuclear antibodies by indirect immunofluorescence and by solid phase assay*. *Autoimmun Rev*, 2011. **10**(12): p. 801-8.

36. Vlahakos, D., et al., *Murine monoclonal anti-DNA antibodies penetrate cells, bind to nuclei, and induce glomerular proliferation and proteinuria in vivo*. J Am Soc Nephrol, 1992. **2**(8): p. 1345-54.
37. Sabbaga, J., et al., *Cross-reactivity distinguishes serum and nephritogenic anti-DNA antibodies in human lupus from their natural counterparts in normal serum*. J Autoimmun, 1990. **3**(2): p. 215-35.
38. Foster, M.H., B. Cizman, and M.P. Madaio, *Nephritogenic autoantibodies in systemic lupus erythematosus: immunochemical properties, mechanisms of immune deposition, and genetic origins*. Lab Invest, 1993. **69**(5): p. 494-507.
39. Sokolove, J., et al., *Autoantibody epitope spreading in the pre-clinical phase predicts progression to rheumatoid arthritis*. PLoS One, 2012. **7**(5): p. e35296.
40. Corsiero, E., et al., *Single cell cloning and recombinant monoclonal antibodies generation from RA synovial B cells reveal frequent targeting of citrullinated histones of NETs*. Ann Rheum Dis, 2016. **75**(10): p. 1866-75.
41. Ingegnoli, F., R. Castelli, and R. Gualtierotti, *Rheumatoid factors: clinical applications*. Dis Markers, 2013. **35**(6): p. 727-34.
42. Ashe, W.K., et al., *Interaction of rheumatoid factor with infectious herpes simplex virus-antibody complexes*. Science, 1971. **172**(3979): p. 176-7.
43. Douvas, A., et al., *Neutralization of HIV type 1 infectivity by serum antibodies from a subset of autoimmune patients with mixed connective tissue disease*. AIDS Res Hum Retroviruses, 1996. **12**(16): p. 1509-17.

44. Brezski, R.J., et al., *Human anti-IgG1 hinge autoantibodies reconstitute the effector functions of proteolytically inactivated IgGs*. J Immunol, 2008. **181**(5): p. 3183-92.
45. Van Snick, J.L., et al., *Enhancement by IgM rheumatoid factor of in vitro ingestion by macrophages and in vivo clearance of aggregated IgG or antigen-antibody complexes*. Eur J Immunol, 1978. **8**(4): p. 279-85.
46. Roosnek, E. and A. Lanzavecchia, *Efficient and selective presentation of antigen-antibody complexes by rheumatoid factor B cells*. J Exp Med, 1991. **173**(2): p. 487-9.
47. Sokolove, J., et al., *Rheumatoid factor as a potentiator of anti-citrullinated protein antibody-mediated inflammation in rheumatoid arthritis*. Arthritis Rheumatol, 2014. **66**(4): p. 813-21.
48. Laurent, L., et al., *IgM rheumatoid factor amplifies the inflammatory response of macrophages induced by the rheumatoid arthritis-specific immune complexes containing anticitrullinated protein antibodies*. Ann Rheum Dis, 2015. **74**(7): p. 1425-31.
49. Anquetil, F., et al., *IgM and IgA rheumatoid factors purified from rheumatoid arthritis sera boost the Fc receptor- and complement-dependent effector functions of the disease-specific anti-citrullinated protein autoantibodies*. J Immunol, 2015. **194**(8): p. 3664-74.
50. Zhao, X., et al., *Circulating immune complexes contain citrullinated fibrinogen in rheumatoid arthritis*. Arthritis Res Ther, 2008. **10**(4): p. R94.

51. Mellors, R.C., et al., *Cellular Origin of Rheumatoid Factor*. J Exp Med, 1959. **110**(6): p. 875-86.
52. Hedstrom, A.K., et al., *Complex Relationships of Smoking, HLA-DRB1 Genes, and Serologic Profiles in Patients With Early Rheumatoid Arthritis: Update From a Swedish Population-Based Case-Control Study*. Arthritis Rheumatol, 2019. **71**(9): p. 1504-1511.
53. Newkirk, M.M., et al., *Chronic smoke exposure induces rheumatoid factor and anti-heat shock protein 70 autoantibodies in susceptible mice and humans with lung disease*. Eur J Immunol, 2012. **42**(4): p. 1051-61.
54. Jonsson, T., et al., *Population study of the importance of rheumatoid factor isotypes in adults*. Ann Rheum Dis, 1992. **51**(7): p. 863-8.
55. Jonsson, T., et al., *Combined elevation of IgM and IgA rheumatoid factor has high diagnostic specificity for rheumatoid arthritis*. Rheumatol Int, 1998. **18**(3): p. 119-22.
56. de Brito Rocha, S., D.C. Baldo, and L.E.C. Andrade, *Clinical and pathophysiologic relevance of autoantibodies in rheumatoid arthritis*. Adv Rheumatol, 2019. **59**(1): p. 2.
57. Myasoedova, E., et al., *Is the epidemiology of rheumatoid arthritis changing? Results from a population-based incidence study, 1985-2014*. Ann Rheum Dis, 2020. **79**(4): p. 440-444.
58. Schellekens, G.A., et al., *Citrulline is an essential constituent of antigenic determinants recognized by rheumatoid arthritis-specific autoantibodies*. J Clin Invest, 1998. **101**(1): p. 273-81.

59. Stastny, P., *Association of the B-cell alloantigen DRw4 with rheumatoid arthritis*. N Engl J Med, 1978. **298**(16): p. 869-71.
60. Ting, Y.T., et al., *The interplay between citrullination and HLA-DRB1 polymorphism in shaping peptide binding hierarchies in rheumatoid arthritis*. J Biol Chem, 2018. **293**(9): p. 3236-3251.
61. Linn-Rasker, S.P., et al., *Smoking is a risk factor for anti-CCP antibodies only in rheumatoid arthritis patients who carry HLA-DRB1 shared epitope alleles*. Ann Rheum Dis, 2006. **65**(3): p. 366-71.
62. Auger, I., et al., *Peptidylarginine Deiminase Autoimmunity and the Development of Anti-Citrullinated Protein Antibody in Rheumatoid Arthritis: The Hapten-Carrier Model*. Arthritis Rheumatol, 2020. **72**(6): p. 903-911.
63. Padyukov, L., et al., *A genome-wide association study suggests contrasting associations in ACPA-positive versus ACPA-negative rheumatoid arthritis*. Ann Rheum Dis, 2011. **70**(2): p. 259-65.
64. Pedersen, M., et al., *Environmental risk factors differ between rheumatoid arthritis with and without auto-antibodies against cyclic citrullinated peptides*. Arthritis Res Ther, 2006. **8**(4): p. R133.
65. Sohrabian, A., et al., *Number of individual ACPA reactivities in synovial fluid immune complexes, but not serum anti-CCP2 levels, associate with inflammation and joint destruction in rheumatoid arthritis*. Ann Rheum Dis, 2018. **77**(9): p. 1345-1353.

66. Meyer, O., et al., *Serial determination of cyclic citrullinated peptide autoantibodies predicted five-year radiological outcomes in a prospective cohort of patients with early rheumatoid arthritis*. *Arthritis Res Ther*, 2006. **8**(2): p. R40.
67. van der Helm-van Mil, A.H., et al., *Antibodies to citrullinated proteins and differences in clinical progression of rheumatoid arthritis*. *Arthritis Res Ther*, 2005. **7**(5): p. R949-58.
68. van Oosterhout, M., et al., *Differences in synovial tissue infiltrates between anti-cyclic citrullinated peptide-positive rheumatoid arthritis and anti-cyclic citrullinated peptide-negative rheumatoid arthritis*. *Arthritis Rheum*, 2008. **58**(1): p. 53-60.
69. Gomez-Puerta, J.A., et al., *Differences in synovial fluid cytokine levels but not in synovial tissue cell infiltrate between anti-citrullinated peptide/protein antibody-positive and -negative rheumatoid arthritis patients*. *Arthritis Res Ther*, 2013. **15**(6): p. R182.
70. Shi, J., et al., *Autoantibodies recognizing carbamylated proteins are present in sera of patients with rheumatoid arthritis and predict joint damage*. *Proc Natl Acad Sci U S A*, 2011. **108**(42): p. 17372-7.
71. Juarez, M., et al., *Identification of novel antiacetylated vimentin antibodies in patients with early inflammatory arthritis*. *Ann Rheum Dis*, 2016. **75**(6): p. 1099-107.
72. Volkov, M., K.A. van Schie, and D. van der Woude, *Autoantibodies and B Cells: The ABC of rheumatoid arthritis pathophysiology*. *Immunol Rev*, 2020. **294**(1): p. 148-163.

73. Thiele, G.M., et al., *Soluble proteins modified with acetaldehyde and malondialdehyde are immunogenic in the absence of adjuvant*. Alcohol Clin Exp Res, 1998. **22**(8): p. 1731-9.
74. Thiele, G.M., et al., *Malondialdehyde-acetaldehyde adducts and anti-malondialdehyde-acetaldehyde antibodies in rheumatoid arthritis*. Arthritis Rheumatol, 2015. **67**(3): p. 645-55.
75. Mikuls, T.R., et al., *Autoantibodies to Malondialdehyde-Acetaldehyde Are Detected Prior to Rheumatoid Arthritis Diagnosis and After Other Disease Specific Autoantibodies*. Arthritis Rheumatol, 2020. **72**(12): p. 2025-2029.
76. Sieghart, D., et al., *Determination of Autoantibody Isotypes Increases the Sensitivity of Serodiagnostics in Rheumatoid Arthritis*. Front Immunol, 2018. **9**: p. 876.
77. Reed, E., et al., *Presence of autoantibodies in "seronegative" rheumatoid arthritis associates with classical risk factors and high disease activity*. Arthritis Res Ther, 2020. **22**(1): p. 170.
78. Sahlstrom, P., et al., *Different Hierarchies of Anti-Modified Protein Autoantibody Reactivities in Rheumatoid Arthritis*. Arthritis Rheumatol, 2020.
79. Kissel, T., et al., *Antibodies and B cells recognising citrullinated proteins display a broad cross-reactivity towards other post-translational modifications*. Ann Rheum Dis, 2020. **79**(4): p. 472-480.
80. Kampstra, A.S.B., et al., *Different classes of anti-modified protein antibodies are induced on exposure to antigens expressing only one type of modification*. Ann Rheum Dis, 2019. **78**(7): p. 908-916.

81. Tilvawala, R., et al., *The Rheumatoid Arthritis-Associated Citrullinome*. Cell Chem Biol, 2018. **25**(6): p. 691-704 e6.
82. Ryall, J., et al., *Expression of nuclear genes encoding the urea cycle enzymes, carbamoyl-phosphate synthetase I and ornithine carbamoyl transferase, in rat liver and intestinal mucosa*. Eur J Biochem, 1985. **152**(2): p. 287-92.
83. Hamano, Y., et al., *Immunocytochemical localization of ornithine transcarbamylase in rat intestinal mucosa. Light and electron microscopic study*. J Histochem Cytochem, 1988. **36**(1): p. 29-35.
84. Takiguchi, M. and M. Mori, *Transcriptional regulation of genes for ornithine cycle enzymes*. Biochem J, 1995. **312 (Pt 3)**: p. 649-59.
85. Papadia, C., et al., *Plasma citrulline concentration: a reliable marker of small bowel absorptive capacity independent of intestinal inflammation*. Am J Gastroenterol, 2007. **102**(7): p. 1474-82.
86. Fujisaki, M. and K. Sugawara, *Properties of peptidylarginine deiminase from the epidermis of newborn rats*. J Biochem, 1981. **89**(1): p. 257-63.
87. Nakashima, K., et al., *Molecular characterization of peptidylarginine deiminase in HL-60 cells induced by retinoic acid and 1alpha,25-dihydroxyvitamin D(3)*. J Biol Chem, 1999. **274**(39): p. 27786-92.
88. Kanno, T., et al., *Human peptidylarginine deiminase type III: molecular cloning and nucleotide sequence of the cDNA, properties of the recombinant enzyme, and immunohistochemical localization in human skin*. J Invest Dermatol, 2000. **115**(5): p. 813-23.

89. Ishigami, A., et al., *Human peptidylarginine deiminase type II: molecular cloning, gene organization, and expression in human skin*. Arch Biochem Biophys, 2002. **407**(1): p. 25-31.
90. Guerrin, M., et al., *cDNA cloning, gene organization and expression analysis of human peptidylarginine deiminase type I*. Biochem J, 2003. **370**(Pt 1): p. 167-74.
91. Chavanas, S., et al., *Comparative analysis of the mouse and human peptidylarginine deiminase gene clusters reveals highly conserved non-coding segments and a new human gene, PADI6*. Gene, 2004. **330**: p. 19-27.
92. Darrah, E., et al., *Peptidylarginine deiminase 2, 3 and 4 have distinct specificities against cellular substrates: novel insights into autoantigen selection in rheumatoid arthritis*. Ann Rheum Dis, 2012. **71**(1): p. 92-8.
93. Takahara, H., et al., *Peptidylarginine deiminase of the mouse. Distribution, properties, and immunocytochemical localization*. J Biol Chem, 1989. **264**(22): p. 13361-8.
94. Mechin, M.C., et al., *The peptidylarginine deiminases expressed in human epidermis differ in their substrate specificities and subcellular locations*. Cell Mol Life Sci, 2005. **62**(17): p. 1984-95.
95. Tarcsa, E., et al., *Protein unfolding by peptidylarginine deiminase. Substrate specificity and structural relationships of the natural substrates trichohyalin and filaggrin*. J Biol Chem, 1996. **271**(48): p. 30709-16.
96. Inagaki, M., et al., *Ca²⁺-dependent deimination-induced disassembly of intermediate filaments involves specific modification of the amino-terminal head domain*. J Biol Chem, 1989. **264**(30): p. 18119-27.

97. Jang, B., et al., *Peptidylarginine deiminase modulates the physiological roles of enolase via citrullination: links between altered multifunction of enolase and neurodegenerative diseases*. *Biochem J*, 2012. **445**(2): p. 183-92.
98. Darrah, E. and F. Andrade, *Rheumatoid arthritis and citrullination*. *Curr Opin Rheumatol*, 2018. **30**(1): p. 72-78.
99. van Beers, J.J., et al., *The rheumatoid arthritis synovial fluid citrullinome reveals novel citrullinated epitopes in apolipoprotein E, myeloid nuclear differentiation antigen, and beta-actin*. *Arthritis Rheum*, 2013. **65**(1): p. 69-80.
100. Wang, F., et al., *Identification of citrullinated peptides in the synovial fluid of patients with rheumatoid arthritis using LC-MALDI-TOF/TOF*. *Clin Rheumatol*, 2016. **35**(9): p. 2185-94.
101. Tuttunen, A.E., B. Fleckenstein, and G.A. de Souza, *Assessing the citrullinome in rheumatoid arthritis synovial fluid with and without enrichment of citrullinated peptides*. *J Proteome Res*, 2014. **13**(6): p. 2867-73.
102. Sharma, M., et al., *Expanding the citrullinome of synovial fibrinogen from rheumatoid arthritis patients*. *J Proteomics*, 2019. **208**: p. 103484.
103. Lugli, E.B., et al., *Expression of citrulline and homocitrulline residues in the lungs of non-smokers and smokers: implications for autoimmunity in rheumatoid arthritis*. *Arthritis Res Ther*, 2015. **17**: p. 9.
104. Vossenaar, E.R., et al., *Expression and activity of citrullinating peptidylarginine deiminase enzymes in monocytes and macrophages*. *Ann Rheum Dis*, 2004. **63**(4): p. 373-81.

105. Chang, X., et al., *Localization of peptidylarginine deiminase 4 (PADI4) and citrullinated protein in synovial tissue of rheumatoid arthritis*. Rheumatology (Oxford), 2005. **44**(1): p. 40-50.
106. Foulquier, C., et al., *Peptidyl arginine deiminase type 2 (PAD-2) and PAD-4 but not PAD-1, PAD-3, and PAD-6 are expressed in rheumatoid arthritis synovium in close association with tissue inflammation*. Arthritis Rheum, 2007. **56**(11): p. 3541-53.
107. Sun, B., et al., *Reciprocal regulation of Th2 and Th17 cells by PAD2-mediated citrullination*. JCI Insight, 2019. **4**(22).
108. Vossenaar, E.R., et al., *PAD, a growing family of citrullinating enzymes: genes, features and involvement in disease*. Bioessays, 2003. **25**(11): p. 1106-18.
109. De Rycke, L., et al., *Synovial intracellular citrullinated proteins colocalizing with peptidyl arginine deiminase as pathophysiologically relevant antigenic determinants of rheumatoid arthritis-specific humoral autoimmunity*. Arthritis Rheum, 2005. **52**(8): p. 2323-30.
110. Gyorgy, B., et al., *Citrullination: a posttranslational modification in health and disease*. Int J Biochem Cell Biol, 2006. **38**(10): p. 1662-77.
111. Suzuki, A., et al., *Functional haplotypes of PADI4, encoding citrullinating enzyme peptidylarginine deiminase 4, are associated with rheumatoid arthritis*. Nat Genet, 2003. **34**(4): p. 395-402.
112. Ikari, K., et al., *Association between PADI4 and rheumatoid arthritis: a replication study*. Arthritis Rheum, 2005. **52**(10): p. 3054-7.

113. Freudenberg, J., et al., *Genome-wide association study of rheumatoid arthritis in Koreans: population-specific loci as well as overlap with European susceptibility loci*. *Arthritis Rheum*, 2011. **63**(4): p. 884-93.
114. Too, C.L., et al., *Polymorphisms in peptidylarginine deiminase associate with rheumatoid arthritis in diverse Asian populations: evidence from MyEIRA study and meta-analysis*. *Arthritis Res Ther*, 2012. **14**(6): p. R250.
115. Terao, C., et al., *The human AIRE gene at chromosome 21q22 is a genetic determinant for the predisposition to rheumatoid arthritis in Japanese population*. *Hum Mol Genet*, 2011. **20**(13): p. 2680-5.
116. Goh, L.L., et al., *NLRP1, PTPN22 and PADI4 gene polymorphisms and rheumatoid arthritis in ACPA-positive Singaporean Chinese*. *Rheumatol Int*, 2017. **37**(8): p. 1295-1302.
117. Chang, X., et al., *PADI2 is significantly associated with rheumatoid arthritis*. *PLoS One*, 2013. **8**(12): p. e81259.
118. Corsiero, E., et al., *NETosis as Source of Autoantigens in Rheumatoid Arthritis*. *Front Immunol*, 2016. **7**: p. 485.
119. Li, P., et al., *PAD4 is essential for antibacterial innate immunity mediated by neutrophil extracellular traps*. *J Exp Med*, 2010. **207**(9): p. 1853-62.
120. Bawadekar, M., et al., *Peptidylarginine deiminase 2 is required for tumor necrosis factor alpha-induced citrullination and arthritis, but not neutrophil extracellular trap formation*. *J Autoimmun*, 2017. **80**: p. 39-47.

121. Khandpur, R., et al., *NETs are a source of citrullinated autoantigens and stimulate inflammatory responses in rheumatoid arthritis*. *Sci Transl Med*, 2013. **5**(178): p. 178ra40.
122. Borregaard, N., *Neutrophils, from marrow to microbes*. *Immunity*, 2010. **33**(5): p. 657-70.
123. Fuchs, T.A., et al., *Novel cell death program leads to neutrophil extracellular traps*. *J Cell Biol*, 2007. **176**(2): p. 231-41.
124. Brinkmann, V., et al., *Neutrophil extracellular traps kill bacteria*. *Science*, 2004. **303**(5663): p. 1532-5.
125. Urban, C.F., et al., *Neutrophil extracellular traps capture and kill *Candida albicans* yeast and hyphal forms*. *Cell Microbiol*, 2006. **8**(4): p. 668-76.
126. Brinkmann, V. and A. Zychlinsky, *Beneficial suicide: why neutrophils die to make NETs*. *Nat Rev Microbiol*, 2007. **5**(8): p. 577-82.
127. Brinkmann, V. and A. Zychlinsky, *Neutrophil extracellular traps: is immunity the second function of chromatin?* *J Cell Biol*, 2012. **198**(5): p. 773-83.
128. Wang, Y., et al., *Histone hypercitrullination mediates chromatin decondensation and neutrophil extracellular trap formation*. *J Cell Biol*, 2009. **184**(2): p. 205-13.
129. Spengler, J., et al., *Release of Active Peptidyl Arginine Deiminases by Neutrophils Can Explain Production of Extracellular Citrullinated Autoantigens in Rheumatoid Arthritis Synovial Fluid*. *Arthritis Rheumatol*, 2015. **67**(12): p. 3135-45.
130. Holmes, C.L., et al., *Insight into Neutrophil Extracellular Traps through Systematic Evaluation of Citrullination and Peptidylarginine Deiminases*. *J Immunol Res*, 2019. **2019**: p. 2160192.

131. Loos, T., et al., *Citrullination of CXCL10 and CXCL11 by peptidylarginine deiminase: a naturally occurring posttranslational modification of chemokines and new dimension of immunoregulation*. *Blood*, 2008. **112**(7): p. 2648-56.
132. Loos, T., et al., *Citrullination of CXCL8 increases this chemokine's ability to mobilize neutrophils into the blood circulation*. *Haematologica*, 2009. **94**(10): p. 1346-53.
133. Kouzarides, T., *Chromatin modifications and their function*. *Cell*, 2007. **128**(4): p. 693-705.
134. Witalison, E.E., P.R. Thompson, and L.J. Hofseth, *Protein Arginine Deiminases and Associated Citrullination: Physiological Functions and Diseases Associated with Dysregulation*. *Curr Drug Targets*, 2015. **16**(7): p. 700-10.
135. Wang, S. and Y. Wang, *Peptidylarginine deiminases in citrullination, gene regulation, health and pathogenesis*. *Biochim Biophys Acta*, 2013. **1829**(10): p. 1126-35.
136. Wang, Y., et al., *Human PAD4 regulates histone arginine methylation levels via demethylination*. *Science*, 2004. **306**(5694): p. 279-83.
137. Lee, Y.H., et al., *Regulation of coactivator complex assembly and function by protein arginine methylation and demethylination*. *Proc Natl Acad Sci U S A*, 2005. **102**(10): p. 3611-6.
138. Levine, A.J., *p53, the cellular gatekeeper for growth and division*. *Cell*, 1997. **88**(3): p. 323-31.
139. Li, P., et al., *Regulation of p53 target gene expression by peptidylarginine deiminase 4*. *Mol Cell Biol*, 2008. **28**(15): p. 4745-58.

140. Nakashima, K., T. Hagiwara, and M. Yamada, *Nuclear localization of peptidylarginine deiminase V and histone deimination in granulocytes*. J Biol Chem, 2002. **277**(51): p. 49562-8.
141. Zheng, L., et al., *Calcium Regulates the Nuclear Localization of Protein Arginine Deiminase 2*. Biochemistry, 2019. **58**(27): p. 3042-3056.
142. Clancy, K.W., et al., *Citrullination/Methylation Crosstalk on Histone H3 Regulates ER-Target Gene Transcription*. ACS Chem Biol, 2017. **12**(6): p. 1691-1702.
143. Musse, A.A., et al., *Peptidylarginine deiminase 2 (PAD2) overexpression in transgenic mice leads to myelin loss in the central nervous system*. Dis Model Mech, 2008. **1**(4-5): p. 229-40.
144. Zhang, X., et al., *Peptidylarginine deiminase 2-catalyzed histone H3 arginine 26 citrullination facilitates estrogen receptor alpha target gene activation*. Proc Natl Acad Sci U S A, 2012. **109**(33): p. 13331-6.
145. McElwee, J.L., et al., *Identification of PADI2 as a potential breast cancer biomarker and therapeutic target*. BMC Cancer, 2012. **12**: p. 500.
146. Beato, M. and P. Sharma, *Peptidyl Arginine Deiminase 2 (PADI2)-Mediated Arginine Citrullination Modulates Transcription in Cancer*. Int J Mol Sci, 2020. **21**(4).
147. Naranbhai, V., et al., *Genomic modulators of gene expression in human neutrophils*. Nat Commun, 2015. **6**: p. 7545.
148. Crowson, C.S., et al., *The lifetime risk of adult-onset rheumatoid arthritis and other inflammatory autoimmune rheumatic diseases*. Arthritis Rheum, 2011. **63**(3): p. 633-9.

149. Engdahl, C., et al., *Periarticular Bone Loss in Arthritis Is Induced by Autoantibodies Against Citrullinated Vimentin*. J Bone Miner Res, 2017. **32**(8): p. 1681-1691.
150. Wegner, N., et al., *Autoimmunity to specific citrullinated proteins gives the first clues to the etiology of rheumatoid arthritis*. Immunol Rev, 2010. **233**(1): p. 34-54.
151. Sur Chowdhury, C., et al., *Enhanced neutrophil extracellular trap generation in rheumatoid arthritis: analysis of underlying signal transduction pathways and potential diagnostic utility*. Arthritis Res Ther, 2014. **16**(3): p. R122.
152. Rebernick, R., et al., *DNA Area and NETosis Analysis (DANA): a High-Throughput Method to Quantify Neutrophil Extracellular Traps in Fluorescent Microscope Images*. Biol Proced Online, 2018. **20**: p. 7.
153. Leppkes, M., et al., *Externalized decondensed neutrophil chromatin occludes pancreatic ducts and drives pancreatitis*. Nat Commun, 2016. **7**: p. 10973.
154. Clark, H.L., et al., *Protein Deiminase 4 and CR3 Regulate Aspergillus fumigatus and beta-Glucan-Induced Neutrophil Extracellular Trap Formation, but Hyphal Killing Is Dependent Only on CR3*. Front Immunol, 2018. **9**: p. 1182.
155. Tatsiy, O. and P.P. McDonald, *Physiological Stimuli Induce PAD4-Dependent, ROS-Independent NETosis, With Early and Late Events Controlled by Discrete Signaling Pathways*. Front Immunol, 2018. **9**: p. 2036.
156. Pratesi, F., et al., *Antibodies from patients with rheumatoid arthritis target citrullinated histone 4 contained in neutrophils extracellular traps*. Ann Rheum Dis, 2014. **73**(7): p. 1414-22.

157. Damgaard, D., et al., *Relative efficiencies of peptidylarginine deiminase 2 and 4 in generating target sites for anti-citrullinated protein antibodies in fibrinogen, alpha-enolase and histone H3*. PLoS One, 2018. **13**(8): p. e0203214.
158. Shelef, M.A., et al., *Peptidylarginine deiminase 4 contributes to tumor necrosis factor alpha-induced inflammatory arthritis*. Arthritis Rheumatol, 2014. **66**(6): p. 1482-91.
159. Bawadekar, M., et al., *Tumor necrosis factor alpha, citrullination, and peptidylarginine deiminase 4 in lung and joint inflammation*. Arthritis Res Ther, 2016. **18**(1): p. 173.
160. Suzuki, A., et al., *Decreased severity of experimental autoimmune arthritis in peptidylarginine deiminase type 4 knockout mice*. BMC Musculoskelet Disord, 2016. **17**: p. 205.
161. Titcombe, P.J., et al., *Pathogenic Citrulline-Multispecific B Cell Receptor Clades in Rheumatoid Arthritis*. Arthritis Rheumatol, 2018. **70**(12): p. 1933-1945.
162. Steen, J., et al., *Recognition of Amino Acid Motifs, Rather Than Specific Proteins, by Human Plasma Cell-Derived Monoclonal Antibodies to Posttranslationally Modified Proteins in Rheumatoid Arthritis*. Arthritis Rheumatol, 2019. **71**(2): p. 196-209.
163. Ioan-Facsinay, A., et al., *Anti-cyclic citrullinated peptide antibodies are a collection of anti-citrullinated protein antibodies and contain overlapping and non-overlapping reactivities*. Ann Rheum Dis, 2011. **70**(1): p. 188-93.
164. Guiducci, E., et al., *Candida albicans-Induced NETosis Is Independent of Peptidylarginine Deiminase 4*. Front Immunol, 2018. **9**: p. 1573.

165. Claushuis, T.A.M., et al., *Role of Peptidylarginine Deiminase 4 in Neutrophil Extracellular Trap Formation and Host Defense during Klebsiella pneumoniae-Induced Pneumonia-Derived Sepsis*. J Immunol, 2018. **201**(4): p. 1241-1252.
166. Neeli, I. and M. Radic, *Opposition between PKC isoforms regulates histone deimination and neutrophil extracellular chromatin release*. Front Immunol, 2013. **4**: p. 38.
167. Halder, L.D., et al., *Factor H Binds to Extracellular DNA Traps Released from Human Blood Monocytes in Response to Candida albicans*. Front Immunol, 2016. **7**: p. 671.
168. Chow, O.A., et al., *Statins enhance formation of phagocyte extracellular traps*. Cell Host Microbe, 2010. **8**(5): p. 445-54.
169. Cuthbert, G.L., et al., *Histone deimination antagonizes arginine methylation*. Cell, 2004. **118**(5): p. 545-53.
170. Nakashima, K., et al., *PAD4 regulates proliferation of multipotent haematopoietic cells by controlling c-myc expression*. Nat Commun, 2013. **4**: p. 1836.
171. Pratesi, F., et al., *Antibodies from patients with rheumatoid arthritis target citrullinated histone 4 contained in neutrophils extracellular traps*. Annals of the rheumatic diseases, 2013.
172. Khan, M.A., et al., *Role of peroxynitrite-modified H2A histone in the induction and progression of rheumatoid arthritis*. Scand J Rheumatol, 2012. **41**(6): p. 426-33.
173. Khan, W.A. and G.S. Zaman, *Detection of 16alpha-Hydroxyestrone-histone 1 Adduct as High-Affinity Antigen for Rheumatoid Arthritis Autoantibodies*. Arch Immunol Ther Exp (Warsz), 2018. **66**(5): p. 379-388.

174. Lloyd, K.A., et al., *Differential ACPA Binding to Nuclear Antigens Reveals a PAD-Independent Pathway and a Distinct Subset of Acetylation Cross-Reactive Autoantibodies in Rheumatoid Arthritis*. *Front Immunol*, 2018. **9**: p. 3033.
175. Tuaille, N., et al., *Antibodies from patients with rheumatoid arthritis and juvenile chronic arthritis analyzed with core histone synthetic peptides*. *Int Arch Allergy Appl Immunol*, 1990. **91**(3): p. 297-305.
176. Holmes CL, P.C., Bier AM, Donlon TZ, Bartels CM, Shelef MA, *Reduced IgG titers against pertussis in rheumatoid arthritis: evidence for a citrulline-biased immune response and medication effects*. *PLOS ONE*, 2019(Under Revision).
177. Katz, J.N., et al., *Sensitivity and positive predictive value of Medicare Part B physician claims for rheumatologic diagnoses and procedures*. *Arthritis Rheum*, 1997. **40**(9): p. 1594-600.
178. Yalavarthi, S., et al., *Release of neutrophil extracellular traps by neutrophils stimulated with antiphospholipid antibodies: a newly identified mechanism of thrombosis in the antiphospholipid syndrome*. *Arthritis Rheumatol*, 2015. **67**(11): p. 2990-3003.
179. Harley, J.B., et al., *Anti-Ro (SS-A) and anti-La (SS-B) in patients with Sjogren's syndrome*. *Arthritis Rheum*, 1986. **29**(2): p. 196-206.
180. Moller, P., et al., *IgA and rheumatoid factor in ankylosing spondylitis*. *Scand J Rheumatol Suppl*, 1988. **75**: p. 276-7.
181. Artandi, S.E., et al., *Monoclonal IgM rheumatoid factors bind IgG at a discontinuous epitope comprised of amino acid loops from heavy-chain constant-region domains 2 and 3*. *Proc Natl Acad Sci U S A*, 1992. **89**(1): p. 94-8.

182. Watanabe, K., et al., *An investigation on rheumatoid factor of different immunoglobulin classes in hepatitis B virus carriers*. Clin Rheumatol, 1991. **10**(1): p. 31-7.
183. Terness, P., et al., *The natural human IgG anti-F(ab')₂ antibody recognizes a conformational IgG1 hinge epitope*. J Immunol, 1995. **154**(12): p. 6446-52.
184. Maibom-Thomsen, S.L., et al., *Immunoglobulin G structure and rheumatoid factor epitopes*. PLoS One, 2019. **14**(6): p. e0217624.
185. Falkenburg, W.J., et al., *Anti-Hinge Antibodies Recognize IgG Subclass- and Protease-Restricted Neopeptides*. J Immunol, 2017. **198**(1): p. 82-93.
186. Borretzen, M., et al., *Control of autoantibody affinity by selection against amino acid replacements in the complementarity-determining regions*. Proc Natl Acad Sci U S A, 1994. **91**(26): p. 12917-21.
187. Shelef, M.A., *New Relationships for Old Autoantibodies in Rheumatoid Arthritis*. Arthritis Rheumatol, 2019. **71**(9): p. 1396-1399.
188. Zheng, Z., et al., *Disordered Antigens and Epitope Overlap Between Anti-Citrullinated Protein Antibodies and Rheumatoid Factor in Rheumatoid Arthritis*. Arthritis Rheumatol, 2020. **72**(2): p. 262-272.
189. Morell, A., et al., *Correlations between the concentrations of the four sub-classes of IgG and Gm Allotypes in normal human sera*. J Immunol, 1972. **108**(1): p. 195-206.
190. Aletaha, D., et al., *2010 rheumatoid arthritis classification criteria: an American College of Rheumatology/European League Against Rheumatism collaborative initiative*. Ann Rheum Dis, 2010. **69**(9): p. 1580-8.

191. Petri, M., et al., *Derivation and validation of the Systemic Lupus International Collaborating Clinics classification criteria for systemic lupus erythematosus*. *Arthritis Rheum*, 2012. **64**(8): p. 2677-86.
192. Amara, K., et al., *A Refined Protocol for Identifying Citrulline-specific Monoclonal Antibodies from Single Human B Cells from Rheumatoid Arthritis Patient Material*. *Bio Protoc*, 2019. **9**(17): p. e3347.
193. Van Avondt, K. and D. Hartl, *Mechanisms and disease relevance of neutrophil extracellular trap formation*. *Eur J Clin Invest*, 2018. **48 Suppl 2**: p. e12919.
194. Liu, Y., et al., *Peptidylarginine deiminases 2 and 4 modulate innate and adaptive immune responses in TLR-7-dependent lupus*. *JCI Insight*, 2018. **3**(23).
195. Mergaert, A.M., et al., *Reduced Anti-Histone Antibodies and Increased Risk of Rheumatoid Arthritis Associated with a Single Nucleotide Polymorphism in PADI4 in North Americans*. *Int J Mol Sci*, 2019. **20**(12).
196. Nakae, S., et al., *Suppression of immune induction of collagen-induced arthritis in IL-17-deficient mice*. *J Immunol*, 2003. **171**(11): p. 6173-7.
197. Stuart, J.M. and F.J. Dixon, *Serum transfer of collagen-induced arthritis in mice*. *J Exp Med*, 1983. **158**(2): p. 378-92.
198. Virelizier, J.L., *Host defenses against influenza virus: the role of anti-hemagglutinin antibody*. *J Immunol*, 1975. **115**(2): p. 434-9.
199. Lewis, H.D. and M. Nacht, *iPAD or PADi-'tablets' with therapeutic disease potential?* *Curr Opin Chem Biol*, 2016. **33**: p. 169-78.
200. Brentville, V.A., et al., *Post-translational modifications such as citrullination are excellent targets for cancer therapy*. *Semin Immunol*, 2020. **47**: p. 101393.

201. Hibi, T. and H.M. Dosch, *Limiting dilution analysis of the B cell compartment in human bone marrow*. Eur J Immunol, 1986. **16**(2): p. 139-45.
202. Jenkins, M.R., et al., *Addition of a prominent epitope affects influenza A virus-specific CD8+ T cell immunodominance hierarchies when antigen is limiting*. J Immunol, 2006. **177**(5): p. 2917-25.
203. Willis, V.C., et al., *N-alpha-benzoyl-N5-(2-chloro-1-iminoethyl)-L-ornithine amide, a protein arginine deiminase inhibitor, reduces the severity of murine collagen-induced arthritis*. J Immunol, 2011. **186**(7): p. 4396-404.
204. Mishra, N., et al., *Cutting Edge: Protein Arginine Deiminase 2 and 4 Regulate NLRP3 Inflammasome-Dependent IL-1beta Maturation and ASC Speck Formation in Macrophages*. J Immunol, 2019. **203**(4): p. 795-800.
205. Franchi, L., T. Eigenbrod, and G. Nunez, *Cutting edge: TNF-alpha mediates sensitization to ATP and silica via the NLRP3 inflammasome in the absence of microbial stimulation*. J Immunol, 2009. **183**(2): p. 792-6.
206. Lubberts, E., et al., *Treatment with a neutralizing anti-murine interleukin-17 antibody after the onset of collagen-induced arthritis reduces joint inflammation, cartilage destruction, and bone erosion*. Arthritis Rheum, 2004. **50**(2): p. 650-9.
207. Fujimoto, M., et al., *Interleukin-6 blockade suppresses autoimmune arthritis in mice by the inhibition of inflammatory Th17 responses*. Arthritis Rheum, 2008. **58**(12): p. 3710-9.
208. Pollinger, B., et al., *Th17 cells, not IL-17+ gammadelta T cells, drive arthritic bone destruction in mice and humans*. J Immunol, 2011. **186**(4): p. 2602-12.

209. Kawalkowska, J., et al., *Abrogation of collagen-induced arthritis by a peptidyl arginine deiminase inhibitor is associated with modulation of T cell-mediated immune responses*. Sci Rep, 2016. **6**: p. 26430.
210. Atassi, M.Z. and R.G. Webster, *Localization, synthesis, and activity of an antigenic site on influenza virus hemagglutinin*. Proc Natl Acad Sci U S A, 1983. **80**(3): p. 840-4.
211. Burton, D.R., *Antibodies, viruses and vaccines*. Nat Rev Immunol, 2002. **2**(9): p. 706-13.
212. Harada, Y., et al., *Unmutated immunoglobulin M can protect mice from death by influenza virus infection*. J Exp Med, 2003. **197**(12): p. 1779-85.
213. Skountzou, I., et al., *Influenza virus-specific neutralizing IgM antibodies persist for a lifetime*. Clin Vaccine Immunol, 2014. **21**(11): p. 1481-9.
214. Hemmers, S., et al., *PAD4-mediated neutrophil extracellular trap formation is not required for immunity against influenza infection*. PloS one, 2011. **6**(7): p. e22043.
215. Srivastava, B., et al., *Host genetic background strongly influences the response to influenza a virus infections*. PLoS One, 2009. **4**(3): p. e4857.
216. Pica, N., et al., *The DBA.2 mouse is susceptible to disease following infection with a broad, but limited, range of influenza A and B viruses*. J Virol, 2011. **85**(23): p. 12825-9.
217. Kim, J.I., et al., *DBA/2 mouse as an animal model for anti-influenza drug efficacy evaluation*. J Microbiol, 2013. **51**(6): p. 866-71.

218. Shin, D.L., et al., *Protection from Severe Influenza Virus Infections in Mice Carrying the Mx1 Influenza Virus Resistance Gene Strongly Depends on Genetic Background*. J Virol, 2015. **89**(19): p. 9998-10009.
219. Choi, E.J., et al., *The effect of mutations derived from mouse-adapted H3N2 seasonal influenza A virus to pathogenicity and host adaptation*. PLoS One, 2020. **15**(1): p. e0227516.
220. Bouvier, N.M. and A.C. Lowen, *Animal Models for Influenza Virus Pathogenesis and Transmission*. Viruses, 2010. **2**(8): p. 1530-1563.
221. Braciale, T.J., et al., *Class I major histocompatibility complex-restricted cytolytic T lymphocytes recognize a limited number of sites on the influenza hemagglutinin*. Proc Natl Acad Sci U S A, 1989. **86**(1): p. 277-81.
222. Boon, A.C., et al., *Host genetic variation affects resistance to infection with a highly pathogenic H5N1 influenza A virus in mice*. J Virol, 2009. **83**(20): p. 10417-26.
223. Raijmakers, R., et al., *Experimental autoimmune encephalomyelitis induction in peptidylarginine deiminase 2 knockout mice*. J Comp Neurol, 2006. **498**(2): p. 217-26.
224. Gasper, D.J., et al., *Effective Respiratory CD8 T-Cell Immunity to Influenza Virus Induced by Intranasal Carbomer-Lecithin-Adjuvanted Non-replicating Vaccines*. PLoS Pathog, 2016. **12**(12): p. e1006064.
225. Granger, V., et al., *Human blood monocytes are able to form extracellular traps*. J Leukoc Biol, 2017. **102**(3): p. 775-781.
226. Sauna, Z.E. and C. Kimchi-Sarfaty, *Understanding the contribution of synonymous mutations to human disease*. Nat Rev Genet, 2011. **12**(10): p. 683-91.

227. Vasilopoulos, Y., et al., *A nonsynonymous substitution of cystatin A, a cysteine protease inhibitor of house dust mite protease, leads to decreased mRNA stability and shows a significant association with atopic dermatitis*. *Allergy*, 2007. **62**(5): p. 514-9.
228. Hutchinson, D., et al., *Are Rheumatoid Factor, Anti-Citrullinated Protein Antibodies, and Anti-Carbamylated Protein Antibodies Linked by Posttranslational Modification of IgG? Comment on the Article by Koppejan et al*. *Arthritis Rheumatol*, 2016. **68**(11): p. 2825-2826.
229. Verheul, M.K., et al., *Pitfalls in the detection of citrullination and carbamylation*. *Autoimmun Rev*, 2018. **17**(2): p. 136-141.
230. Nielen, M.M., et al., *Specific autoantibodies precede the symptoms of rheumatoid arthritis: a study of serial measurements in blood donors*. *Arthritis Rheum*, 2004. **50**(2): p. 380-6.
231. Cornelis, R., et al., *Stromal Cell-Contact Dependent PI3K and APRIL Induced NF-kappaB Signaling Prevent Mitochondrial- and ER Stress Induced Death of Memory Plasma Cells*. *Cell Rep*, 2020. **32**(5): p. 107982.
232. Wang, T.T., et al., *Vaccination with a synthetic peptide from the influenza virus hemagglutinin provides protection against distinct viral subtypes*. *Proc Natl Acad Sci U S A*, 2010. **107**(44): p. 18979-84.
233. Okuno, Y., et al., *Rapid focus reduction neutralization test of influenza A and B viruses in microtiter system*. *J Clin Microbiol*, 1990. **28**(6): p. 1308-13.

234. Turesson, C., et al., *Extra-articular disease manifestations in rheumatoid arthritis: incidence trends and risk factors over 46 years*. Ann Rheum Dis, 2003. **62**(8): p. 722-7.
235. Koivula, M.K., et al., *Are there autoantibodies reacting against citrullinated peptides derived from type I and type II collagens in patients with rheumatoid arthritis?* Ann Rheum Dis, 2005. **64**(10): p. 1443-50.
236. Burkhardt, H., et al., *Epitope-specific recognition of type II collagen by rheumatoid arthritis antibodies is shared with recognition by antibodies that are arthritogenic in collagen-induced arthritis in the mouse*. Arthritis Rheum, 2002. **46**(9): p. 2339-48.
237. Harris, M.L., et al., *Association of autoimmunity to peptidyl arginine deiminase type 4 with genotype and disease severity in rheumatoid arthritis*. Arthritis Rheum, 2008. **58**(7): p. 1958-67.
238. Smolen, J.S., D. Aletaha, and I.B. McInnes, *Rheumatoid arthritis*. Lancet, 2016. **388**(10055): p. 2023-2038.
239. Cantaert, T., et al., *Presence and role of anti-citrullinated protein antibodies in experimental arthritis models*. Arthritis Rheum, 2013. **65**(4): p. 939-48.
240. Chang, M.H. and P.A. Nigrovic, *Antibody-dependent and -independent mechanisms of inflammatory arthritis*. JCI Insight, 2019. **4**(5).
241. Hill, J.A., et al., *Arthritis induced by posttranslationally modified (citrullinated) fibrinogen in DR4-IE transgenic mice*. J Exp Med, 2008. **205**(4): p. 967-79.
242. Courtenay, J.S., et al., *Immunisation against heterologous type II collagen induces arthritis in mice*. Nature, 1980. **283**(5748): p. 666-8.

243. Butz, D.E., et al., *A mechanistic approach to understanding conjugated linoleic acid's role in inflammation using murine models of rheumatoid arthritis*. *Am J Physiol Regul Integr Comp Physiol*, 2007. **293**(2): p. R669-76.
244. Holmdahl, R., et al., *Collagen induced arthritis as an experimental model for rheumatoid arthritis. Immunogenetics, pathogenesis and autoimmunity*. *APMIS*, 1989. **97**(7): p. 575-84.
245. Trentham, D.E., *Collagen arthritis as a relevant model for rheumatoid arthritis*. *Arthritis Rheum*, 1982. **25**(8): p. 911-6.
246. Holmdahl, R., M. Andersson, and A. Tarkowski, *Origin of the autoreactive anti-type II collagen response. I. Frequency of specific and multispecific B cells in primed murine lymph nodes*. *Immunology*, 1987. **61**(3): p. 369-74.
247. Bajtner, E., et al., *Chronic development of collagen-induced arthritis is associated with arthritogenic antibodies against specific epitopes on type II collagen*. *Arthritis Res Ther*, 2005. **7**(5): p. R1148-57.
248. Schulte, S., et al., *Arthritis-related B cell epitopes in collagen II are conformation-dependent and sterically privileged in accessible sites of cartilage collagen fibrils*. *J Biol Chem*, 1998. **273**(3): p. 1551-61.
249. Kidd, B.A., et al., *Epitope spreading to citrullinated antigens in mouse models of autoimmune arthritis and demyelination*. *Arthritis Res Ther*, 2008. **10**(5): p. R119.
250. Inglis, J.J., et al., *Collagen-induced arthritis in C57BL/6 mice is associated with a robust and sustained T-cell response to type II collagen*. *Arthritis Res Ther*, 2007. **9**(5): p. R113.

251. Holmdahl, R., et al., *High antibody response to autologous type II collagen is restricted to H-2q*. Immunogenetics, 1986. **24**(2): p. 84-9.
252. Holmdahl, R., et al., *Localization of a critical restriction site on the I-A beta chain that determines susceptibility to collagen-induced arthritis in mice*. Proc Natl Acad Sci U S A, 1989. **86**(23): p. 9475-9.
253. Campbell, I.K., J.A. Hamilton, and I.P. Wicks, *Collagen-induced arthritis in C57BL/6 (H-2b) mice: new insights into an important disease model of rheumatoid arthritis*. Eur J Immunol, 2000. **30**(6): p. 1568-75.
254. Sato, T., et al., *Citrullinated fibrinogen is a target of auto-antibodies in interstitial lung disease in mice with collagen-induced arthritis*. Int Immunol, 2020. **32**(8): p. 533-545.
255. Dunussi-Joannopoulos, K., et al., *B-cell depletion inhibits arthritis in a collagen-induced arthritis (CIA) model, but does not adversely affect humoral responses in a respiratory syncytial virus (RSV) vaccination model*. Blood, 2005. **106**(7): p. 2235-43.
256. Yanaba, K., et al., *B cell depletion delays collagen-induced arthritis in mice: arthritis induction requires synergy between humoral and cell-mediated immunity*. J Immunol, 2007. **179**(2): p. 1369-80.
257. Webb, L.M., M.J. Walmsley, and M. Feldmann, *Prevention and amelioration of collagen-induced arthritis by blockade of the CD28 co-stimulatory pathway: requirement for both B7-1 and B7-2*. Eur J Immunol, 1996. **26**(10): p. 2320-8.
258. Gabay, C., *IL-1 inhibitors: novel agents in the treatment of rheumatoid arthritis*. Expert Opin Investig Drugs, 2000. **9**(1): p. 113-27.

259. Dowty, M.E., et al., *Preclinical to clinical translation of tofacitinib, a Janus kinase inhibitor, in rheumatoid arthritis*. J Pharmacol Exp Ther, 2014. **348**(1): p. 165-73.
260. Williams, R.O., M. Feldmann, and R.N. Maini, *Anti-tumor necrosis factor ameliorates joint disease in murine collagen-induced arthritis*. Proc Natl Acad Sci U S A, 1992. **89**(20): p. 9784-8.
261. Kim, E.J., H.R. Collard, and T.E. King, Jr., *Rheumatoid arthritis-associated interstitial lung disease: the relevance of histopathologic and radiographic pattern*. Chest, 2009. **136**(5): p. 1397-1405.
262. Li, P. and E.M. Schwarz, *The TNF-alpha transgenic mouse model of inflammatory arthritis*. Springer Semin Immunopathol, 2003. **25**(1): p. 19-33.
263. Miyazaki, Y., et al., *Expression of a tumor necrosis factor-alpha transgene in murine lung causes lymphocytic and fibrosing alveolitis. A mouse model of progressive pulmonary fibrosis*. J Clin Invest, 1995. **96**(1): p. 250-9.
264. Lundblad, L.K., et al., *Tumor necrosis factor-alpha overexpression in lung disease: a single cause behind a complex phenotype*. Am J Respir Crit Care Med, 2005. **171**(12): p. 1363-70.
265. Douni, E., et al., *Transgenic and knockout analyses of the role of TNF in immune regulation and disease pathogenesis*. J Inflamm, 1995. **47**(1-2): p. 27-38.
266. Keffer, J., et al., *Transgenic mice expressing human tumour necrosis factor: a predictive genetic model of arthritis*. Embo J, 1991. **10**(13): p. 4025-31.

Appendix: Rheumatoid Arthritis: Two Murine Models

This manuscript was submitted to *Methods in Cell Biology* (2021)

Funding for this work was provided support by the National Institutes of Health's National Heart, Lung, and Blood Institute [T32 HL007899] to A.M.M.

This manuscript was submitted to *Methods in Cell Biology* (2021)

Funding for this work was provided support by the National Institutes of Health's National Heart, Lung, and Blood Institute [T32 HL007899] to A.M.M.

Rheumatoid Arthritis: Two Murine Models

Aisha M. Mergaert^{1,2}, Thomas F. Warner², Miriam A. Shelef^{1,3}

¹Department of Medicine, University of Wisconsin-Madison, Madison, WI 53705, USA.

²Department of Pathology and Laboratory Medicine, University of Wisconsin-Madison, Madison, WI 53705, USA.

³William S. Middleton Memorial Veterans Hospital, Madison, WI 53705, USA.

AM contributed to the manuscript by writing the abstract, introduction and CIA methods; performing CIA experiments; making all of the CIA figures; reviewing and editing the final manuscript.

4.1 Abstract

Rheumatoid arthritis is an incurable chronic inflammatory disease for which the pathophysiology is not fully understood, and treatment options are flawed. Thus, animal models are used to dissect disease pathogenesis and to develop improved therapeutics. However, accurately modeling all aspects of human rheumatoid arthritis in mice is not possible, and each model has pros and cons. Two useful murine models of rheumatoid arthritis are collagen induced arthritis and TNF induced arthritis. Both recapitulate the chronic inflammatory, erosive arthritis of human rheumatoid arthritis. Collagen induced arthritis has the added similarity to human rheumatoid arthritis of pathogenic autoantibodies. However, collagen induced arthritis tends to have highly variable arthritis severity with optimal arthritis requiring a specific genetic background, two features analogous to human rheumatoid arthritis, but challenging for experiments. In contrast, TNF induced arthritis is not genetic background dependent and tends to be uniform. Here we describe the benefits, limitations, and details for both models to help investigators select and implement the correct model to achieve the goals of their experiments.

4.2 Introduction

Rheumatoid arthritis (RA) is a chronic autoimmune, inflammatory arthritis that, particularly if untreated, can lead to joint destruction. RA is also a systemic disease with a variety of extra-articular manifestations including interstitial lung disease, pericarditis, cutaneous vasculitis, subcutaneous nodules, keratoconjunctivitis sicca, scleritis, and more [234]. Most people with RA generate autoimmune antibodies, classically anti-citrullinated protein antibodies, which are used diagnostically [24] and have pathogenic

capabilities [149]. Autoantibodies detected in RA can also target the Fc portion of IgG (rheumatoid factor), [19] carbamylated antigens [70], acetylated antigens [71], MAA-adducted proteins [74], collagen [235, 236], the peptidylarginine deiminases (enzymes that citrullinate proteins) [237], and more. In addition to these contributions from B lineage cells, there is clear evidence for the involvement of T cells, neutrophils, macrophages, osteoclasts, and other cells in RA [238]. Thus, given the range of organs affected, antigens targeted, and cells involved, RA is an extremely complicated disease.

Modeling RA in mice is important to study disease mechanisms and to test therapeutics. Given the complexity of human disease and the significant genetic and immunologic differences between mice and humans, no model perfectly recapitulates human RA. Rather, different murine arthritis models simulate different features of the pathophysiology of RA. Arthritis models may be acute or chronic, antibody-independent or antibody-dependent, and differentially mimic autoimmunity against citrullinated proteins [158, 203, 239-241]. Investigators must select the correct model to achieve the goals of their experiments. Here, we will focus on two forms of murine inflammatory arthritis that are chronic and differentially model the adaptive and innate immune response in RA.

Collagen induced arthritis (CIA) is a frequently used model to study RA due to similar disease manifestations and autoantibody reactivity. In this model, arthritis is induced by injecting type II collagen with adjuvant [242, 243]. Mice with CIA develop a polyarthritis with synovitis and destruction of bone and cartilage (Figure 1), all of which are observed in human RA [244, 245]. Also similar to human RA, a variety of autoantibodies develop in CIA, including rheumatoid factor [246], antibodies against type

II collagen [236, 247, 248], and antibodies against citrullinated antigens [203, 249]. However, unlike anti-citrullinated protein antibodies in human RA [58], there does not appear to be a strong preference for targeting citrullinated epitopes, as opposed to unmodified epitopes, in CIA [203, 249]. The anti-collagen antibodies are pathogenic with the capacity to induce arthritis in naïve mice [197]. Also analogous to RA, major histocompatibility complex (MHC) haplotypes contribute to CIA, as mice with the H-2q genotype, like DBA/1J mice, are highly susceptible to this model of arthritis, whereas mice with other MHC haplotypes can develop arthritis only under certain conditions [59, 250-253]. Finally, mice with CIA develop an interstitial lung disease similar to human RA-associated lung disease [254]. Given the many similarities with human RA, CIA has proved useful in successfully testing therapeutics, including rituximab, abatacept, IL-1 receptor antagonists, tofacitinib, and TNF-alpha inhibitors [255-261]. However, a significant drawback to this model is that arthritis is often highly variable from paw to paw, mouse to mouse, experiment to experiment, and facility to facility. The full explanation for this variability is unknown, but exact experimental conditions including microbiome differences may contribute. Also, using this model with transgenic or knockout lines can be challenging due to the need to back-cross to the DBA/1J background for optimal arthritis.

A second chronic model of RA in mice is TNF-induced arthritis (TIA), an arthritis model in which human TNF alpha is overexpressed, leading to a chronic, erosive arthritis (Figure 2) like human RA [262]. These mice also develop interstitial lung disease with some comparable features to human RA-associated lung disease [159, 263, 264]. TIA is thought to primarily be a model of the innate arm of the immune response in RA, although

B cells and T cells do become activated [158]. Also, autoantibodies form against native and citrullinated antigens in this model, but without citrulline-specificity [158]. Although there are multiple TNF transgenic lines [265, 266], Tg3647, with one copy of the TNF transgene, is arguably the most useful. Mice with more transgene copies develop arthritis faster, but are challenging to breed. Advantages to TIA include arthritis that is 100% penetrant and reproducible as well as ease of crossing TNF-overexpressing mice with other genetically modified mice [120, 158, 262]. The precise methodology for implementing the CIA and TIA models is outlined below.

4.3 Collagen Induced Arthritis

4.3.1 Making the Collagen Emulsion

1. All steps of emulsion preparation should be performed on ice and with cold reagents.
2. Attach a one-way stopcock (Cadence Science, Cranston, USA) to the end of a 10ml luer lock syringe, with the plunger removed and saved (Figure 2a). Ensure the stopcock is in the closed position.
3. Place the syringe with the attached stopcock in a bucket of ice with the stopcock pointed down and the opening of the syringe accessible (Figure 2b).
4. At a ratio of 1:1 by volume, add complete Freund's adjuvant (BD, Franklin Lakes, USA) and a 2mg/ml solution of chick type II collagen (Chondrex, Redmond, USA) to the opening of the syringe, ensuring that as little solution as possible remains on the sides of the syringe shaft.

5. Using an electric tissue homogenizer with a small blade (5 mm or less), mix the solution on high for 1.5 minutes. Pause for 1 minute.
6. Repeat step 5 two additional times, for a total of three rounds of emulsification.
7. Allow the emulsion to cool for 5-10 minutes on ice.
8. Perform a drop test to ensure that the emulsion is correctly made. To do so, add tap water to a clean beaker. Using an 18 gauge needle and a 3 ml syringe, draw up a small amount of emulsion. Gently expel the emulsion a few inches above the water. If the emulsion is good, the droplet will remain whole in the water. If the droplet disperses, repeat steps 4 and 5 until the drop test is successful.
9. Remove the 10 ml syringe that contains the emulsion from the bucket of ice. Remove all ice particles from the syringe and stopcock, including ice lodged inside the valve of the stopcock.
10. To the 10 ml syringe, insert the plunger that was previously removed, but do not depress.
11. Connect a 1 ml luer lock glass syringe (Hamilton, Reno, USA) to the opposite end of the stopcock (Figure 2c).
12. While covering the open end of the glass syringe with a tissue, depress the plunger into the 10 ml syringe.
13. Once the emulsion is completely inside the glass syringe, add the appropriate plunger to the glass syringe.
14. Depress the plunger into the glass syringe so that the entire emulsion moves into the 10 ml syringe.
15. Using the 10 ml syringe plunger, move the emulsion back into the glass syringe.

16. Close the stopcock and remove the 10 ml syringe.
17. Move the air pocket in the emulsion toward the stopcock by flicking the syringe with the syringe held so that the plunger is pointed downwards and not depressed. This process may take some time. Check for partially transparent air pockets by holding the syringe up to a bright light.
18. Remove the stopcock and replace it with a 27 gauge, ½ inch needle. Slowly expel air until a small amount of emulsion emerges from the needle (Figure 2d).
19. Place the glass syringe on ice and use within 1 hour.

4.3.2 CIA Induction

1. Anesthetize 8 to 9 week old DBA/1J mice (Jackson Laboratory, Bar Harbor, USA) with an approved reagent such as isoflurane. Use toe pinch to ensure proper anesthesia.
2. At approximately the middle of the tail, looking at the dorsal side, identify the dark tail veins. In between the tail veins, there is pale tissue, which will be the site of intradermal injection.
3. With the needle pointed toward the mouse and parallel to the tail, insert the needle bevel down into the pale space of the tail. Avoid the tail veins. With a thumb and forefinger, pinch the needle, holding it in place.
4. Slowly inject 100 µl of emulsion into the tail. The emulsion will slowly move up the tail within the skin towards the body of the mouse. Monitor this progression to prevent the emulsion from moving past the tail base.
5. Remove the needle and wipe away excess emulsion from the tail.

6. Allow the mouse to recover from anesthesia.
7. From this point on, maintain mice on a breeder diet such as Teklad Global 19% Protein Extruded Rodent (Envigo, Indianapolis, USA).
8. After three weeks, make an emulsion as in section 3.1, but substitute *incomplete* Freund's adjuvant (BD) for *complete* Freund's adjuvant for the first boost injection.
9. Although typically intradermal injection is used to deliver 100 μ l of this emulsion, we found that intraperitoneal injection works well to induce arthritis and also reduces the frequency of tail necrosis. No anesthesia is needed for intraperitoneal injection.
10. Given the variability of CIA induction, we repeat Steps 8 & 9 to deliver a second boost of collagen in *incomplete* Freund's adjuvant six weeks after the initial injection (three weeks after the first boost) to ensure arthritis induction.

4.3.3 CIA Scoring

1. Limbs should be evaluated regularly for arthritis. We typically score arthritis weekly starting on the date of the second boost.
2. For caliper measurements, each mouse should be hand restrained, and each paw measured with a digital caliper (Swiss Precision Instruments, Melville, USA) while the mouse is not moving its paw. Measurements should be taken at the pad of the paw in the same place for each mouse. Measurements for all paws can be averaged for each date.

3. We perform visual scoring according to Table 1. Each limb is scored according to each parameter. Scores for all limbs are averaged for each mouse to create a final score.

4.4. TNF Induced Arthritis

1. As noted above, we recommend Tg3647 mice, with one copy of the TNF transgene. These mice are maintained by several investigators, typically on a C57BL/6 background, with permission for their use required by Biomedical Sciences Research Centre Alexander Fleming.
2. Mice are typically bred by crossing heterozygous Tg3647 males with wild-type females. Heterozygous Tg3647 females can be bred with wild-type males, but Tg3647 females tend not to breed well.
3. Pups are genotyped with 50% of the litter expected to be heterozygous for the TNF transgene. DNA prepared from ear punches or tail snips by standard methods can be used for PCR with the following primers: TACCCCCTCCTTCAGACACC and GCCCTTCATAATATCCCCCA. PCR conditions that work well are 94°C for 3 minutes, then 30 cycles of 94°C for 30 seconds, 60°C for 35 seconds, and 72°C for 90 seconds, followed by 72°C for 10 minutes.
4. Arthritis typically starts mildly at one month of age. Scoring can be performed weekly, but monthly may be sufficient given slow progression of disease.
5. Our scoring definitions are in Table 2. We typically score the front paws and use the average. Grip strength is tested by the allowing the mouse to resist being lifted from a wire cage top.

4.5 Concluding remarks

Above we describe two chronic models of RA in mice and provide clear methods for implementing them. Given the different benefits and limitations of RA models, investigators must choose a model that best fits their experimental goals according to both pathology and logistics. We find CIA and TIA to be broadly applicable to the study of RA and easily established with the above protocols.

4.6 Notes

- All experiments should include negative and positive controls. Typically a negative control is a mouse in which arthritis is not induced and a positive control is a mouse in which arthritis is induced, but no treatment or experimental condition is provided.
- Each cage should contain at least one positive control mouse and one mouse with each experimental condition to reduce microbiome or other cage-specific effects.
- Experimental and control mice should always be age- and sex-matched. Age-matched mice are typically born within 5 days of each other.
- If using the TIA model crossed with a transgenic or knock-out line from a different strain, littermates should be used for control and experimental mice.
- Given subjectivity, scoring always should be performed in a blinded manner. Additionally, using a single investigator to score arthritis reduces variability between mice and time points. Adding a second investigator to score all mice adds robustness.
- DBA/1J mice are very jumpy and can be difficult to handle.

- For CIA, sometimes 100 μ l of emulsion cannot be injected. Typically 50 μ l is sufficient.
- In a minority of mice in which CIA has been induced, tail damage may occur after intradermal injection. Tissue damage varies from irritation at the injection site to necrosis of the tail distal to the injection site.
- For CIA, arthritis onset will usually occur between 5 and 8 weeks after the first injection. However, arthritis is very variable and a minority of mice may never develop arthritis.
- Use of the caliper must be possible with one hand, as the other will be holding the mouse. A digital caliper is recommended. Alternatively, a second investigator or a restraining device would be needed.
- Tg3647 mice are not very hardy. Depending on stressors or pathogens in the facility, some mice may not live much past four months of age. They almost never live past six months of age. Additionally, as arthritis progresses, breeding success declines.

4.7 Figures

Table 1. Collagen Induced Arthritis Scoring

Score	Range of Motion*	Usage**	Swelling	Erythema**
0	Normal	Normal	None	None
1	Reduced in digits	Abnormal weight bearing or loss of grip strength	Any digit	Slight
2	Reduced in wrist/ankle	Non-use	Paw	Extreme
3	Not applicable	Not applicable	Wrist/ankle	Not applicable
4	Not applicable	Not applicable	Entire limb	Not applicable

* Maximum score is 2.

** Minimum score is 2.

Table 2. TNF Induced Arthritis Scoring

Score	Joint Deformity	Swelling	Grip Strength
0	none	none	normal
0.5	mild	mild	normal
1	moderate	moderate	normal
1.5	moderate/severe	moderate	reduced
2	severe	moderate	none
2.5	severe	moderate/severe	none
3	severe	severe	none

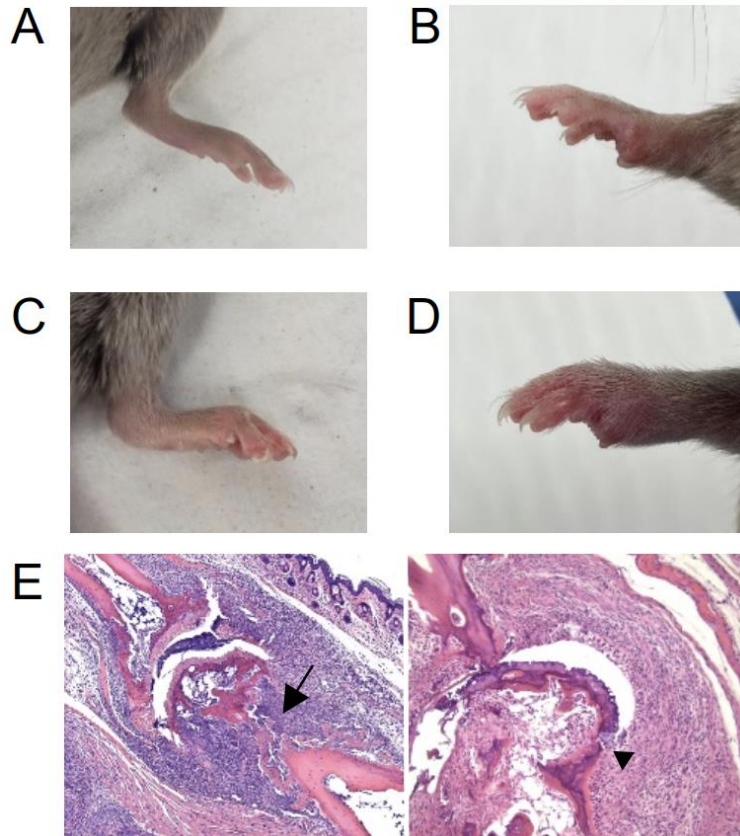


Figure 1. Collagen Induced Arthritis (CIA). Images of a normal rear paw (A) and front paw (B) from a DBA/1J mouse without CIA, both with scores of 4, as well as a rear paw with a score of 9 (C) and front paw with a score of 8 (D) from a mouse with CIA. E. Hematoxylin and eosin stained histology images from a CIA mouse paw showing synovitis and erosion of cartilage (arrow head) and bone (arrow).

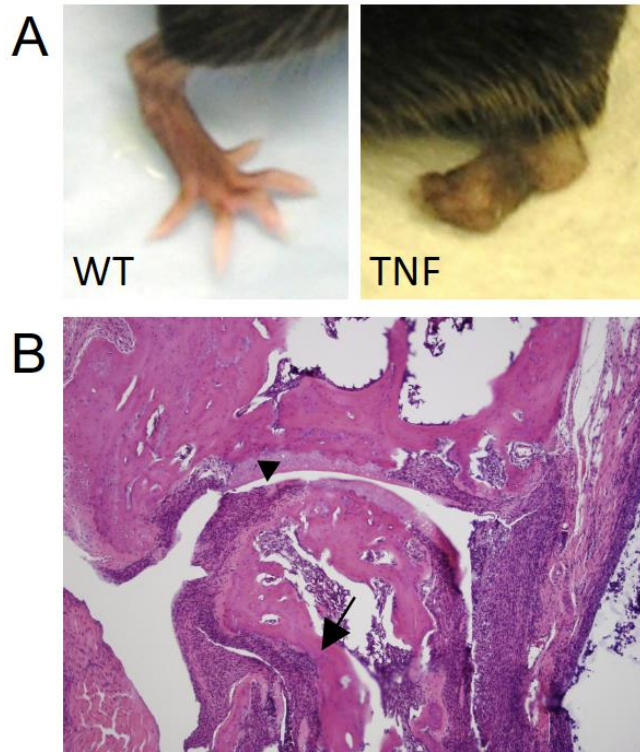


Figure 2. TNF Induced Arthritis. A. Images of a paw from a wild-type (WT) mouse with a score of 0 and a Tg3647 mouse (TNF) with a score of 3. B. Hematoxylin and eosin stained histology image from a Tg3647 mouse joint showing synovitis and erosion of cartilage (arrow head) and bone (arrow).

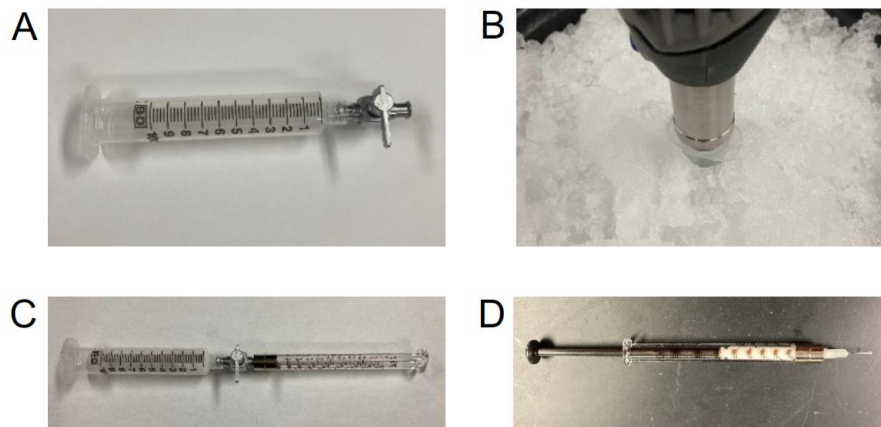


Figure 3. Key supplies for making the collagen emulsion. A. Luer lock syringe (10 ml) with plunger removed attached to a one-way stopcock. B. Syringe with stopcock from (A) pointing downwards in ice with homogenizer inserted into the syringe C. Glass syringe attached to the 10 ml syringe via the stopcock. D. Glass syringe filled with collagen emulsion with stopcock removed and replaced with a 27 gauge needle.